Journal of Membrane Science 640 (2021) 119802

Contents lists available at ScienceDirect

Journal of Membrane Science

journal homepage: www.elsevier.com/locate/memsci

Polycrystalline metal-organic framework (MOF) membranes for molecular separations: Engineering prospects and challenges

Mohamad Rezi Abdul Hamid [a,1], Yutian Qian [b,1], Ruicong Wei [c,1], Zhen Li [c,1], Yichang Pan [d], Zhiping Lai [c,*], Hae-Kwon Jeong [b,**]

[a] Department of Chemical and Environmental Engineering, Faculty of Engineering, Universiti Putra Malaysia, Serdang, Selangor, 43400, Malaysia
[b] Artie McFerrin Department of Chemical Engineering and Department of Materials Science and Engineering, Texas A&M University, College Station, TX, 77843-3122, United States
[c] Chemical Engineering Program, Division of Physical Sciences and Engineering, King Abdullah University of Science and Technology (KAUST), Thuwal, 23955-6900, Saudi Arabia
[d] College of Chemical Engineering, State Key Laboratory of Materials-Oriented Chemical Engineering, Nanjing Tech University, Nanjing, 210009, China

ARTICLE INFO

Keywords:
Metal-organic frameworks
Zeolitic-imidazolate frameworks
Polycrystalline membranes
Gas separations
Engineering challenges

ABSTRACT

Metal-organic frameworks (MOFs), owing to their ordered porous structure, ease of synthesis, and versatility of surface functionalization have attracted significant research interests for membrane-based separations. Zeolitic-imidazolate frameworks (ZIFs), a subclass of MOFs, have drawn the most research attention by virtue of their ease of forming high-quality membranes and potential in hydrocarbon mixture separations. Other MOF-based membranes such as IRMOFs, HKUST-1, MILs, UiOs, etc., were also well-studied for hydrogen purification and carbon capture. In this review, we summarize a chronological development of MOF membranes for gas separations, focusing on ZIF-8 membranes for C_3H_6/C_3H_8 separation. Other MOF membranes for H_2/CO_2, CO_2/CH_4, and CO_2/N_2 separations are also reviewed. Following this, we provide a thorough assessment and evaluation of the engineering challenges, including cost-effectiveness, module design, and membrane stability and reproducibility for industrial scale-up. Finally, we provide our point of view on future research and development in the area.

1. Introduction and background

1.1. Overview of the status of industrial chemical separations

The industrial revolution in the 19th century has empowered humans to explore natural resources such as natural gas, crude oil, and seawater. These resources are processed to produce a huge amount of chemical mixtures, which require various separation and purification processes for further use. The industrial separation processes can be generally divided into two forms: gas and liquid, as summarized in Fig. 1. Hydrogen recovery, carbon capture, and light hydrocarbon separations are among the challenging yet important gas separations. The demand for hydrogen has been increasing exponentially in recent years, driven by the clean energy transformation worldwide ranging from electricity generation to energy storage (e.g., hydrogen battery) [1,2]. Hydrogen recovery from natural gas or refinery mixtures (H_2/CH_4) is an attractive way to collect this energy carrier. In addition, hydrogen purification from syngas (H_2/CO_2) is another important industrial separation for fuel decarbonization [3]. Decarbonization also involves carbon capture (CO_2/N_2), which has attracted significant industrial efforts, especially with the rising concerns of climate change and global warming.

Natural gas purification to strip away CO_2 from CH_4 is essential to meet natural gas pipeline specifications, making CO_2/CH_4 an important industrial separation [4]. Meanwhile, hydrocarbon mixtures derived from crude oil refinery needs to be further separated and purified for downstream processing. For example, the separation involving alkene/alkane (e.g., C_2H_4/C_2H_6, C_3H_6/C_3H_8, and C_4H_8/C_4H_{10}) has been the most industrially important process. Alkenes (e.g., C_2H_4, C_3H_6, and C_4H_8) are important chemicals for polymer productions including, but

* Corresponding author.
** Corresponding author.
E-mail addresses: zhiping.lai@kaust.edu.sa (Z. Lai), hjeong7@tamu.edu (H.-K. Jeong).
[1] The authors contribute equally.

https://doi.org/10.1016/j.memsci.2021.119802
Received 27 June 2021; Received in revised form 17 August 2021; Accepted 25 August 2021
Available online 27 August 2021

not limited to polyethylene, polypropylene, polyvinyl chloride, polyester, polystyrene, and polybutene [5–7]. Alkanes such as ethane, on the other hand, can be used as chemical feedstocks to produce acetic acid. Propane, a popular fuel source, has recently been considered as a potential candidate for anti-freeze applications. Other separation pairs include alkene/alkyne (e.g., C_2H_4/C_2H_2), and isomers (e.g., n-C_4H_8/i-C_4H_8 and n-C_4H_{10}/i-C_4H_{10}) also play important roles in the industrial processes. Acetylene is widely used as fuel gas for welding and feedstock for plastic production. Butane isomers such as i-butene and i-butane also involve in various industrial applications, with the former is used as a feedstock to produce butyl-rubber while the latter is used to produce alkylate or i-octane.

Water treatment, organic solvent or hydrocarbon separation, and chiral resolution are the three major processes for liquid-based separations. Water treatments represent a major industrial segment that involves desalination and wastewater treatment/recycle/purification. These separation processes include salt rejection and contaminant removals such as dyes, organic solvents, and heavy metals. Chiral resolution is particularly important in agrochemical, pharmaceutical, and food industries as chiral isomers can trigger different responses in living organisms [8,9].

1.2. Conventional separation technologies

1.2.1. Gas separations

Adsorption, absorption, and distillation are the main technologies employed for gas separations due to their best combinations in process economics and producing high purity products compared to other alternatives.

Pressure-swing adsorption (PSA) and temperature-swing adsorption (TSA) are the two common methods to separate gas mixtures based on the difference in individual gas sorption at a specific pressure or temperature. Product purity and recovery are highly dependent on chemical interactions between the adsorbent and target molecule. PSA and TSA are commercially available in several important gas separations such as oxygen purification, nitrogen enrichment, and CO_2-based separations. This technology is mainly employed in medium scale separation as the scale-up is linearly correlated with the amount of adsorbents [10].

Chemical absorption is mainly employed in CO_2 separations such as carbon capture from exhaust gas or natural gas sweetening [4,11]. The main principle behind this is to use basic liquid amines to react with CO_2 to form carbamic acid [12]. The unstable carbamic acid then releases CO_2 at elevated temperatures via decomposition through which amine is regenerated. Amine-based absorption is a continuous process, thereby allowing high purity CO_2 to be obtained with high recovery rates. However, one of the main disadvantages of this process is continuous heating and cooling, which requires a large amount of energy input [13]. Another drawback is the high chemical reactivity of amines: some amines can react with SO_2 and NO_x to form salts, while other amines might degrade with O_2 and form corrosive substances [5,14]. These undesirable side reactions require continuous replenishment of amines and regular cleaning or replacement of the associated operation modules.

The separation of hydrocarbon mixtures, especially alkane/alkene, is typically achieved through thermally-driven distillation. The purity of the distilled chemicals depends on various operating parameters, including feed composition and their associated intrinsic physical properties, flow rate, reflux ratio, stage temperature, and pressure. The optimum operational condition requires extensive heat integration and long start-up and shut-down [10]. In addition, due to similar physicochemical properties of alkene/alkane pairs (e.g., C_2H_4/C_2H_6 and C_3H_6/C_3H_8), the distillation tower needs more than 200 separation stages to fulfill the purity requirement, placing C_2 and C_3 splitters among the most energy intensive industrial processes [15]. High operation cost is another issue for distillation. For example, a distillation process producing 500 × 10^3 tons of C_2H_4 annually is estimated to incur ~$800

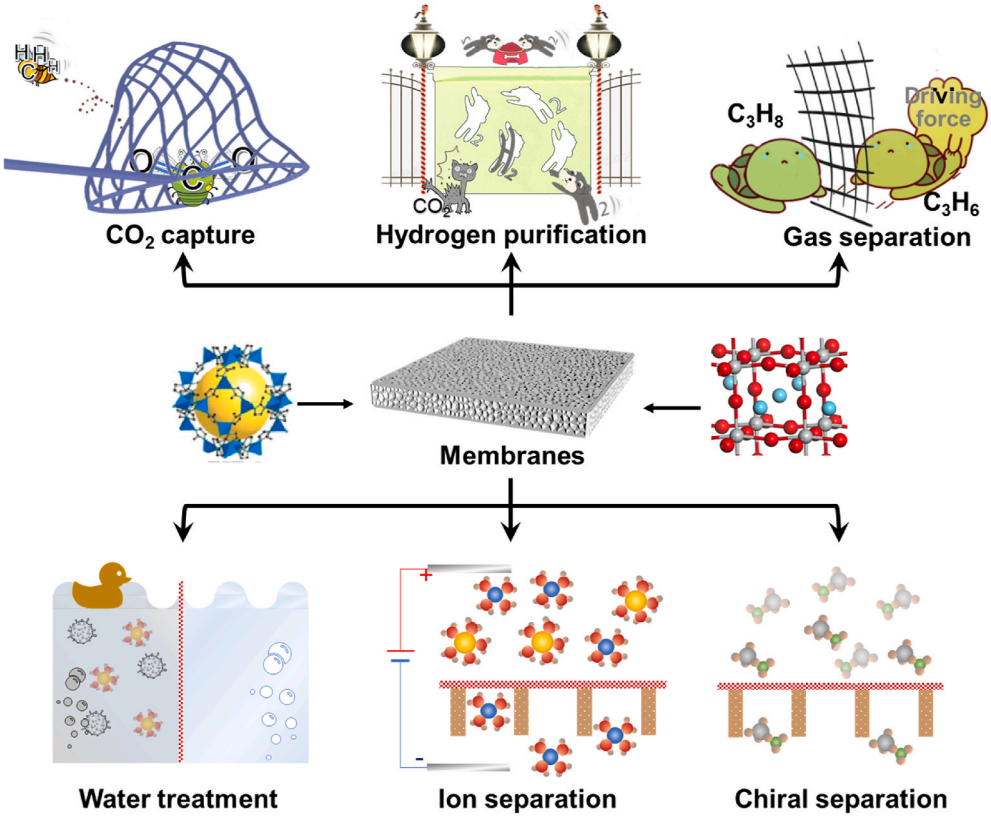

Fig. 1. Important gas and liquid phase separations using membranes.

million in total capital cost and ~$9.2 million•year^{-1} in operating cost, among which gas pressurization and condensation account for the most [10]. According to the statistics of 2016 shown in Fig. 2, distillation accounts for ~50% of industrial energy consumption, which corresponds to ~10–15% of global energy consumption [16,17]. Application of membrane technology to replace conventional distillation can potentially save up to 90% of energy, making membrane an attractive choice for chemical separations. One important point to highlight here is the 90% energy saving is obtained based on a comparison of net thermal energy consumption between thermal desalination plant and reverse osmosis plant [18].

A relative energy consumption of different separation technologies is presented in Fig. 3. From the figure it is well-established that thermal processes (e.g., distillation, drying, etc.) consume more energy than non-thermal processes (e.g., membrane, crystallization, etc.) because they are based on enthalpy of vaporization of at least one component. When comparing different separation technologies, we should not easily draw a conclusion that thermal processes, especially distillation as inherently energy intensive compared to non-thermal processes without a proper system analysis of each of the process. A recent study by Agrawal et al. [18] showed that heat pump distillation to recover 98.7% C_3H_6 (mole purity of 99.6%) from C_3H_6/C_3H_8 feed (70/30 mol%) performed better in term of effective fuel use compared to membranes (membrane consume 40% more fuel). This however does not necessarily mean that heat pump distillations are always perform better than membranes. The same study also suggest that membrane still remains a better choice to recover C_3H_6 with slightly lower mole purity (~90%).

Research efforts have been made towards upgrading the distillation system by using heat pumps to increase energy efficiency [21], but challenges such as economic feasibility [22], operational and control, and heat integration in the context of the entire distillation system [23] need to be further addressed to make this energy integration design

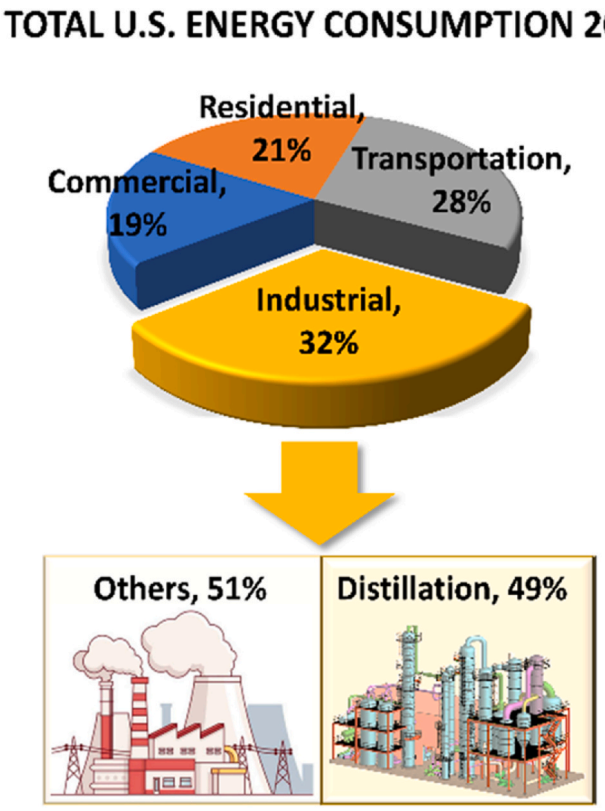

Fig. 2. Breakdown of the U.S. total energy consumption in 2016. Data obtained from Ref. [19]. Application of membrane technology as an alternative to distillation can potentially reduce industrial energy consumption.

industrially viable. Due to issues mentioned above, application of membrane can be an attractive alternative for hydrocarbon separations.

1.2.2. Liquid-phase separations

Liquid-phase separations are considered more advanced than those gas-phase separations in terms of commercialization, especially in water treatment. Commercialized liquid separation processes include flocculation-sedimentation-filtration [24,25], ozonation [25], adsorption [26,27], ultrasonication [28,29], and membranes [30,31]. More than 90% of the membranes used in liquid-phase separation are made of polymers, making the separation process suffer from fouling and low membrane stability, thereby requiring frequent membrane replacement. Researchers are currently investigating other materials such as zeolites to solve this problem. LTA-Na zeolite membranes are the first commercialized polycrystalline membranes for solvent dehydration (e.g., ethanol, propanol, and acetonitrile), with over 200 separation plants being operated all over the world today [32–35], paving the way for other polycrystalline membranes to be industrialized [36].

1.3. Potential of MOF membranes for gas separations

1.3.1. Limitations of polymeric membranes

As discussed above, membrane technology has been widely commercialized for liquid separations. For gas separations, polymeric membranes have been industrially employed in four major applications (i.e., hydrogen purification, vapor recovery, nitrogen enrichment, and natural gas treatment) with a combined annual sales in the range of $1.0–1.5 billion. In natural gas treatment, polymeric membranes account for only a small portion (10%) of the market share. The rest is occupied by amine-based separations [11]. In general, gas separation in polymers follows a solution-diffusion mechanism through which gas dissolves into the membrane with the diffusion rate depending on feed pressure and concentration gradient. This phenomenon is subject to Robeson upper bound [10,37,38]. Numerous research efforts have been made to push membrane separation performances beyond this boundary [37,39–44]. However, compared with polycrystalline materials, there is always a bottleneck for polymeric membranes in terms of permeability owing to its intrinsic lower porosity. The application of polymeric membranes to other gas separations such as alkene/alkane mixture is also limited due to its non-uniform pore distribution and solution-diffusion separation mechanism. Small size difference and similar chemical properties between alkene and alkane (e.g., C_2H_4/C_2H_6 and C_3H_6/C_3H_8) dwarf polymers to be a good candidate for such separations.

Polymeric membrane is a good candidate for carbon capture, especially in the post-combustion process. In this process, industry standard for CO_2 capture requires a membrane with a selectivity of 30–50 and CO_2 permeance of 1000–5000 gas permeation units, GPU (1 GPU = 3.35×10^{-10} mol $m^{-2}{\cdot}s^{-1}{\cdot}Pa^{-1}$). This standard is established based on a typical 550 MW power plant that produces 2 MMscf·min^{-1} flue gas containing 12–14 mol% of CO_2 [10]. For pre-combustion CO_2 capture, membranes with H_2/CO_2 selectivity of 20 and H_2 permeance of 200 GPU are required for the technology to be an attractive replacement of PSA. However, high-temperature operation at 300–500 °C would impose a major barrier for polymeric membranes [45,46].

Recently, polymeric membrane technology has been extended in biomethane production, shown in Fig. 4. The entire process able to recover more than 95% of CH_4 from a biogas mixture with a composition of 50–70% of CH_4, 30–50% of CO_2, and a trace amount of H_2S, O_2, and N_2 [45–47], making a milestone for membranes to be used in a biorefinery plant.

Besides carbon capture, the application of membrane technology for energy-intensive alkene/alkane separations is highly desirable, as described in the previous section. Here, we use C_3H_6/C_3H_8 separation as an example to demonstrate the potential of membrane-based processes. Single-stage membrane with C_3H_6 permeance of 20–40 GPU and

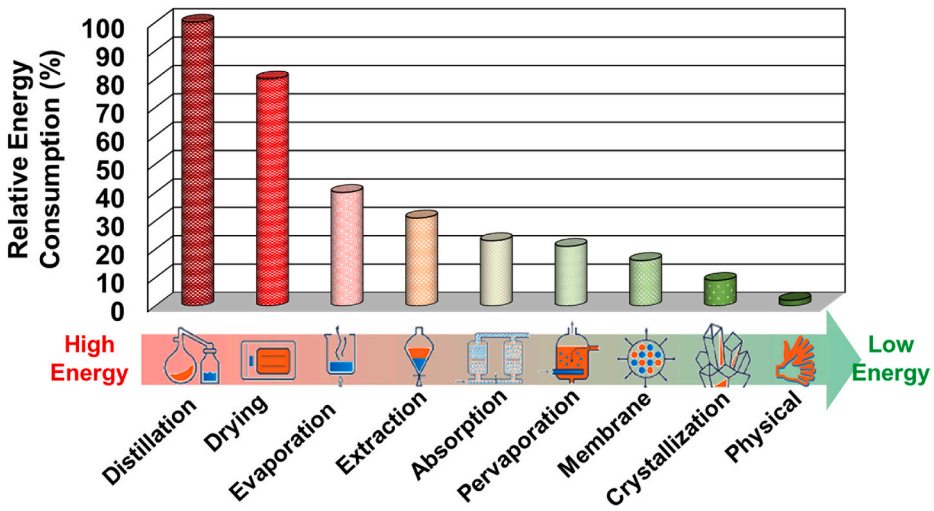

Fig. 3. Relative energy consumption of all types of separation technologies in the industry with data obtained from Ref. [16] and icons reproduced with permission from Ref. [20].

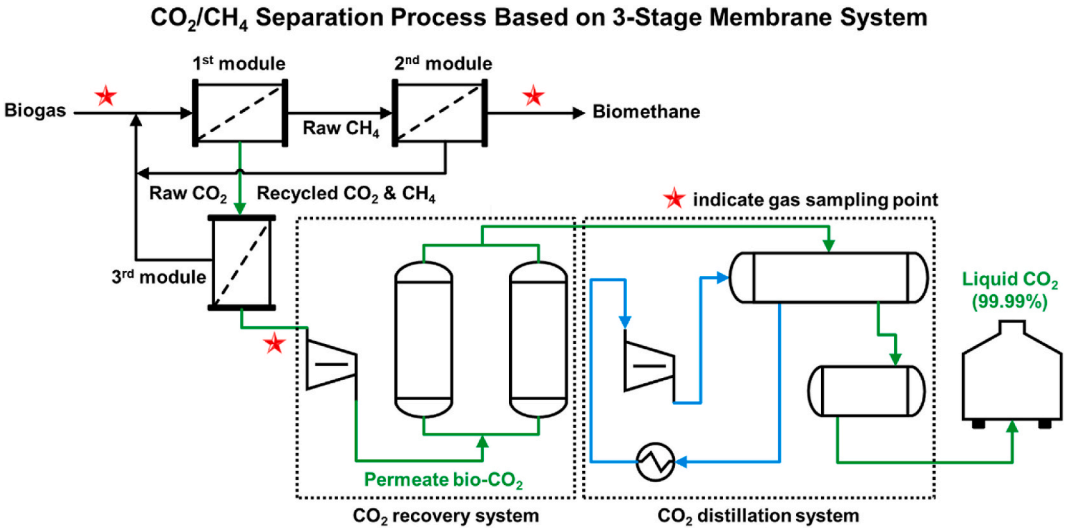

Fig. 4. A schematic illustration of the CO_2/CH_4 separation process based on the three-stage membrane separation and CO_2 recovery unit [47]. Red star symbol indicates the gas sampling points. Image is prepared based on ref. [47] Copyright 2019 The Royal Society of Chemistry. (For interpretation of the references to color in this figure legend, the reader is referred to the Web version of this article.)

selectivity of 6–10 could recover 90% of C_3H_6 from the reactor purge stream [10]. A complete replacement of C_2 or C_3 distillation columns is possible for membranes with moderate selectivity of 15–20 [48].

Despite the great potential of membrane technology in gas separations, its commercial deployment is mainly limited to four main applications and of which are intended for the separation of non-condensable gases [11,49]. Currently, 90% of commercial membranes were developed before the 1990s and are made of less than 10 polymers, including polyimides, polysulfone, polyphenylene oxide, substituted polycarbonates, silicone rubber, and cellulose acetate [10]. Despite their wide commercial use, the majority of polymer membranes suffer from physical and structural instability. Plasticization, triggered mainly by the high-pressure operation, is a major concern that needs to be dealt with. Increasing feed gas pressure will push the polymers to swell due to the intrinsic flexible network of polymers, causing an increased diffusivity for all gases, resulting in a significant loss of selectivity. Aging is another major issue mainly occurring in glassy polymers such as polymers with intrinsic microporosity (PIM). The rigid backbones in glassy polymers restrict the flexibility of the chains to stochastically occupy the spaces, resulting in 'nonequilibrium free volume' [10]. The chains will slowly reconstruct themselves to an equilibrium state over time, diminishing the free volume, leading to a reduction in the gas diffusivity. To date, the majority of the reported polymeric membranes with high flux were made of PIMs, highlighting the development of new materials with permanent porosity.

Recognizing the intrinsic limitation of polymers, research efforts have been shifted towards inorganic and/or polycrystalline membranes, including carbon molecular sieves [50], zeolites [51], and MOFs [52]. Compared with amorphous materials (e.g., polymers, amorphous ceramics, and carbon molecular sieves), crystalline materials (e.g., zeolites and MOFs) possess ordered and tunable frameworks, high porosities, and high versatility in term of surface functionalization, making them ideal membrane materials that can overcome several limitations of polymers.

1.3.2. Polycrystalline MOF membranes

MOFs have several advantages over zeolites owing to their structural diversities, thereby finding a broader range of applications ranging from

catalysts, batteries to gas storage and separations. In general, MOFs are nanoporous crystalline materials made of metal ions coordinated with polydentate organic ligands. The first report on MOFs can be traced back to as early as the 1950s, when the structure of MOF-2 was reported [53]. MOFs started to gain more research attentions since 1995 when the Yaghi's group comprehensively explained the concept of MOFs [54] and reported MOF-5 in 1999 [55]. Since then, numerous research efforts have been contributed to this field, with around ~20,000 MOF structures reported so far. As shown in Fig. 5, classic MOFs can be briefly categorized into 5 groups: isoreticular MOFs (IRMOFs), HKUST-1, MILs, UiOs, and zeolitic-imidazolate frameworks (ZIFs). The potential applications of these materials, in particular as separation membranes, have also been extensively reported [56–61].

Compared with zeolites, MOFs offer several advantages for membrane-based separations as summarized in the following: (i) MOFs have a versatile structural tunability through simple manipulation of metal ions and ligands. The ease of structure design and synthesis enables MOFs to be tailored to target applications. In contrast, creating new zeolites requires tedious work in template design and synthesis. A targeted structure is not guaranteed to be achieved; (ii) MOFs have higher porosity and surface area than zeolites, enabling them to accommodate more molecules. This allows the molecules to diffuse faster through the cavities, resulting in higher gas permeances; (iii) MOFs are more flexible than zeolites, enabling their use in the separation involving larger molecules than their aperture sizes; (iv) MOFs are more versatile to be functionalized via tuning ligand functional groups, exchanging metal ions or ligands, or introducing foreign ions/molecules into the frameworks. This versatility empowers MOF membranes to be employed in a broader range of separations; (v) MOFs can be synthesized and activated under much milder conditions, even in an ambient environment. This advantage enables MOFs to be synthesized onto polymer substrates. Zeolites, in contrast, are normally synthesized under harsher conditions (temperature >150 °C) followed by calcination to remove structure-directing agents.

2. Recent developments in MOF-based membranes

2.1. Chronological development of MOF crystalline membranes in the past decade

MOF membrane research for gas separations can be traced back to 2009 when a pioneering work by Lai and Jeong et al. [68] fabricated the first continuous MOF-5 membrane using an *in-situ* growth approach, opening a door for MOF membrane development in gas separations. Other approaches, including seeding and secondary growth, contra-diffusion, layer-by-layer growth, vapor phase synthesis, and electrochemical synthesis, were also established for MOF membrane fabrications in the following decade (Fig. 6). The majority of MOF membrane research focused on ZIF-8 due to its impressive C_3H_6/C_3H_8 separation properties, ease of synthesis, and the feasibility of forming high-quality membranes. Thus, in the following sections, our main focus is on the development of ZIF-8 membranes. After briefly reviewing the chronological development of MOF membrane fabrication up to date in Section 2.1, we then concentrate on ZIF-8 membranes for C_3H_6/C_3H_8 separation in Section 2.2. The development for other MOF membranes will be reviewed in Section 2.3.

2.1.1. In-situ growth

In-situ growth is the simplest approach to fabricate MOF membranes. In this approach, a pristine or chemically modified support is directly immersed into a precursor solution, allowing for heterogeneous nucleation and membrane growth. Depending on the synthesis system, energy

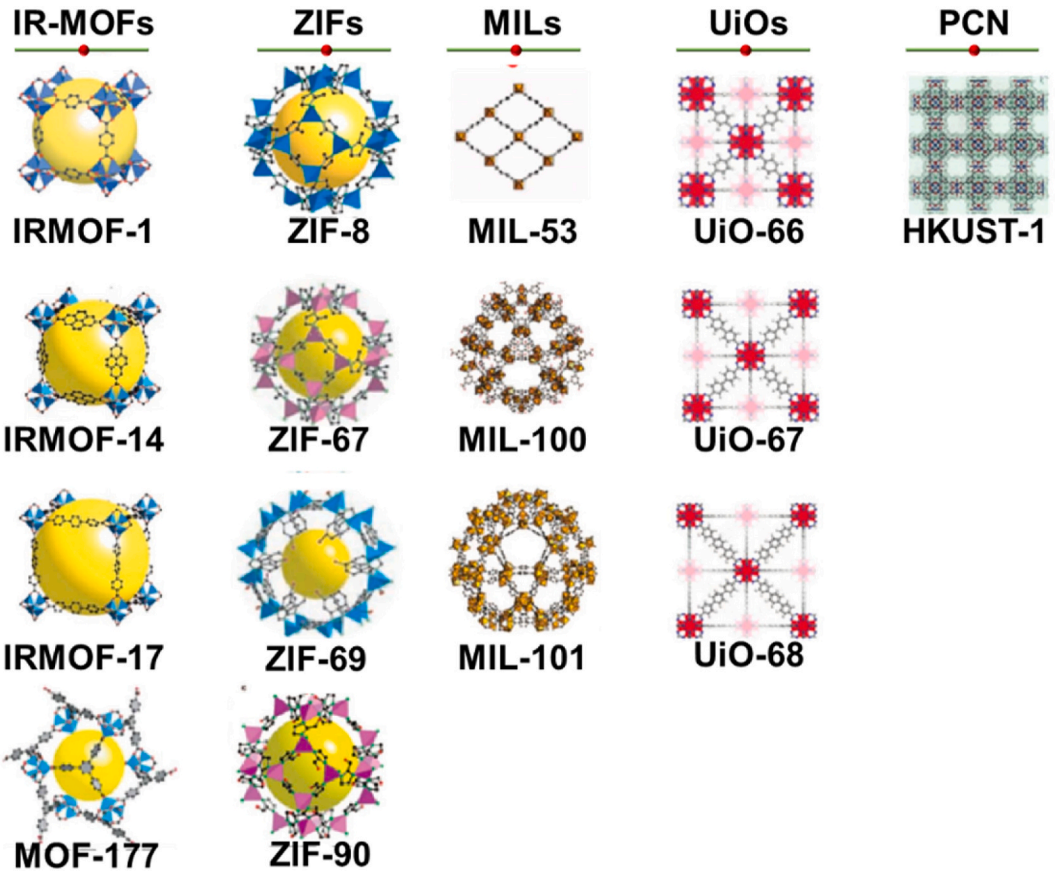

Fig. 5. A summary of typical MOF frameworks classified into five main categories: IRMOFs, HKUST-1, MILs, UiOs, and ZIFs. Images of MOF structures are reproduced with permission from Refs. [62–67].

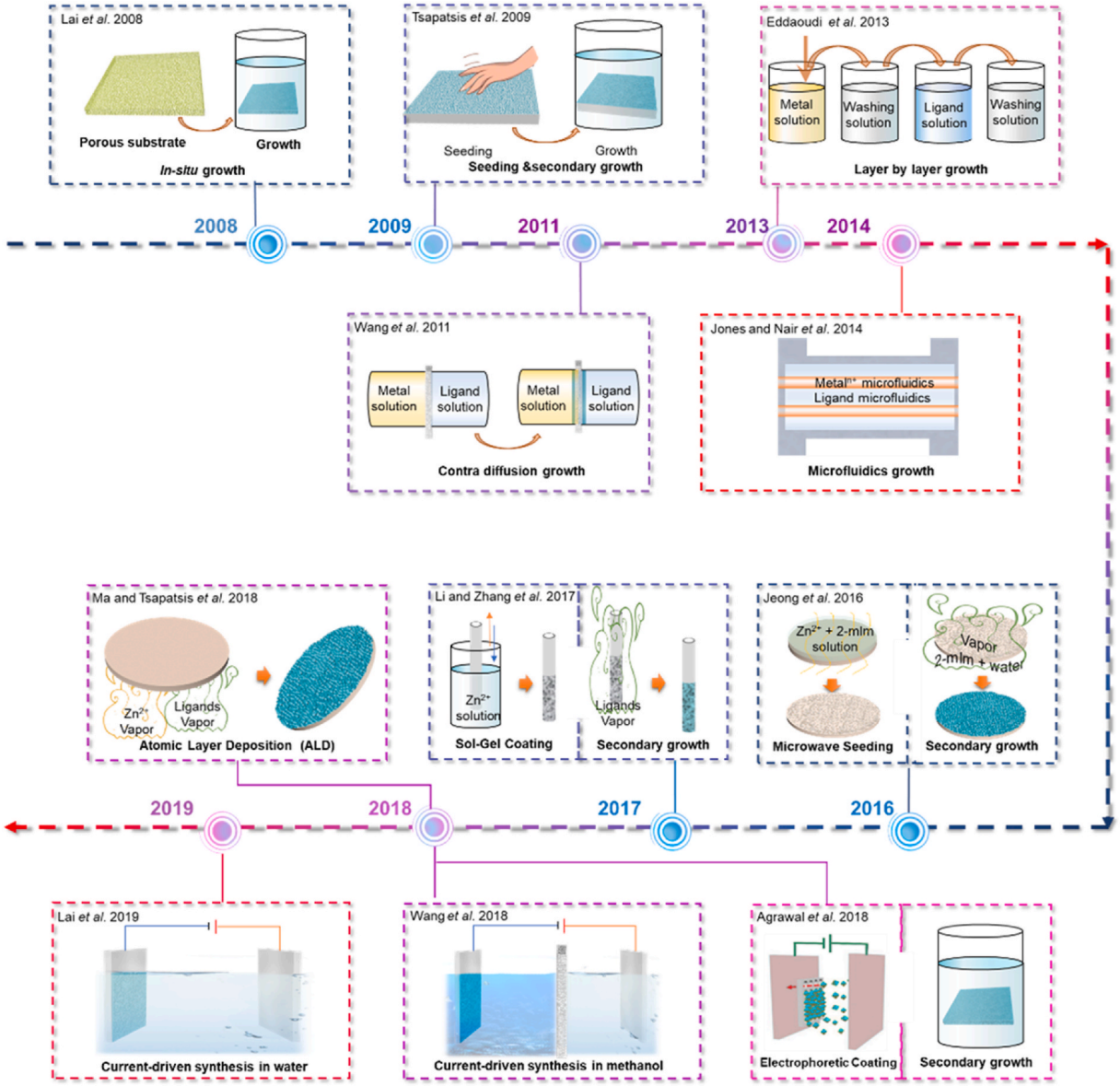

Fig. 6. Chronological development of MOF membranes for gas separation from 2008 – today. (2008) *In-situ* growth was firstly reported by Lai and Jeong et al. [68], followed by Zhu and Qiu et al. [69]. (2009) Seeding and secondary growth by reported by Tsapatsis et al. [70]. (2011) Contra-diffusion growth reported by Wang et al. [71], followed by interfacial microfluidic processing reported by Jones and Nair et al. [72] in 2014. (2013) Layer-by-layer growth reported by Eddaoudi et al. [73]. (2016) Microwave-assisted seeding and ligand/water vapor secondary growth reported by Jeong et al. [74]. (2017) Zn gel coating and ligand vapor phase transformation reported by Li and Zhang et al. [75]. (2018) All vapor-phase conversion of ZnO layer via ALD reported by Ma and Tsapatsis et al. [76], electrophoretic nuclei assembly and secondary growth reported by Agrawal et al. [77], followed by methanol-based current-driven synthesis reported by Wang et al. [78]. (2019) Aqueously cathodic deposition (ACD) reported by Lai et al. [79].

input such as heating, microwave, sonication, etc., are used to either assist in overcoming the reaction energy barrier or shorten the synthesis time [80–86]. In 2008, Lai et al. [68] successfully fabricated a continuous MOF-5 membrane on unmodified Al_2O_3 support using an *in-situ* growth approach as shown in Fig. 7a. The thickness of the MOF-5 membrane could be tuned by varying membrane synthesis time. Membrane obtained were tested using probe gases with different molecular sizes (e.g., H_2, N_2, CO_2, and SF_6). The resultant linear relationship between single component permeabilities and square root inverse of penetrant molecular weight in Fig. 7b indicated that gas transport through the membrane mainly follows the Knudsen type diffusion. Later in the same year, the first MOF membrane for gas separations was developed by Qiu et al. [69], who grew an HKUST-1 membrane on a copper net. They tested the membrane for H_2/N_2, H_2/CH_4, and H_2/CO_2 separations and found that the membrane had one-to two-fold higher permeance than zeolite membranes. Since then, a number of MOF membranes including ZIF-8 [87], ZIF-69 [88], UiO-66, and MOF-74 on various supports (e.g., alumina, titania, and polymer) [89,90] were reported.

It is worth noting that not all MOFs can be *in-situ* grown into high-quality films on porous substrates. UiO-66 is one such MOF. The reason is that these MOFs readily undergo homogenous nucleation, thereby preferentially nucleating and growing in the precursor solution rather than on the support. Another reason is that there are insufficient nucleation sites on unmodified substrates, disabling uniform MOF nucleation on the supports. As a result, the obtained membrane is discontinuous and exhibits extensive surface defects. One way to solve the problem is to modify the support with either organic molecules or associated metals (or metal compounds). Organic molecules have active functional groups (e.g., –COOH, –NH_2, –OH, etc.) that can coordinate

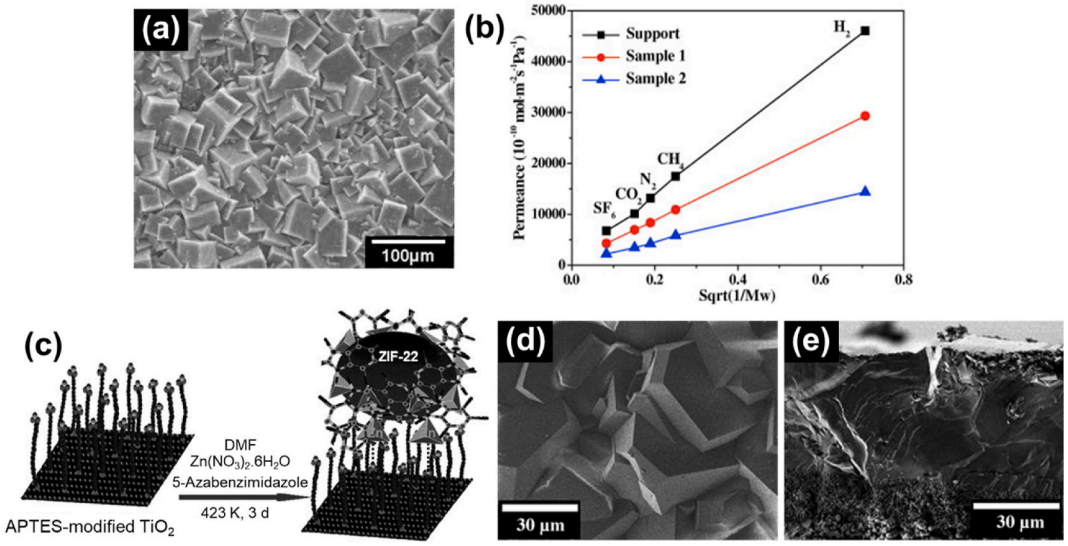

Fig. 7. (a) SEM image of MOF-5 membrane. (b) Single-component gas permeances through α-alumina support (black square), 25 μm thick MOF-5 membrane (red circle), and 85 μm thick MOF-5 membrane (blue triangle) measured at 1.06 bar. (c) Preparation of a ZIF-22 membrane using 3-aminopropyltriethoxysilane (APTES) as a covalent linker between the ZIF-22 membrane and the titania support. (d) Top and (e) cross-section view of the prepared ZIF-22 membrane. Reproduced with permission from Ref. [68] Copyright 2008 Elsevier B.V. and ref. [91] Copyright 2010 Wiley VCH. (For interpretation of the references to color in this figure legend, the reader is referred to the Web version of this article.)

with the metal ions in the precursor, triggering nucleation. On the other hand, metal or metal compounds can serve as a metal source to anchor the ligand by coordination, providing nucleation sites for membrane growth.

There have been several reports on support surface functionalization for MOF film fabrications. For example, a MOF-5 film successfully grown on a –COOH functionalized gold (Au) substrate [92,93]. Using a similar functionalization method, oriented $Cu_3(BTC)_2$ and $Zn_2(bdc)_2(dabco)$ films were successfully synthesized [94]. Caro et al. [91] were among the first to apply a similar concept to prepare a ZIF-22 membrane on alumina substrate modified with 3-aminopropyltriethoxysilane (APTES) modified alumina substrate (Fig. 7c – e). Following this research, various ZIF membranes, including ZIF-7, ZIF-8, ZIF-90, and ZIF-100 grown on porous supports modified with various functional molecules, were reported [95–97]. Among the functional molecules, dopamine (DPA) was the most popular choice. Jeong et al. [98] further extended this strategy and reported a ZIF-7 membrane grown on a benzimidazole (bIm) modified alumina support. This method could also be extended to ZIF-8 membranes using 2-methylimidazole (2-mIm) modified support, demonstrating the versatility of the ligand functionalization method to synthesize various ZIF membranes [98]. Another interesting report is the synthesis of HKUST-1 membrane using a poly(methyl methacrylate) (PMMA) coated substrate. A freestanding membrane could be obtained by dissolving the PMMA in chloroform, providing insight for free-standing membrane fabrications [99].

For the metal or metal compounds modification method, a typical example is an HKUST-1 film synthesized using copper mesh [69]. The copper mesh was firstly heat-treated to convert copper into copper oxide. Then, the treated mesh was immersed into precursor containing both copper ions and ligand. Both copper oxide and copper ions from the support and precursor solution, respectively, were believed to participate in crystal growth. Finally, an HKUST-1 membrane was formed on the mesh [69]. This method sometimes does not require a metal source present in the precursor solution. For example, $Ni_2(L\text{-}asp)_2(bipy)$ film in Fig. 8a was fabricated on a nickel mesh with the precursor containing only ligand [100]. This method was later used in ZIF membrane fabrications using substrates coated by zinc oxide or zinc hydroxide, as depicted in Fig. 8d [101,102].

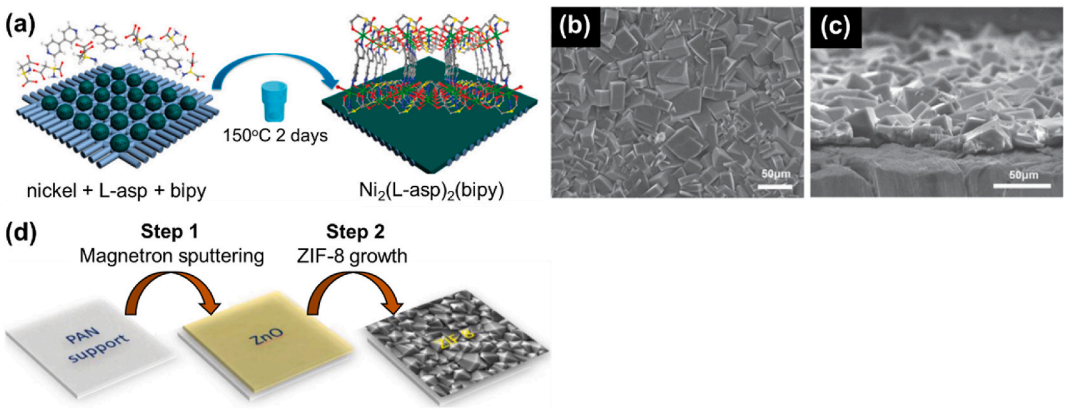

Fig. 8. (a) Schematic diagram of homochiral MOF membrane synthesis on nickel net by *in-situ* growth. (b) Top and (c) cross-section SEM images of the $Ni_2(l\text{-}asp)_2(bipy)$ membrane. (d) Schematic diagram demonstrating a ZIF-8 membrane deposition on polyacrylonitrile (PAN) substrates. Bare PAN was coated with a thin layer of ZnO via sputtering to enhance ZIF-8 nucleation density. Reproduced with permission from Ref. [100] Copyright 2013 The Royal Society of Chemistry and ref. [101] Copyright 2015 Elsevier B.V.

2.1.2. Secondary (seeded) growth

The *in-situ* growth approach sometimes suffers from either a slow rate of nucleation or non-uniform nucleation, causing defect formation throughout the membrane. To overcome this issue, a secondary (seeded) growth approach can be employed. In this approach, a layer of seed crystals is deposited on a substrate followed by secondary growth in a dilute precursor solution. The seed layer can trigger faster and more uniform heterogeneous nucleation, forming a membrane with relatively low defect density. Sometimes, a third or more growth are needed to heal membrane defects and improve grain boundary structures. The qualities of the seed layer, including crystal size, crystal orientation, seed layer thickness, and seed-support adhesion, play important roles in this approach. Thus, a plethora of seeding methods such as rub coating, dip coating, spin coating, titration coating, electrospinning, and thermal/microwave seeding was developed (Fig. 9).

Conventional seeding (e.g., rub coating, titration coating, dip coating, and spin coating) followed by secondary growth method was firstly employed by Tsapatsis et al. [70], who synthesized a continuous Cu (4,4′-(hexafluoroisopropylidene)-bis(benzoic acid)) membrane in 2009. Basically, they used the rub coating method through which the dry MOF particles were rubbed on an alumina substrate functionalized by polyethyleneimine (PEI). The seeded substrate was then subjected to secondary growth to form a continuous membrane. The titration coating, dip coating, and spin coating are similar in which a layer of colloidal seed rather than dry powder is applied onto the support. For example, an NH_2-MIL-53(Al) membrane was prepared by firstly coating a thin layer of NH_2-MIL-53(Al) seed colloidal solution onto a pre-treated glass frit via titration. The wet layer was dried overnight at room temperature, followed by a secondary growth at 150 °C for 3 days [103]. Spin coating and dip coating are more common for seeding. There are a number of reported membranes such as ZIF-7, ZIF-8, and HKUST-1 prepared using either spin or dip coating methods [104,105]. Another interesting coating method is electrospinning which was firstly used in ZIF-8 membrane fabrication. In the electrospinning setup shown in Fig. 10a, an automatic syringe was filled with a seed colloidal solution to coat the surface of macroporous SiO_2 support [106].

The seeding methods mentioned above were mostly conducted at room temperature, which could result in loosely bound seeds due to weak chemical bonds or purely physical attachment. To improve seed-substrate adhesion, a microwave-induced thermal deposition (MITD) method was introduced by Jeong et al. [83] in 2009 (Fig. 10b). In this method, the seed layer was *in-situ* grown on a graphite-coated α-alumina disc by microwave heating for 1.5–2 min. After a secondary growth, a continuous MOF-5 membrane was achieved. MITD method however requires a conductive substrate to ensure a strong interaction between substrate surface and microwave irradiation. A more generic method was developed in which the seed layer was deposited under thermal heating (Fig. 10c) [107]. The seed stability was found to be improved after heat treatment, and a continuous HKUST-1 film was obtained after secondary growth.

In general, both microwave and thermal heating improve the seed-substrate adhesion by forming stronger chemical bonds at elevated temperatures. To further increase this adhesion, the support can be functionalized by organic or metal/metal compounds similar to the *in-situ* method mentioned in Section 2.1.1.

2.1.3. Contra-diffusion

For *in-situ* and secondary growth approaches, reactant concentration in the precursor reduces at the later stage of the synthesis. Consequently, defects could be formed on the membrane due to a lack of reactants near the support. To solve this problem, Wang et al. [71] first developed a contra-diffusion approach for ZIF-8 membrane fabrication (Fig. 11a). In this method, metal and ligand solution were placed inside two parallel compartments separated by porous nylon support, allowing the crystallization to take place on the support in a counter diffusion manner. As a result, the reactants near the support could be replenished by the bulk solution, improving the crystal growth rate on the support.

Later, a modified version named interfacial microfluidic membrane processing (IMMP) was developed by Nair et al. [72] in 2014, who used polymer hollow fibers as supports (Fig. 11b). In this approach, metal and ligand source were dissolved in water and 1-octanol, respectively. The aqueous metal source was introduced from the outer shell of the support, while the ligand solution was supplied from the bore of the support via a continuous pumping process. Since water and 1-octanol are immiscible, a membrane was formed at the interface of the two solutions. IMMP allows for positional control of membrane formation (inner or outer shell) via controlling the sequence of the precursor supply and the solution cycling place (inner or outer shell) [72,108–111]. Compared to static growth, dynamic growth via solution cycling improved product yield and crystallization rate [72,108]. This phenomenon was further

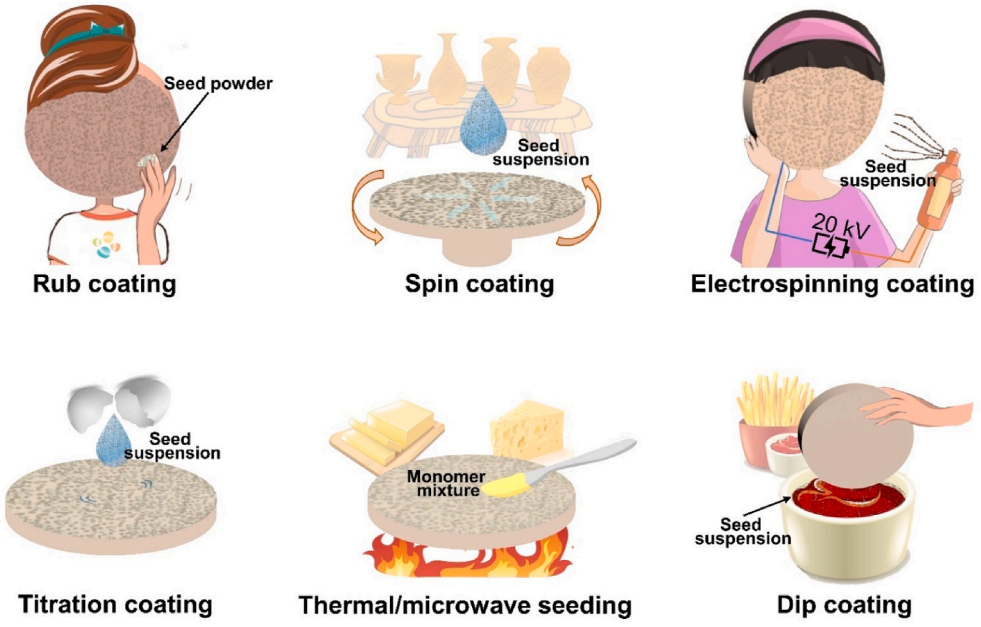

Fig. 9. A symbolic summary of various seeding methods before membrane growth.

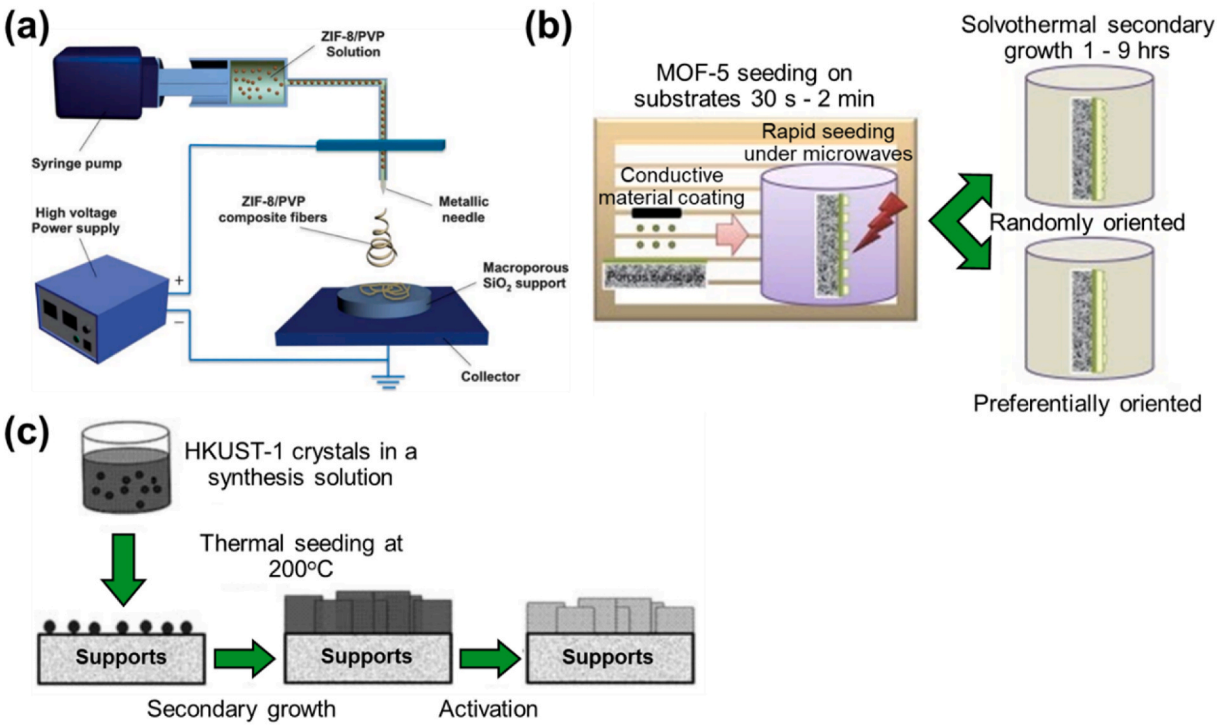

Fig. 10. Schematic illustration of (a) electrospinning coating process, (b) microwave-assisted seeding and secondary growth, and (c) thermal heating assisted seeding and secondary by Jeong's group [83,107]. Images were modified based on ref. [106] Copyright 2012 The Royal Society of Chemistry, ref. [83] Copyright 2009 Elsevier B.V, and ref. [107] Copyright 2010 The Royal Society of Chemistry.

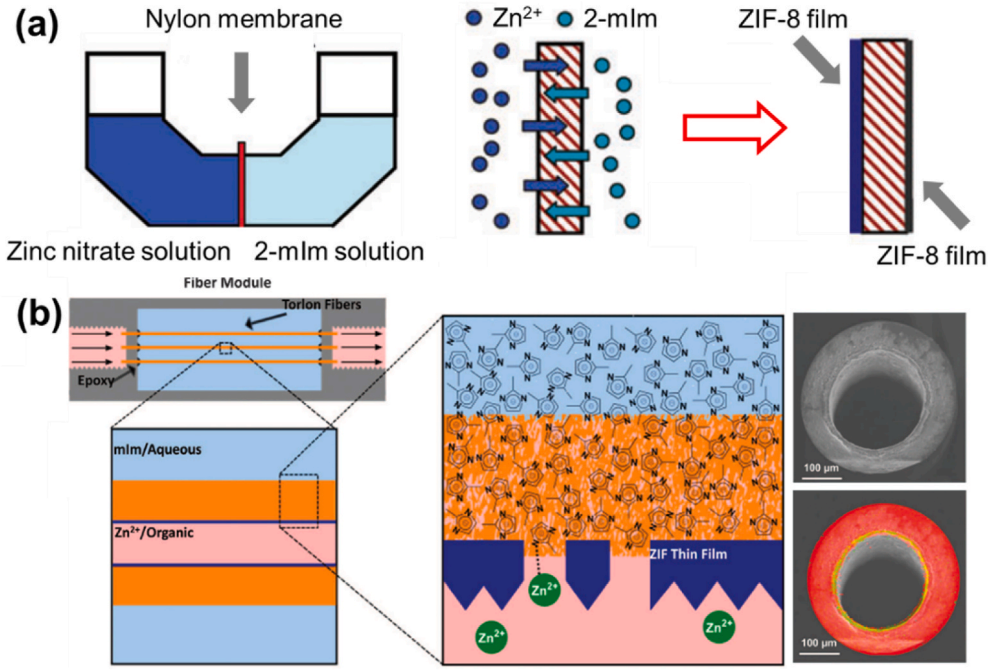

Fig. 11. Schematic illustration of (a) contra-diffusion approach and (b) interfacial microfluidic membrane processing (IMMP) approach to prepare ZIF-8 membranes on porous substrates. Reproduced with permission from Ref. [71] Copyright 2011 The Royal Society of Chemistry and ref. [72] Copyright 2014 American Association for the Advancement of Science.

proved by *in-situ* TEM observation on ZIF-8 crystals [112]. Combining all the advantages of contra-diffusion, this approach could be considered as a versatile approach for the continuous production of MOF membranes.

2.1.4. *Layer-by-layer deposition*

The layer-by-layer (LbL) deposition was first reported by Wöll et al., in 2007 to form surface-mounted MOFs (SURMOFs) [113]. An HKUST-1 film was successfully obtained by adopting this approach. In this approach, the support is immersed into the metal and ligand solutions in

a sequence to allow for the stepwise MOF growth. An organic layer normally functionalizes the support with reactive functional groups (e.g., –COOH, –OH, and $–NH_3$) that can coordinate with the metal ions. Thus, the support is firstly immersed in the metal solution to form a layer of coordination site followed by immersion in the ligand solution. Between each immersion, the support is washed with a solvent to remove unreacted liquor. The thickness of the obtained MOF films can be tuned by controlling immersion time and number of LbL cycles. Interestingly, oriented SURMOFs can be formed using this method probably due to the so-called 'controlled reaction' through which the thermodynamic equilibrium is favored towards a certain crystal direction. This approach has been used to synthesize a number of MOF films [103]. In 2013, Eddaoudi et al. [73] extended this approach to fabricate MOF membranes (Fig. 12) [73]. A (110) oriented ZIF-8 membrane with thickness as thin as ~0.5 μm was obtained and tested for gas separations, showing a relatively good sieving effect for the separation of H_2 from larger molecules such as CO_2, N_2, CH_4, and C_3H_8.

2.1.5. Vapor phase synthesis

All the conventional methods discussed above were solution-based, which could be a hurdle for scale-up production due to environmental and cost concerns. A lot of reported syntheses used hazardous organic solvents such as methanol or dimethylformamide (DMF), which could potentially impose some risks to the environment. Furthermore, during membrane synthesis, only a small portion of reactants is involved in membrane formation, leaving many residuals to be either recycled or disposed. Consequently, a high cost could be incurred for the post-synthesis treatment and waste management. To overcome these disadvantages, the idea of vapor-phase synthesis was proposed in 2016. Stassen et al. [114] were the first to demonstrate the deposition of ZIF thin film on a silicon wafer via chemical vapor deposition (CVD). In this work, ZnO was firstly deposited on the support via atomic layer deposition (ALD), followed by a ligand vapor phase secondary growth. The idea of vapor phase growth was later adopted by Jeong et al. [74] for ZIF-8 membrane fabrications (Fig. 13a – c). A layer of seeds previously deposited onto alumina support under microwave treatment was exposed to a vapor environment composed of a mixture of water and ligand, transforming the seed layer into membranes. Later, Li et al. [75] established a sol-gel vapor deposition method to deposit ZIF-8 membrane on the shell side of ethylenediamine-modified PVDF hollow fiber in Fig. 13d. In this method, a layer of zinc gel, $Zn(CH_3COO)_2$, was coated onto the hollow fiber followed by 2-methylimidazole vapor treatment at 150 °C.

In 2018, Ma and Tsapatsis et al. [76] developed an all-vapor-phase approach using the atomic layer deposition (ALD) technique as depicted in Fig. 13e. Three steps were involved in this approach, as explained in the following. Firstly, a macroporous α-alumina substrate was coated by a layer of mesoporous γ-alumina with a thickness ~5 μm. Secondly, the coated substrate was subjected to a diethylzinc vapor in which the metal source reacted with the hydroxyl groups of the γ-alumina to form hydroxylated ZnO in the presence of water vapor. The ZnO deposits could fully fill the mesopores of γ-alumina by 10 ALD cycles, resulting in a gas impermeable ZnO-γ-alumina layer. Finally, the ZnO-γ-alumina was treated by ligand vapor using ALD, from which the ZnO deposit was transformed to a ZIF-8 membrane. This all-vapor ALD-based method eliminates use of solvent and can be a general approach for other MOF membrane fabrications.

2.1.6. Electrochemical synthesis

Another novel development in recent years is the electrochemical synthesis approach. In the past decade, this approach has been used for MOF particulate or MOF film synthesis [115,116]. A number of MOF films such as MOF-5, HKUST-1, UiO-66, and ZIFs were reported. The key advantage of electrochemical-based synthesis is the 'defect self-healing' mechanism during membrane formation. A conductive electrode will be covered by a non-conductive MOF layer during the synthesis, leaving the uncovered surface to be continually deposited by MOF crystals. Membrane growth will continue until the entire electrode surface becomes non-conductive due to the full coverage by the MOF membrane. The defects could be gradually healed by the electric current in this process, forming a continuous membrane with relatively low defect density.

In 2018, Agrawal et al. [77] developed an electrophoretic nuclei assembly approach referred to ENACT to grow ZIF-7 and ZIF-8 membranes. They used electric current to deposit a layer of negatively charged seeds on anodized aluminum oxide (AAO) support, followed by a secondary growth for 10 h. Later on, Wang's group [78] established a "fast current-driven synthesis" (FCDS) to fabricate ZIF-8 membranes on AAO discs. In this method, the anode and cathode were separated into two compartments containing the same precursor solution prepared by dissolving zinc acetate and 2-mIm in methanol. A macroporous membrane separated the two compartments, with one located at the anode and the other situated at the cathode. A continuous membrane was obtained at the cathode under a current density of 0.7 mA cm^{-2}. In 2019, Lai et al. [79] established an aqueous cathodic deposition (ACD) approach. The authors used a simple apparatus set-up with only a beaker and a power source, as shown in Fig. 14. A ZIF-8 membrane was successfully fabricated in a precursor using water as a solvent. The authors identified an optimal current density that ensures both rapid membrane growth and low water hydrolysis. A continuous ZIF-8 membrane with thickness of 500 nm was formed at cathode in 1 h under a current density of 0.13 mA cm^{-2}.

2.2. Development of polycrystalline ZIF-8 membranes for gas separations

2.2.1. ZIF-8 membrane fabrications

Chen et al. [117] firstly reported ZIFs followed by Yaghi et al. [64] in 2006. Among many ZIFs, ZIF-8 with sodalite (SOD) topology is most extensively investigated for gas separations. ZIF-8 framework is built by periodic coordination of zinc ions and 2-methyimidazoles (2-mIm). The framework has a crystallographically defined six-membered ring aperture of ~3.4 Å (blue dashed line in Fig. 15a). This makes ZIF-8 a potential candidate for carbon capture applications such as CO_2/N_2 and

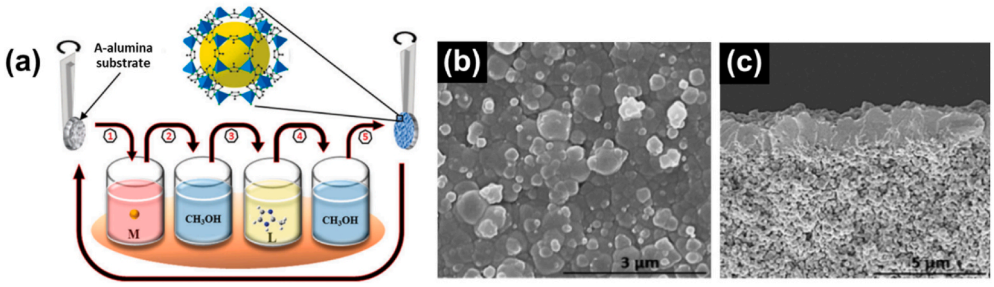

Fig. 12. (a) Schematic representation of the liquid phase epitaxy (LPE) approach for the synthesis of ZIF-8 membrane. (b) Top and (c) cross-section view of SEM images of the prepared ZIF-8 membranes. Reproduced with permission from Ref. [73] The Royal Society of Chemistry.

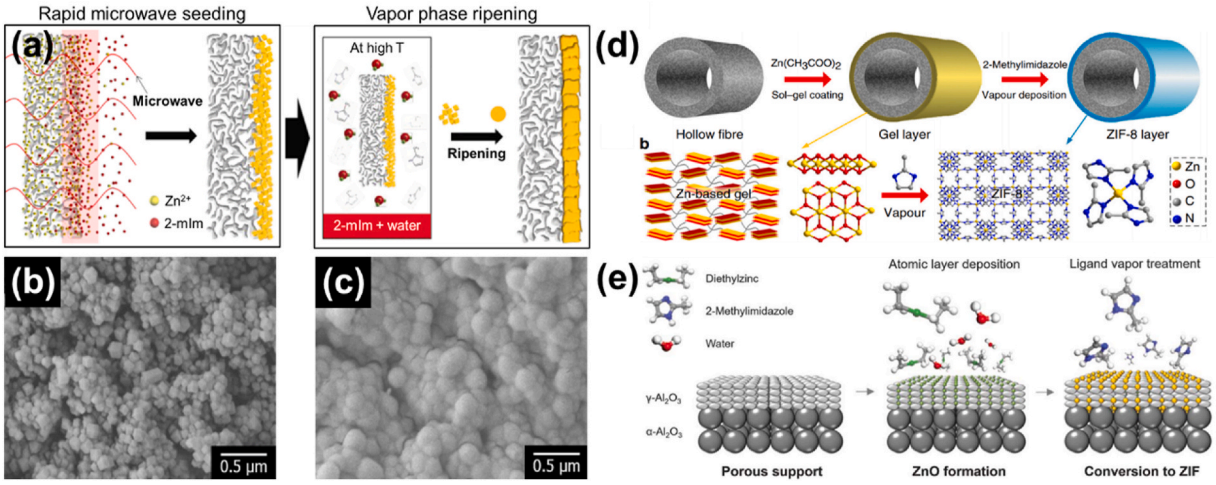

Fig. 13. (a) A schematic illustration of the defect-induced ripening process. SEM images of supported ZIF-8 seed crystal layers (b) before and (c) after exposure to a vapor environment composed of 2-methylimidazolate and water at 145 °C for 9 h. (d) A schematic illustration of sol-gel vapor deposition method transforming Zn gel layer on shell side PVDF hollow fiber into ZIF-8 (e) A schematic illustration of all-vapor-phase synthesis. ZnO layer deposited using ALD was transformed into ZIF-8 under a ligand vapor environment. Reproduced with permission from Ref. [74] Copyright 2016 The Royal Society of Chemistry, ref. [75] Copyright 2017 Springer Nature, and ref. [76] Copyright 2018 The American Association for the Advancement of Science.

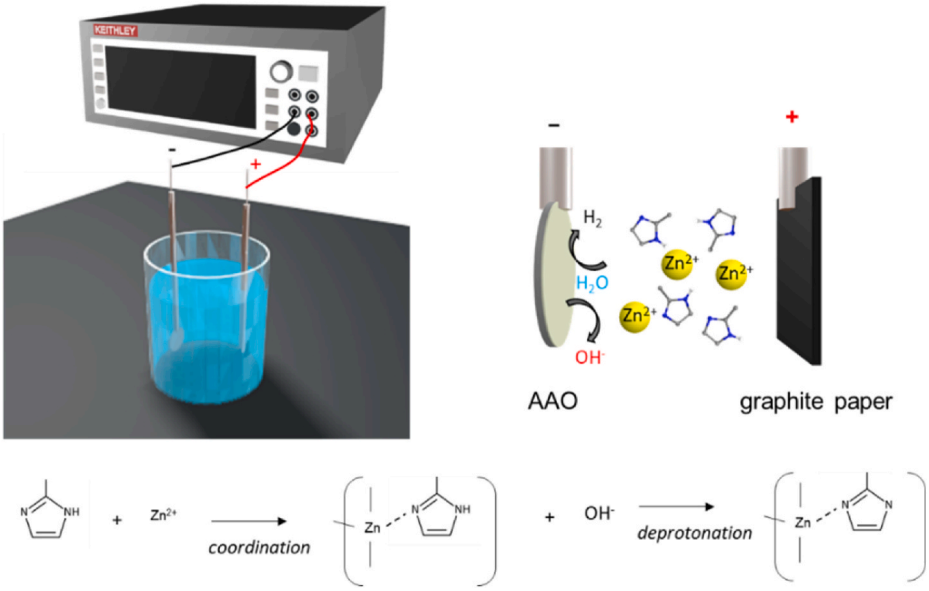

Fig. 14. Schematic illustration of aqueous cathodic deposition (ACD) method for ZIF-8 membrane fabrication on AAO disc. Reproduced with permission from Ref. [79] Copyright 2019 Wiley VCH.

CO_2/CH_4 separations as the aperture size perfectly sits between molecule size of CO_2 and N_2. However, it was found that ZIF-8 does not exhibit a satisfactory sieving property towards these molecules [118, 119]. An adsorption study conducted by Li and co-workers [120] showed that ZIF-8 is a suitable material for kinetic separation of C_3H_6 from C_3H_8 with an ideal diffusion selectivity of ~125 [120]. Later, Zhang et al. [121] found that besides C_3H_6 (kinetic diameter: 4.03 Å) and C_3H_8 (kinetic diameter: 4.16 Å), even larger molecules (e.g., n-C_4H_8, i-C_4H_8, n-C_4H_{10}, and i-C_4H_{10}) can diffuse through ZIF-8. These findings suggest that the aperture of ZIF-8 is not rigid and therefore can accommodate larger molecules during gas adsorption. This phenomenon was further studied by a computational simulation [119], showing that the swing motion of 2-mIm linkers in ZIF-8 widen the six-membered ring aperture size to ~4.0 Å which is exactly sitting between the sizes of C_3H_6 and C_3H_8.

Caro et al. [87] synthesized the first ZIF-8 membrane in 2009. They demonstrated ZIF-8 membrane could be a good candidate for hydrogen purification. In 2012, Lai et al. [122] first proved that ZIF-8 membranes were promising for C_3H_6/C_3H_8 separation with a selectivity of 45 and C_3H_6 permeance of 61 GPU. The separation performance was shown to have surpassed both polymer and carbon molecule sieve (CMS) membranes (Fig. 16a – b). Since then, the majority of the research efforts on ZIF-8 membrane have gravitated towards C_3H_6/C_3H_8 separations. Advancement in ZIF-8 membrane synthesis continues with the development of a green synthesis protocol. Lai et al. [123] first reported ZIF-8 synthesis in an aqueous solution at room temperature and later applied a similar concept for the fabrication of ZIF-8 membranes on the shell side of ceramic hollow fibers (Fig. 16c – d). Since then, many reports have adopted similar synthesis protocols, opening up more opportunities for ZIF-8 membranes for other separations.

ZIF-8 membrane synthesis in the early studies before 2015 generally used conventional methods, including *in-situ*, seeding and secondary

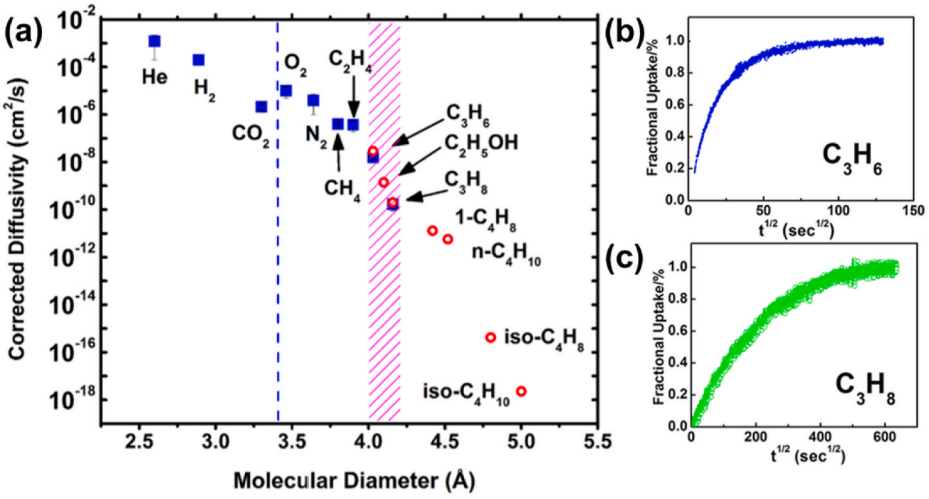

Fig. 15. (a) Corrected diffusivities in ZIF-8 at 35 °C versus molecular diameter of probe molecules (b) Kinetic uptake curves in ZIF-8 at 35 °C of (a) C_3H_6 and (b) C_3H_8 in the 162 μm ZIF-8 crystal. Reproduced with permission from Ref. [121] Copyright 2012 American Chemical Society.

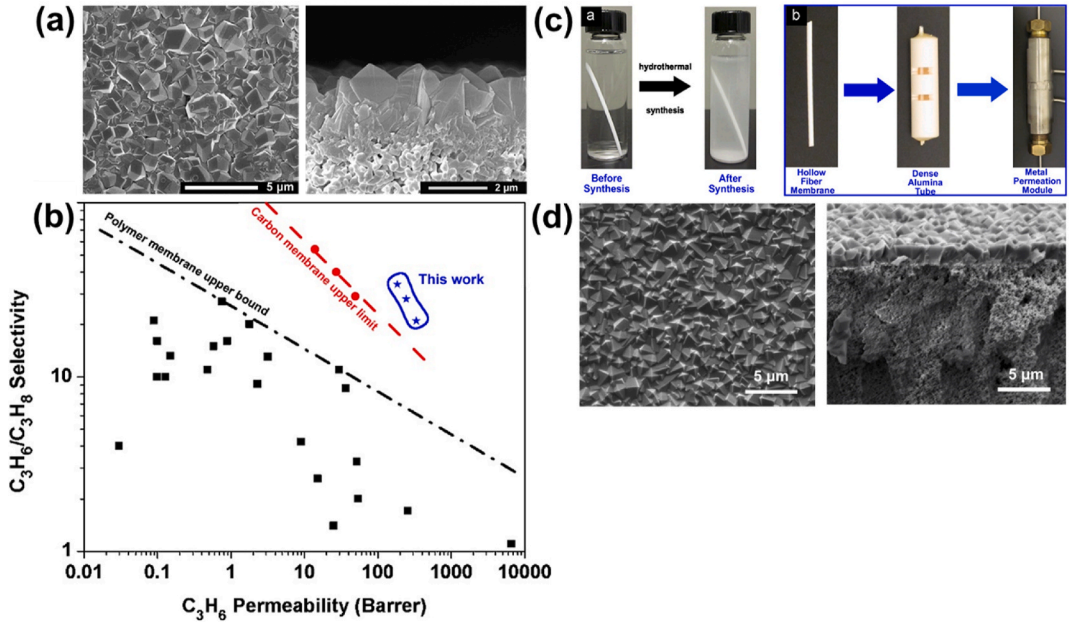

Fig. 16. (a) Top and cross-section SEM images of the ZIF-8 membranes prepared by Lai and co-workers [122]. (b) C_3H_6/C_3H_8 separation performances of the membranes in comparison with CMS and polymer membranes. (c) Schematic illustration of the synthesis of ZIF-8 membranes on yttria-stabilized zirconia (YSZ) hollow fibers by Pan et al. [124] (d) Top and cross-section SEM images of the membranes. Reproduced with permission from Ref. [122] Copyright 2011 and ref. [124] Copyright 2012 Elsevier B.V.

growth, and contra-diffusion. Caro et al. [87] were the first to adopt the *in-situ* method to fabricate ZIF-8 membranes. They used titania as the support with the synthesis assisted by microwave. Sodium formate was added into the precursor to facilitate the deprotonation of 2-mIm linkers [87,125]. The resultant membrane had a thickness of ~30 μm and exhibited a selectivity of ~11 for H_2/CH_4 gas pair. *In-situ* growth of ZIF-8 membrane was also reported on Si_3N_4 hollow fiber and the resultant membrane had an H_2/CO_2 selectivity of ~12 [126]. Various ZIF-8 membranes for gas separations synthesized on modified supports using covalent linkers such as 3-aminopropyltriethoxysilane (APTES) [127,128], 3-(2-imidazolin-1-yl)propyltriethoxysilane (IPTES) [129], polydopamine [95], and ZnO have been reported.

Secondarily grown ZIF-8 membranes on α-alumina supports by Lai et al. [122] had a thickness of ~2.2 μm and displayed much higher C_3H_6 permeance than its polymer and CMS counterparts as illustrated in Fig. 16a – b. Later, a (100) oriented ZIF-8 membrane on PEI-modified alumina support was successfully fabricated using this approach [130]. The membrane showed a sharp molecular sieving for H_2/C_3H_8 gas pair with a selectivity of ~300. Seeding and secondary growth method were also applied to hollow fiber supports [124,131–134]. For example, a 2 μm thick ZIF-8 membrane was grown on the shell side of yttria-stabilized zirconia (YSZ) hollow fiber (Fig. 16c – d) and achieved high H_2 permeance of 5077 GPU and H_2/C_3H_8 ideal selectivity of 500 [124]. In general, research works mentioned above mainly used standard coating methods (e.g., dip coating). In contrast, a 'direct seed synthesis' method was reported by Jin et al. [110], who introduced the seed precursor onto the bore of the hollow fiber and allowed the seeds to grow on the support surface directly.

Contra-diffusion and its variance, interfacial microfluidic processing previously discussed in Section 2.1.3 were firstly developed for ZIF-8

membrane fabrications. Both of the resultant membranes were tested for H_2/N_2 and C_3H_6/C_3H_8 separations, with the latter showed C_3H_6/C_3H_8 selectivity of ~12 [72]. Membrane selectivity and permeance can be improved to ~70 and ~80 GPU, respectively, by tuning synthesis parameters such as nature of the metal salts and modulator (e.g., sodium formate) to ligand ratio [135]. Later, a number of ZIF-8 membranes fabricated using this approach were reported [136–139].

Membrane separation performances could be improved via sol-gel vapor deposition method from which a ZIF-8 membrane with a thickness of ~87 nm was achieved [75] and exhibited exceptional C_3H_6 permeance of 836 GPU while maintaining a satisfactory C_3H_6/C_3H_8 selectivity of 67. The membrane thickness could be further downsized to ~17 nm, making it the thinnest membrane reported so far. The ultra-thin membrane was tested by single gas permeation and exhibited C_3H_6 permeance of ~2500 GPU with a selectivity of ~45. The all-vapor-phase approach using atomic layer deposition (ALD) technique resulted in a ZIF-8 membrane with an excellent C_3H_6/C_3H_8 selectivity (~100) with high C_3H_6 permeance (>300 GPU) [76]. The membrane can sustain this separation performance up to 7 bars, making it to be extremely attractive for industrial scale-up.

For electrochemical synthesis, ZIF-8 membrane obtained from electrophoretic nuclei assembly approach by Agrawal et al. [77] exhibited high C_3H_6 permeance of 298 GPU with a C_3H_6/C_3H_8 selectivity of ~32. The selectivity could be improved via "fast current-driven synthesis" (FCDS), from which the obtained ZIF-8 membrane exhibited extremely high C_3H_6/C_3H_8 selectivity of ~305 (highest reported to date) while maintaining good C_3H_6 permeance of ~52 GPU [78]. The extremely high selectivity is attributed to distortion of ZIF-8 lattices by an electric field which partially transformed ZIF-8 into a new polymorph (i.e., monoclinic Cm space group) with stiffer networks (Fig. 17a). This lattice distortion decreased the pore aperture of ZIF-8 from 3.4 to 3.6 Å to 3.1 Å, resulting in an improved sieving effect. This observation was supported by an online C_3H_6/C_3H_8 gas testing of a ZIF-8 membrane via switching on and off the electric field at 500 V m^{-1} in Fig. 17b [140]. The FCDS approach was later used to deposit a ZIF-8 membrane on polypropylene support [141]. The resultant ZIF-8 membrane exhibited a C_3H_6/C_3H_8 selectivity of ~122 with a permeance of ~16 GPU. A bending test was performed to assess mechanical strength of the ZIF-8 membrane with an initial C_3H_6/C_3H_8 selectivity of ~110 and C_3H_6 permeance of ~4 GPU (Fig. 18a). The membrane separation performance was well maintained after bending with a curvature of <92 m^{-1}, suggesting high flexibility and mechanical strength. This study provides an insight to fabricate flexible ZIF-8 membranes for C_3H_6/C_3H_8 separation. Further research however is encouraged to improve C_3H_6 permeance to make the membrane performance more competitive.

ZIF-8 membrane with stiff frameworks synthesized using the FCDS approach could increase selectivity but come at the expense of permeance. Meanwhile, the aqueous cathodic deposition (ACD) approach by Lai et al. [79] significantly improved the permeance of C_3H_6 to 182 GPU while maintaining a high C_3H_6/C_3H_8 selectivity of 142 (Fig. 18b – c). One important thing to highlight here is that the ACD approach adopts water as the solvent and the synthesis is carried out at room temperature in an open environment, enabling an environmentally friendly synthesis protocol. Combined with a simple synthesis setup, ACD could be a potential candidate for scale-up production of MOF membranes.

2.2.2. *Pushing separation limit of ZIF membranes for C_3H_6/C_3H_8 separation*

There have been constant efforts to further improve ZIF-8 membrane performances for C_3H_6/C_3H_8 separation. It is worth mentioning that, like any other gas separation membranes, ZIF-8 membranes also suffer from a trade-off between selectivity and permeance. For selectivity improvement, defect elimination is the first priority. This can be done via support functionalization, delicate synthesis approach, secondary or even tertiary growth, and post-synthetic treatment. The synthesis approaches discussed in the previous sections have demonstrated the importance of the synthesis process to minimize defects. For the post-synthetic treatment, one strategy to consider is to apply a thin layer of polymer to seal membrane defects [142]. It has been proved that polydimethylsiloxane (PDMS) coating could improve the C_3H_6/C_3H_8 selectivity by up to ~20 times for ZIF-8 membranes [142].

Another strategy for selectivity improvement is to increase framework rigidity (i.e., suppressing the linker swing motion). It has been discussed in the previous section that this can be achieved by applying an electric field. Another way is to use mixed metal or mixed ligand approach. ZIF-8 and ZIF-67 are iso-structures with the same SOD topology but with different metal centers (i.e., Co ions for ZIF-67 and Zn ions for ZIF-8). ZIF-67 has a more rigid framework and slightly smaller aperture size than ZIF-8, which could improve membrane selectivity. Jeong et al. [143] employed this strategy to fabricate a composite ZIF-8/ZIF-67 membrane (Fig. 19a – c). They used a heteroepitaxial growth approach from which a layer of ZIF-8 seed was firstly deposited on the substrate, followed by a secondary growth in the ZIF-67 precursor. The resultant membrane underwent a tertiary growth in the ZIF-8 precursor to improve membrane grain boundaries. The formed ~1 μm thick ZIF-8/ZIF-67 membrane exhibited an exceptional C_3H_6/C_3H_8 separation performance with a selectivity of ~200 and C_3H_6 permeance of ~110 GPU.

This strategy is further explored by Caro and Wang et al. [144], who mapped the relationship between Co/Zn ratio and C_3H_6/C_3H_8 separation performances. They used the FCDS method to synthesize a series of bimetallic ZIF-8 membranes with different Co/Zn ratios and compared the resulting C_3H_6/C_3H_8 separation performances. They demonstrated

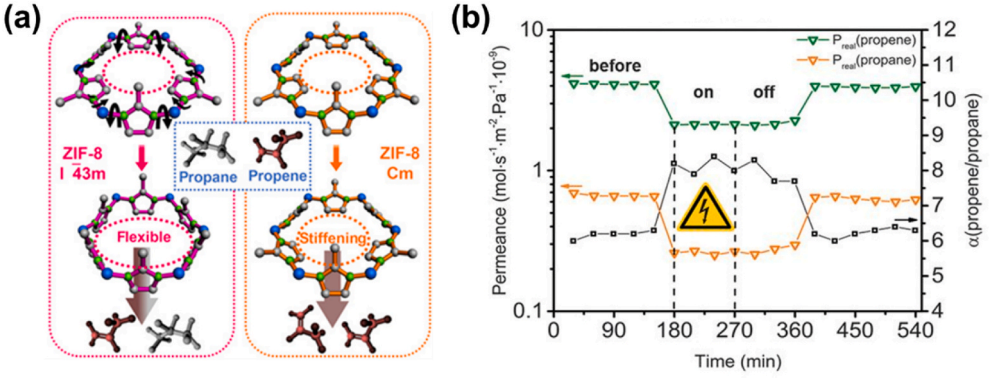

Fig. 17. (a) Schematic illustration of ZIF-8 structural transformation from cubic I-43 to monoclinic Cm polymorph. (b) C_3H_6/C_3H_8 separation performance induced by switching on and off the electric field. Reproduced with permission from Ref. [78] Copyright 2018 and ref. [140] Copyright 2017 American Association for the Advancement of Science.

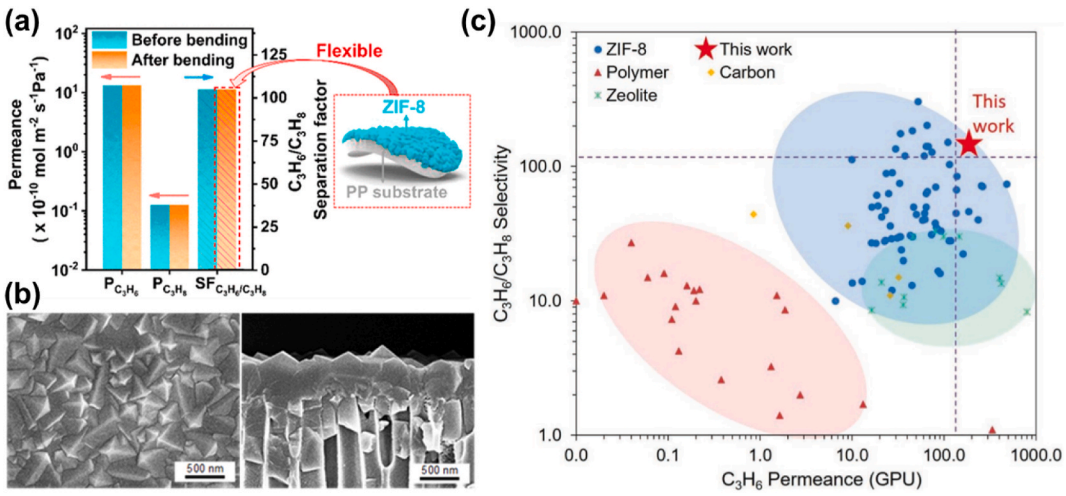

Fig. 18. (a) C_3H_6/C_3H_8 separation performance of polypropylene supported ZIF-8 obtained from fast current-driven synthesis (FCDS) before and after bending test. (b) Top and cross-section SEM images and (c) C_3H_6/C_3H_8 separation performance of ZIF-8 membrane obtained from aqueous cathodic deposition (ACD) approach. Reproduced with permission from Ref. [141] Copyright 2020 American Chemical Society, and ref. [79] Copyright 2019 Wiley VCH.

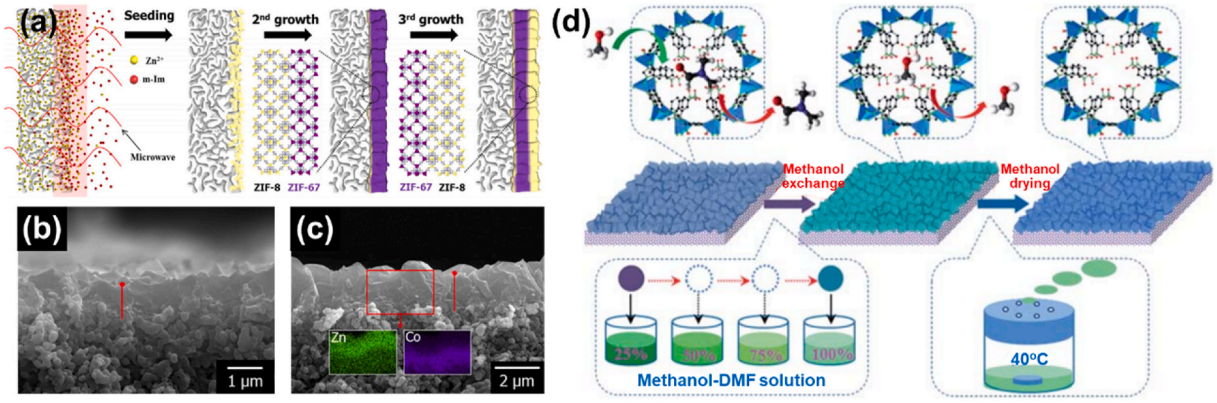

Fig. 19. (a) A schematic illustration of heteroepitaxial growth approach for ZIF-8/ZIF-67 membrane formation. (b) Cross-section SEM images and (c) energy-dispersive X-ray elemental mapping of the membranes. (d) Schematic illustration of ZIF-78 membrane activation thorough slow drying approach. Reproduced with permission from Ref. [143] Copyright American Chemical Society and ref. [145] Copyright 2012 The Royal Society of Chemistry.

that with the optimum Co/Zn ratio of 82/18, the hybrid membrane could give a selectivity of 200 with a permeance of 42 GPU. The high performance was believed to originate from the (100) oriented growth, which increases the framework rigidity and reduces the grain boundary defects.

Three strategies have been applied for permeance improvement: a) thorough membrane activation, b) membrane thickness reduction, and c) post-synthetic modification via linker exchange. The ZIF-8 membrane obtained from solution-based synthesis usually requires activation to remove the residual water and reactants within the pore. Otherwise, the impurities could block the pore and significantly reduce the gas permeance. Our unpublished data suggest that the gas permeance could be improved by 4–5 times after a careful membrane activation. The activation is usually conducted by immersing the membrane in a methanol solution for a few days following by a drying process via heating, vacuum, or ambient condition evaporation. During drying, there is a large concentration gradient of methanol between the pore and the surroundings. Rapid diffusion of methanol could damage MOF structures, creating defects. To avoid this, Jin et al. [145] developed a method in which the membrane was slowly dried under a methanol vapor environment (Fig. 19d). This method better preserved the quality of the membrane, and hence its gas separation performance. The approach was proven to be effective in improving gas separation performance of ZIF-8 membranes [146]. The recently developed all vapor phase ZIF-8 membrane synthesis can literally avoid the activation process. The membrane showed a significant improvement in C_3H_6 permeance while maintaining good C_3H_6/C_3H_8 selectivity when compared to ZIF-8 membranes prepared using the conventional solution-based approach [76,146].

Improving permeance through thickness reduction is the most straightforward way used in many published works. It has been found that seeding and secondary growth could reduce the membrane thickness from ~30 μm [87] to ~2 μm [122]. Recently published works have demonstrated that synthesizing an even thinner ZIF membrane (thickness <1 μm) using a secondary growth approach is possible. For example, Lee et al. [147] fabricated 800 nm thick ZIF-8 membrane on the lumen side of Matrimid® 5218 hollow fiber using microwave seeding followed by secondary growth. Vapor phase synthesis and current-driven synthesis can produce even thinner ZIF membranes (thickness <500 nm). These ultrathin membranes exhibited high C_3H_6 permeance (>100 GPU) while maintaining a good selectivity (>30) [79,144]. Recently, Zhong et al. [148] fabricated an ultrathin ZIF-8 membrane (45–150 nm) via interface layer polarization induction as illustrated in Fig. 20a – c. The membrane was deposited onto a PDMS modified polysulfone (PSF) (named ZIF-8-PDMS-PSF hereafter) and exhibited an ultrahigh C_3H_6 permeance of 2000–3000 GPU and a selectivity of 90–120.

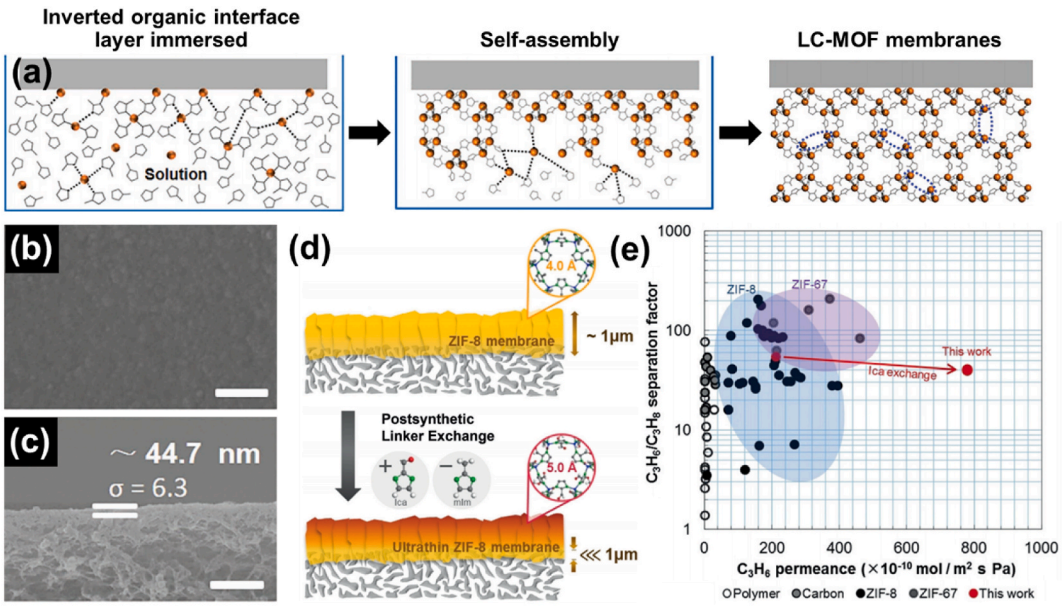

Fig. 20. (a) Schematic illustration of the interface layer polarization induction method. Electron micrographs of ZIF-8-PDMS-PSF: (b) top and (c) cross-section view. (d) Schematic illustration of post-synthetic linker exchange strategy to tune the effective thickness of ZIF-8 membranes. (e) C_3H_6/C_3H_8 separation performances of ZIF-8 membranes after Ica linker exchange. Reproduced with permission from Ref. [149] and ref. [148], Copyright 2018 and Copyright 2020, respectively, Wiley VCH.

A post-synthetic strategy was brought onto the table to further push the gas permeance beyond activation and synthesis. Jeong et al. [149] developed a post-synthetic linker-exchange (PSLE) method to enlarge the pore size of the ZIF-8 membrane after synthesis shown in Fig. 20d – e. In this method, as-synthesized ZIF-8 membrane was immersed in a methanolic solution of 2-imidazolecarboxaldehyde (Ica) to allow for linker exchange followed by treatment with dodecylamine. After the treatment, the membrane surface has linkers being exchanged by Ica and become more hydrophobic due to condensation reaction between Ica and dodecylamine. The membrane was then tested for C_3H_6/C_3H_8 separation and showed a 4-fold higher C_3H_6 permeance (~233 GPU) than those without linker exchange without a significant decrease of membrane selectivity (40).

In general, most of the ZIF-8 membranes have better C_3H_6/C_3H_8 separation performance compared to polymeric membranes. It is worth mentioning here that performances of polymeric membranes are often reported in permeability (Barrer) while MOF membranes are in permeance (GPU). To give a direct comparison, Smith et al. [10] introduced a score metric system (named as 'Smith score metric' hereafter). The authors first drew a Robeson upper bound in which the permeabilities of polymeric membranes were converted to permeances by assuming that the membranes are 100 nm in thickness. Then, each polycrystalline MOF membrane was scored by comparing the perpendicular distance between the data point and the boundary line on the graph. A positive value will be given if the data sit above the line. Fig. 21 plotted the top-performing ZIF membranes. It is clear that the majority of data sitting beyond the boundary (red line) are ZIF-8-based membranes, which strongly indicates that ZIF-8 serves as a much better candidate for C_3H_6/C_3H_8 separation when compared to polymeric membranes.

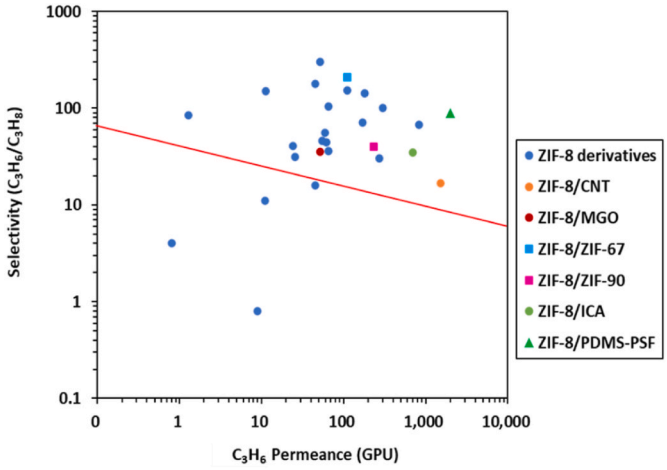

Fig. 21. Top-performing ZIF-8-based membranes for C_3H_6/C_3H_8 separations. The Upper bound is drawn assuming a polymeric membrane thickness of 100 nm based on the data published by Smith et al. [10].

2.3. Polycrystalline MOF membranes for other gas separations

While ZIF-8 membranes have been most extensively studied for C_3H_6/C_3H_8 separation, they also remain the most popular candidate for other gas separations. Beside ZIF-8, other types of MOFs including other ZIFs (e.g., ZIF-L, ZIF-7, ZIF-9, ZIF-22, ZIF-67, ZIF-68, ZIF-69, ZIF-90, ZIF-93, ZIF-94, and ZIF-100), HKUST-1 derivatives, UiO-66 derivatives, and MILs were also studied for gas separations. A number of industrially important gas pairs such as H_2/CO_2, CO_2/N_2, CO_2/CH_4, N_2/CH_4, and N_2/O_2 were studied. Recently, applications of MOF membranes have also been extended to capture other gases such as Xenon from air [150] and ammonia from H_2 and/or N_2 [151].

In this section, we briefly reviewed the reported MOF membranes for H_2/CO_2, CO_2/N_2, and CO_2/CH_4 separations as they attracted the most industrial and research attentions. We used the 'Smith score metric' [10] as a reference and selected a range of typical MOFs that could represent the separation performance within their associated material class.

2.3.1. H_2/CO_2 separation

By virtue of its small molecular size, hydrogen is relatively easy to be separated compared with other gases. Fig. 22 shows the H_2/CO_2 separation performances of the reported MOF membranes when compared to polymeric boundary (red line) drawn based on the 'Smith score metric'.

It is no surprise that ZIF-8 remains the top candidate for H_2/CO_2

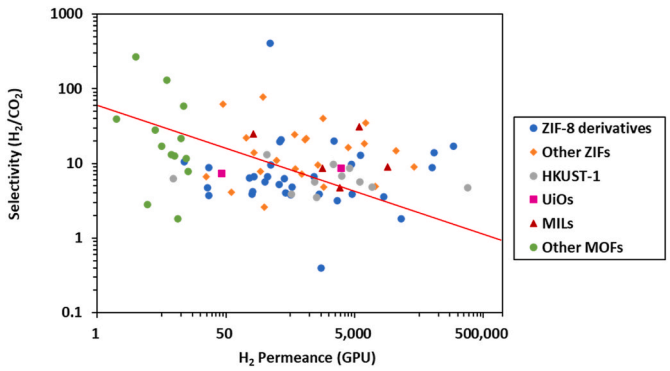

Fig. 22. Top-performing MOF membranes for H_2/CO_2 separation. Upper bound drawn assuming a polymeric membrane thickness of 100 nm based on Smith et al. [10].

separation due to its small pore size and well-designed membrane structures. Wang et al. [152] fabricated a highly H_2-selective ZIF-8 membrane by growing membranes onto graphene oxide (GO) nanosheets via an alternate source immersion method. The GO was firstly immersed to the Zn^{2+} source to anchor the metal ions onto the GO surface, followed by a secondary reaction in the ligand source. The resulting membrane showed an excellent H_2/CO_2 separation performance with a selectivity of 406 and H_2 permeance of 240 GPU [152]. Another high-performance ZIF-8 membrane (thickness of 100–200 nm) was prepared on a CNT/PTA-coated alumina support, showing unprecedentedly high H_2 permeance of 85,736 GPU with a selectivity of 14 [153]. High H_2 permeance membrane could also be fabricated on an APTES-modified alumina tubular support via contra-diffusion, showing exceptional H_2 permeance of 171,000 GPU with an H_2/CO_2 selectivity of 17 [154].

Support modification method was also extended to other ZIFs. For example, Zhong et al. [155] fabricated a ZIF-9 membrane (thickness, 50 μm) on APTES-modified support, showing high H_2 permeance of 22,200 GPU and selectivity of ~14. The high performance was attributed to the APTES functionalized surface, which induced a pore size shrinkage from 4.3 Å to 3.2 Å, improving the sieving effects towards CO_2. To further improve the selectivity of ZIF-9, a post-modification strategy could be adopted. For example, the as-synthesized ZIF-9 membrane was coated by a layer of ionic liquid/CNT mixture, which improved the H_2/CO_2 selectivity to 40 while maintaining satisfactory H_2 permeance of 1627 GPU [156]. An APTES modified support was used for ZIF-95 membrane synthesis, resulting in H_2 permeance of 7340 GPU with an H_2/CO_2 selectivity of 35 [157]. The H_2 permeance is promising in light of the relatively high thickness of the membrane (~30 μm). It is worth pointing out that the ZIF-95 membrane has exceptionally high thermal stability hence able to tolerate high temperatures up to 500 °C.

Other than ZIFs, NH_2-MIL-53(Al) and NH_2-Mg-MOF-74 are two potential candidates with standout performances for H_2/CO_2 separation. Zhang et al. [103] fabricated a 15 μm thick NH_2-MIL-53(Al) membrane on a macroporous glass frit via a seeding and secondary growth approach. The resultant membrane has an ideal H_2/CO_2 selectivity of 18.5, which could be further improved to 31 in a mixture gas separation. The authors attributed this improvement to competitive gas adsorption. The membrane on-stream stability study showed a ~20% reduction in H_2/CO_2 selectivity when the temperature was increased from 25 °C to 80 °C. An NH_2-Mg-MOF-74 membrane was fabricated on a MgO modified alumina support followed by a post-modification using ethylenediamine as illustrated in Fig. 23a – c [158]. Diamine on the functionalized surface imposes a 'pore blocking' effect and reduces CO_2 mobility via CO_2-amino group interactions. H_2/CO_2 selectivity of the membrane was improved from 10.5 to 28 after post-modification. It is somewhat counter-intuitive considering the pore aperture of MOF-74 (11 Å) is far beyond the CO_2 kinetic size (3.3 Å).

The membranes for H_2/CO_2 separation mentioned above are all based on 3D MOFs. In recent years, there is a prolific development of 2D MOFs for various applications. The potential of 2D MOF membranes for gas separation has also been reported. Peng et al. [159] successfully exfoliated $Zn_2(bIM)_3$ nanosheets (thickness of 1.6 nm) via a top-down approach using wet ball-milling and ultrasonication of 3D crystals (Fig. 23d). A nanosheet suspension was then deposited onto a preheated alumina support and dried at the same temperature for 1 h. The obtained membrane showed a high H_2/CO_2 selectivity of 130 with H_2 permeance of 3136 GPU. The excellent performance is attributed to the pore size of $Zn_2(bIM)_3$ nanosheet, which has an aperture of 2.9 Å perfectly sitting between the kinetic diameters of H_2 (2.89 Å) and CO_2 (3.3 Å).

Another interesting 2D MOF is MAMS-1 which could be exfoliated into 12–40 nm nanosheets in Fig. 24 [160]. The nanosheet has dual pore apertures perpendicular to each other. One pathway (PW1) has a pore size of ~2.9 Å and is perpendicular to the basal plane, while the other

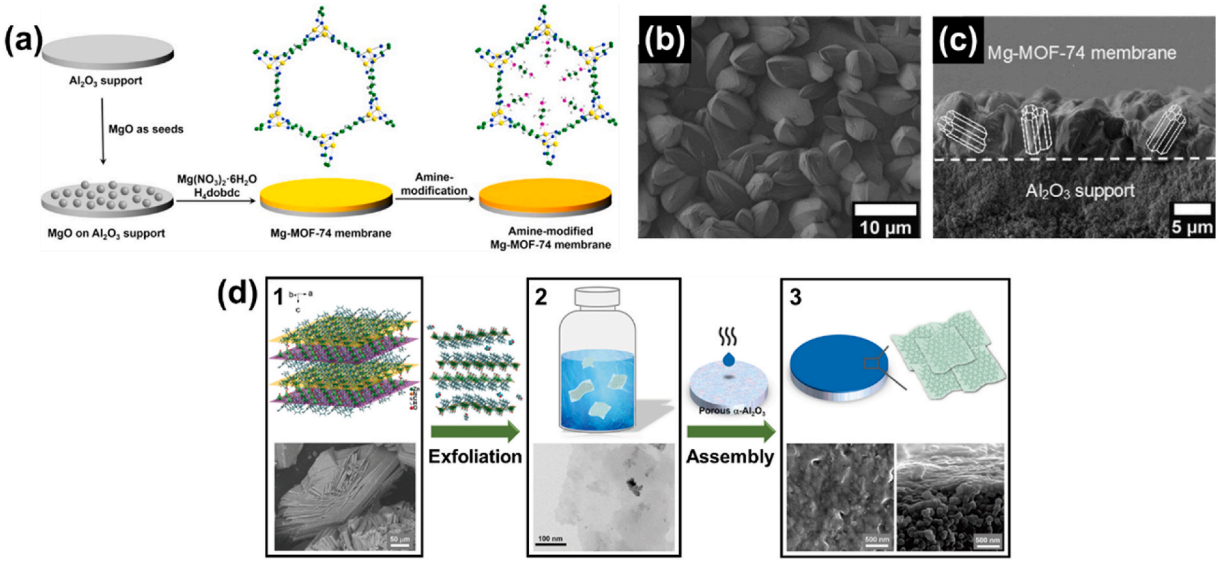

Fig. 23. (a) A schematic representation of the fabrication method for NH_2-Mg-MOF-74 membrane. (b) Top and (c) cross-section SEM images of the NH_2-Mg-MOF-74 membrane. (d) Schematic illustration of the nanosheet exfoliation and membrane fabrication process of $Zn_2(bIM)_3$. Reproduced with permission from Ref. [158] Copyright 2014 Elsevier B.V and ref. [159] Copyright 2017 Wiley VCH.

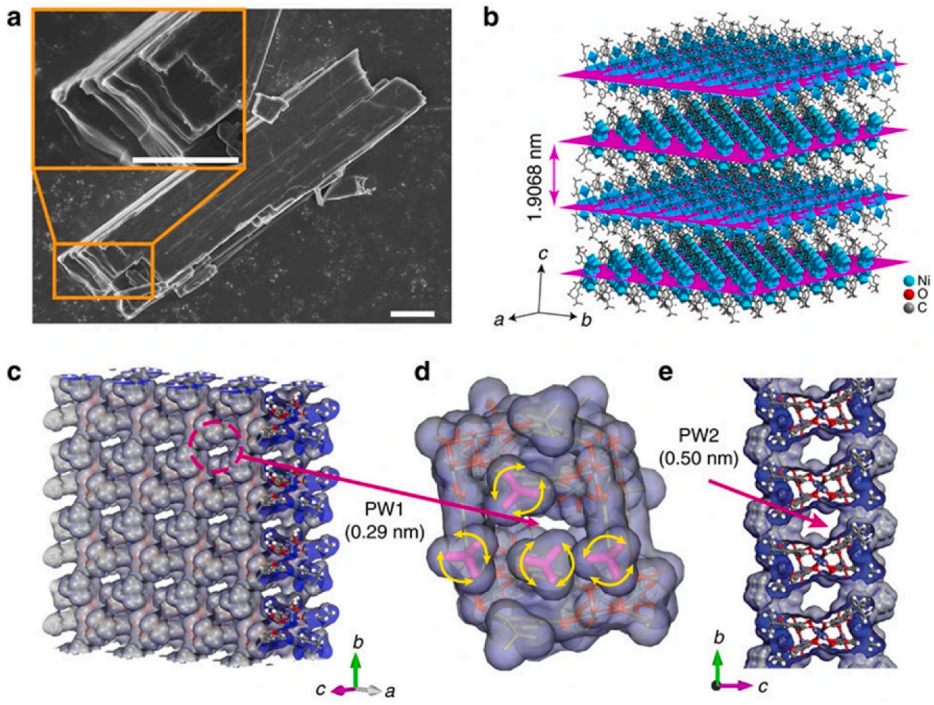

Fig. 24. (a) An SEM image of MAMS-1. (b), (c), (d), and (e) illustrate the crystal structures of MAMS-1. All the images were reproduced with permission from Ref. [160] Copyright 2017 Springer Nature.

(PW2) has a pore size of 5.0 Å and is parallel with the basal plane. PW1 functions for H_2 sieving while PW2 facilitates rapid gas redistribution. The synergistic effects of the two channels make the MAMS-1 nanosheet a promising material for high flux and high H_2-selective membranes. The nanosheets were coated onto an AAO support to create a membrane showing an exceptionally gas separation performance with a selectivity 268 and permeance of 800 GPU, which represents one of the best H_2/CO_2 separation performances based on the 'Smith score metric' [10]. The MAMS-1 membrane also showed a thermal-switchable response up to 100 °C towards H_2 permeance due to structural flexibility. The permeance increased with temperature from –20 °C to 40 °C but decreased with temperature from 40 °C to 100 °C. The H_2 permeance was partially reversible when the temperature was reduced from 100 °C to 40 °C. In contrast, CO_2 permeance remains stable at around 1–3 GPU. Overall, the membrane demonstrates the best gas separation performance at 40 °C.

Based on the works we reviewed for H_2/CO_2 separation, the following comments can be made:

- MOF membranes offer high H_2/CO_2 separation performances surpassing that of polymer membranes.
- The majority of the reported MOF membranes readily achieve a satisfactory H_2 permeance >200 GPU. This is because of two reasons. Firstly, H_2 has intrinsically high diffusivity owing to its small kinetic size. Secondly, support functionalization by carbon-based materials can improve H_2 permeance, which has been observed in a number of ZIF membranes [152,153]. This is somewhat expected since carbon-based materials (e.g., GO, CNT, etc.) can facilitate molecular diffusion which has been well-documented in liquid separations.
- Kinetic-based gas separation is more attractive than equilibrium-based separation for high-resolution H_2/CO_2 separation, as observed in $Zn_2(blM)_3$ and MAMS-1 membranes.

2.3.2. CO_2/CH_4 separation

Removal of CO_2 from natural gas to meet pipeline specifications is an important step before the gas is transported. Pursuing a MOF membrane for CO_2/CH_4 separation has been an interest in the membrane community. Fig. 25 shows the CO_2/CH_4 separation performances of the reported MOF membranes compared with polymer upper bound (red line) drawn based on the 'Smith metric score'.

Similar to H_2/CO_2 separation, ZIF-8 remains one of the most studied MOFs for CO_2/CH_4 separation. However, the majority of reported ZIF-8 membranes showed CO_2/CH_4 selectivity of 3–10 and CO_2 permeance of 100–10,000 GPU, suggesting that the material is not a good candidate for CO_2/CH_4 separation in terms of selectivity. To further explore its potential, a post-modification strategy was adopted. For example, Jomekian et al. [161] fabricated a ZIF-8 membrane on a polyphenylsulfone (PPSF) followed by a PDMS coating. They found that the selectivity of CO_2/CH_4 could be improved from 6.4 to 14.1 while retaining high CO_2 permeance of 925 GPU. In addition, they compared the separation performances of ZIF-8 membranes prepared by different approaches and demonstrated that the LbL approach resulted in a better separation performance compared with the *in-situ* growth approach [161]. Agrawal et al. [162] recently introduced a post-synthetic heat

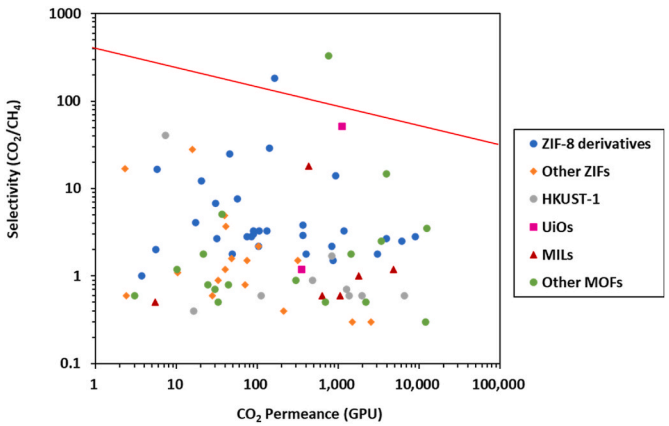

Fig. 25. Top-performing MOF membranes for CO_2/CH_4 separation. Upper bound drawn assuming a polymeric membrane thickness of 100 nm based on Smith et al. [10].

treatment strategy that treated the as-synthesized ZIF-8 membrane at a high temperature (~360 °C) for a few seconds. The heat-treated membrane (hereafter, Heat-ZIF-8) exhibited a significant improvement in CO_2/CH_4 separation with the CO_2/CH_4 selectivity increased from 3 to 30. The CO_2 permeance decreased from 4876 GPU to 120 GPU after the heat treatment. The authors attributed the improved gas selectivity to the stiffened ZIF-8 framework induced by the heat treatment.

Another strategy to improve the CO_2/CH_4 separation performance of the ZIF-8 membrane is through a mixed-linker approach. Wang and co-workers [163] incorporated benzimidazole (bIm, ZIF-7 ligand) to ZIF-8 precursor and fabricated a ZIF-7/ZIF-8 hybrid dual-linker membrane (hereafter, ZIF-7-8) on AAO support. ZIF-8 membrane with 22% bIm incorporation in the framework (i.e., ZIF-7_{22}-8_{78}) exhibited a CO_2/CH_4 selectivity of 25 with CO_2 permeance of ~45 GPU, which is a significant improvement compared with its original selectivity (~3.4). Yeo et al. [164] fabricated a ZIF-8/Zeolite T hybrid membrane via seeding and secondary growth approach. A layer of ZIF-8 seed was firstly coated onto alumna support, followed by a secondary growth of zeolite T. The obtained composite membrane exhibited a CO_2/CH_4 selectivity of 181 with CO_2 permeance of 163 GPU. This hybrid material is the second MOF-based membrane and the only ZIF-8-based membrane sitting beyond the polymer boundary for CO_2/CH_4 separations, as clearly shown in Fig. 25.

Other ZIF-based membranes, including ZIF-9, ZIF-22, ZIF-93, ZIF-94, etc., were also reported, but the majority of them suffer from low selectivity (<5). Among them, the ZIF-94 membrane fabricated by Cacho-Bailo et al. [165] exhibited slightly better performance. The membrane was grown on a P84 hollow fiber via a microfluidic approach followed by a post-modification using nonylamine. The membrane after post-modification showed a CO_2/CH_4 selectivity of 27.8 with a significant improvement in the CO_2 permeance (15.7 GPU) compared with its unmodified counterpart (3.5 GPU). The permeance improvement was attributed to the enhanced CO_2 sorption capacity in the alkyl-modified membrane in which ZIF-94 underwent a topological transformation from SOD to RHO. This transformation could weaken the CO_2-aldehyde interaction owing to the relatively less dense RHO framework.

Other MOFs besides ZIFs were also extensively studied for CO_2/CH_4 separation. Among them, HKUST-1, MIL-53-NH_2, CAU-1, UiO-66, and IRMOF-1 are highlighted here owing to their relatively better CO_2/CH_4 separation performances. HKUST-1 membrane with a thickness of ~40 μm was fabricated onto a hollow alumina fiber using a contra-diffusion approach [166]. The resultant membrane had a high CO_2/CH_4 selectivity of 40.7 but suffered from a relatively low CO_2 permeance (7.32 GPU). Similar to ZIFs, separation performances of the membranes can be improved by synthesizing hybrid materials. For example, MIL-53-N-H_2(Al)/organosilica hybrid membrane with a thickness ~100 nm was fabricated onto silica-modified ceramic support [167]. An as-synthesized MIL-53-NH_2(Al) was firstly mixed with organosilica followed by a dip coating onto support. The coated support underwent a heat treatment at 300 °C under N_2 atmosphere. The membrane obtained was further coated by another layer of organosilica followed by drying and calcination. The resulting composite membrane exhibited a good CO_2/CH_4 separation performance with a CO_2/CH_4 selectivity of 18.3 and CO_2 permeance of 430 GPU. A CAU-1 membrane was fabricated via a seeding and secondary growth approach, as shown in Fig. 26a – d [168]. Energy dispersive X-ray (EDX) elemental mapping shows the alumina support provides some aluminum source during secondary growth, improving the adhesion between the membrane and the support. The obtained membrane has high CO_2 permeance (3940 GPU) with a CO_2/CH_4 selectivity of 14.8. High selectivity was due to increased CO_2 sorption and diffusion in the CAU-1 frameworks compared to other gases.

Compared with CAU-1, a UiO-66 membrane modified by polydopamine (named as UiO-66/PDA hereafter) presented in Fig. 26e – g had a better CO_2/CH_4 selectivity (51.6) while maintained good CO_2 permeance (1115 GPU) [169]. This membrane was fabricated by depositing a layer of PDA on an as-synthesized membrane supported on the AAO disc. The improved CO_2/CH_4 separation performance, compared with pure UiO-66, was attributed to a combination of preferred CO_2 adsorption and the defect healing effect of PDA. The membrane was also tested under humid gas conditions and showed consistent performances attributable to high intrinsic hydrothermal stability of UiO-66.

An IRMOF-1 membrane was fabricated via seeding and secondary growth approach on alumina support (Fig. 27) [170]. The resulting

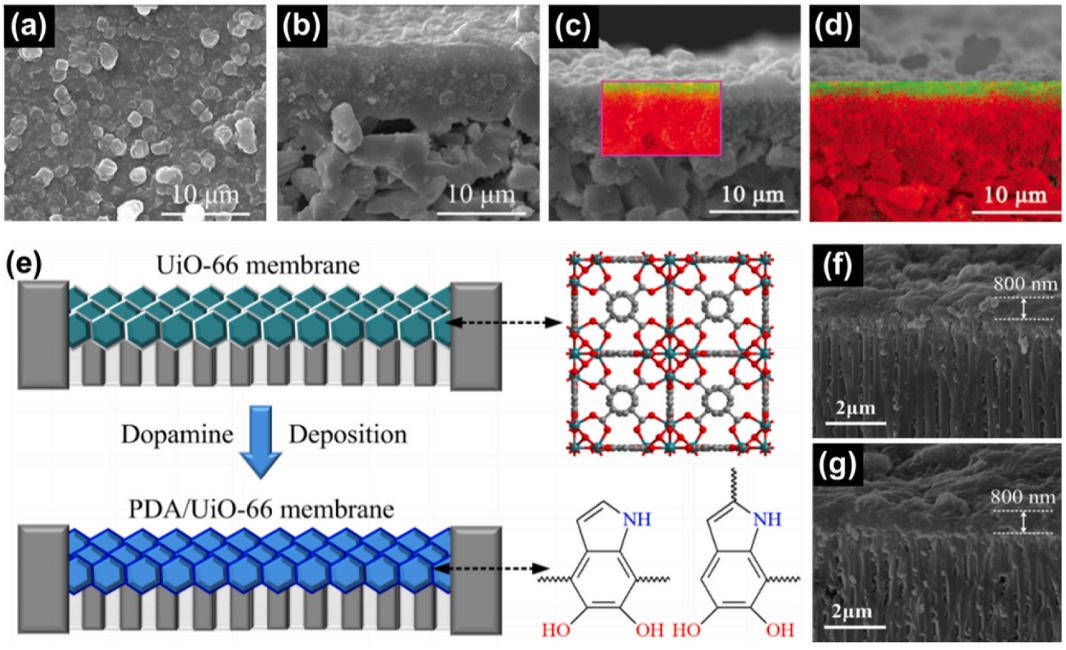

Fig. 26. (a–b) SEM image of the surface and cross-section of the CAU-1 membrane. (c–d) EDX elemental mapping of the membrane and alumina tubes (green = C and red = Al). Images were taken from Ref. [168] Copyright 2014 The Royal Society of Chemistry. (e) A schematic representation of the fabrication method for UiO-66/PDA membrane. SEM images of UiO-66 membrane (f) before and (g) after PDA modification Reproduced with permission from Ref. [169] Copyright 2019 American Chemical Society. (For interpretation of the references to color in this figure legend, the reader is referred to the Web version of this article.)

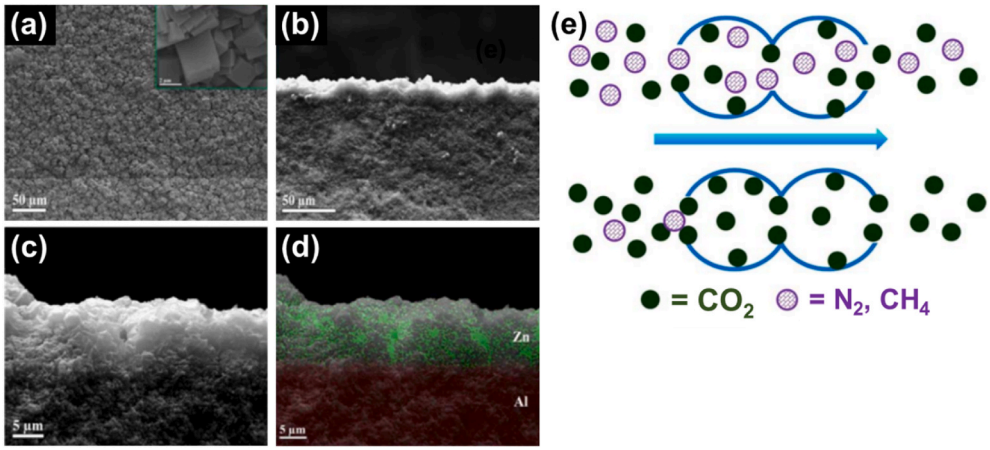

Fig. 27. SEM images and EDX of the IRMOF-1 membrane: (a) top, (b–c) cross-section, and (d) EDX elemental mapping of membrane cross-section in (c), color code: green = Zn, red = Al. (e) Gas transport mechanism through IRMOF-1 membranes under low CO_2 content and high CO_2 content. Reproduced with permission from Ref. [170] Copyright 2016 John Wiley and Sons. (For interpretation of the references to color in this figure legend, the reader is referred to the Web version of this article.)

membrane has a CO_2/CH_4 selectivity below 10 when the feed mixture has CO_2 content below ~60%. Surprisingly, membrane selectivity was increased to a maximum of 328 with CO_2 permeance of 761.2 GPU when CO_2 content was increased to ~80%. Further increasing CO_2 content towards 100% gradually decreased the selectivity from 328 to ~100. This phenomenon was attributed to an adsorption-diffusion mechanism. At lower to moderate CO_2 content, the strong adsorption of CO_2 on the pore walls reduces the concentration gradient of CH_4, thus, its associated diffusivity. The lower diffusion rate of CH_4 also reduces the CO_2 diffusion rate due to multicomponent effects. At higher CO_2 content, a higher amount of CO_2 adsorption occurs within the pores, significantly blocking the diffusion path of CH_4. As a result, the CO_2/CH_4 selectivity increased sharply. Further increase in CO_2 content weakened the driving force of the concentration gradient, reducing the CO_2 diffusivity. As a result, CH_4 diffusivity increased due to multicomponent effects, lowering the CO_2/CH_4 selectivity [170]. The phenomenon observed was not reported for other IRMOFs, demanding further study to understand the mechanism fully. Since the IRMOF-1 membrane requires the feed gas of high CO_2 content, it is a potential candidate for low-grade CO_2 upgrading.

Table 1 shows all the top-performing MOF membranes mentioned above, along with their associated CO_2/CH_4 separation performances. Based on the data and scientific content reviewed in this section, the following comments can be made.

- Most of the reported CO_2/CH_4 separations are based on adsorption selectivity.
- Pure ZIF-8 membranes without post-modification are not capable to provide a satisfactory performance for CO_2/CH_4 separation.
- IRMOF-1 and ZIF-8/Zeolite-T composite are the only two reported membranes that sit beyond the Robeson boundary based on the 'Smith score metric' so far.
- CAU-1 membrane is a potential candidate to compete with the commercially available polymeric membranes (selectivity of ~10 and permeance of ~100 GPU) in its pure form.
- UiO-66/PDA serves as the best candidate for CO_2/CH_4 separation considering its ease of fabrication and high hydrothermal stability.

2.3.3. Carbon capture (CO_2/N_2)

Carbon capture has become an increasingly important topic with the rising awareness of climate change. Driven by the global demand, MOF membranes for CO_2/N_2 separation have also drawn an extensive research effort. Fig. 28 shows the CO_2/N_2 separation performance of the reported MOF membranes when compared with polymeric boundary (red line) drawn based on the 'Smith metric score'.

Similar to CO_2/CH_4, pure ZIF-8 membranes without post-modifications are unable to provide satisfactory CO_2/N_2 separation performances. Post-modification or hybrid strategy can be adopted to improve performances of the membranes. Owing to the relatively similar kinetic size of N_2 (3.64 Å) and CH_4 (3.8 Å), some of the reported ZIF-8 membranes (e.g., Heat-ZIF-8, ZIF-7-8) that showed excellent separation performances for CO_2/CH_4 gas pair also performed well for CO_2/N_2 gas pair. The CO_2/N_2 separation performances of the top-performing MOF membranes are summarized in Table 2. To further improve the

Table 1
A summary of CO_2/CH_4 separation performance of top-performing MOF membranes.

MOF Films	CO_2 (GPU)	CH_4 (GPU)	CO_2/CH_4 Selectivity	[a]Smith Metric Score Ranking	Ref.
IRMOF-1	761.2	2.3	328	1(+)	[170]
ZIF-8/ zeolite T	163	0.9	181.1	2(+)	[164]
UIO-66/ PDA	1115	21.6	51.6	3(−)	[169]
Heat-ZIF-8	140.3	4.8	28.8	4(−)	[162]
ZIF-7-8	45	1.8	25	5(−)	[163]
CAU-1	3940	266	14.8	6(−)	[168]
ZIF-8/ PDMS	925.4	65.7	14.1	7(−)	[161]
MIL-53-NH_2	430.1	23.6	18.2	8(−)	[167]

The ranking is based on Smith Metric Score; the '+' and '-' in the bracket indicate the data point sits on the upper (+) or the lower (−) of the Robeson boundary shown in Fig. 25.

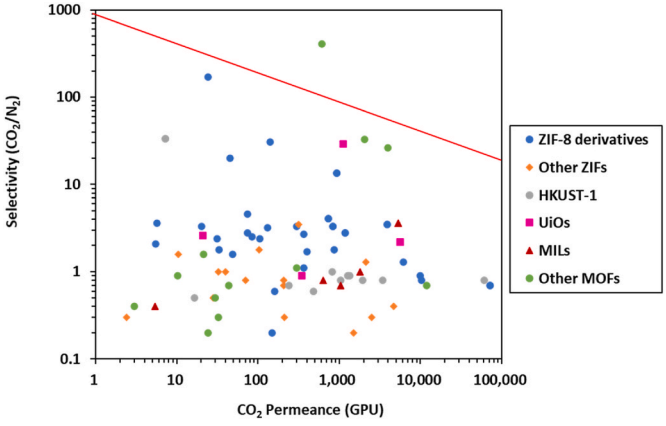

Fig. 28. Top-performing MOF membranes for CO_2/N_2 separation. Upper bound drawn assuming a polymeric membrane thickness of 100 nm based on Smith et al. [10].

Table 2
A summary of CO_2/N_2 separation performance of top-performing MOF membranes.

MOF Films	CO_2 (GPU)	N_2 (GPU)	CO_2/N_2 Selectivity	[a]Smith Metric Score Ranking	Ref.
IRMOF-1	614.9	1.50	410	1(+)	[170]
ZIF-8@carbonic anhydrase	24.20	0.10	169	2(−)	[171]
ZnTCPP	2070	62.7	33.0	3(−)	[172]
CAU-1	3940	150	26.3	4(−)	[168]
UiO-66/PDA	1115	21.6	28.9	5(−)	[169]
Heat-ZIF-8	140.3	4.60	30.6	6(−)	[162]
ZIF-7-8	45.00	2.20	20.0	7(−)	[163]
HKUST-1	7.300	0.20	33.3	8(−)	[166]

The ranking is based on Smith Metric Score; the '+' and '-' in the bracket indicate the data point sits on the upper (+) or the lower (−) of the Robeson boundary shown in Fig. 28.

CO_2/N_2 selectivity, Zhang et al. [171] fabricated a composite membrane by embedding carbonic anhydrase enzymes into ZIF-8 frameworks (ZIF-8@carbonic anhydrase). The membrane was fabricated via an *in-situ* growth approach in which the enzyme reactants were directly mixed with ZIF-8 precursors. PAN modified with a layer of halloysite nanotube served as the support. The resultant membrane was tested under humid gas conditions and showed an exceptional CO_2/N_2 separation performance (CO_2/N_2 selectivity of 165.5 and CO_2 permeance of 24 GPU). The authors attributed the impressive CO_2/N_2 separation performance to an enzyme-H_2O assisted process involving continuous CO_2 hydration and conversion.

For other MOF-based membranes such as HKUST-1, CAU-1, and IRMOF-1, the detailed synthesis and associated separation mechanism have already been discussed in Section 2.3.2. The associated CO_2/N_2 separation performances of the membranes were tabulated in Table 2. One interesting MOF to be highlighted here is ZnTCPP (zinc(II) tetrakis (4-carboxy phenyl)porphyrin) nanosheets which were fabricated as a gutter layer to facilitate the gas transport of a polymeric membrane, as shown in Fig. 29 [172]. The resulting bilayer membrane exhibited good CO_2 permeance of 2070 GPU and CO_2/N_2 selectivity of 33. The high CO_2 permeance was attributed to the gutter layer of ZnTCPP, which could significantly enhance the gas transport rate compared with its PDMS counterpart. The ZnTCPP could also improve the structural integrity of the membrane under mechanical stress, enabling the membrane to remain intact after bending [172].

In summary, though some reported MOF membranes have shown good CO_2/N_2 separation performances, it seems that there is no reported MOF membrane with attractive CO_2/N_2 separation performance for post-combustion carbon capture (CO_2 permeance >1000 GPU and CO_2/N_2 selectivity >30). While a ZnTCPP gutter membrane seems to meet the requirement, the membrane is technically a polymer membrane.

3. Engineering challenges and prospects of polycrystalline MOF membranes

Technological advances in MOF membrane synthesis especially using vapor phase and electrochemical syntheses over the recent years, are nothing short of promising. Membrane scientists have been making great strides in combining conventional approaches and various post-synthetic modifications to prepare better performing MOF membranes. However, the majority of the reported membranes are limited to laboratory scale synthesis with a membrane area of several square centimeters only. Significant research efforts should be targeted at the refinement of the membrane processing towards larger scale synthesis for commercial applications. Despite much enthusiasm over the impressive performances of MOF membranes, in particular ZIF-8 membranes for C_3H_6/C_3H_8 separation, we might not see the membranes find their way to the commercial market unless membrane scale-up challenges are successfully addressed. After reviewing recent development in the synthesis and applications of MOF membranes for gas separations, we identify several focus areas requiring immediate attention.

In this section, we provide perspectives concerning membrane scale-up and membrane stabilities under realistic conditions and discuss where the research focus should be directed in the near future. Note that a large portion of the discussion will be on the ZIF-8 membranes and their hybrids, given their large volume of scientific work.

3.1. Processing convenience and cost attractiveness

Cost attractiveness and ease of processing are the barriers that hinder further development of inorganic membranes. Ideally, large scale membrane manufacturing should be robust, inexpensive, continuous, and reproducible. For scaling up, one important question that we must ask ourselves is whether we can take advantage of the existing technologies without requiring significant changes in the setup to prepare large area MOF membranes. This is where mixed matrix membrane (MMM) approach has the upper hand. MOF-based MMMs combine the spinnability properties of pure polymer with the excellent transport properties of MOF fillers [173]. One can take advantage of the already mature polymer hollow fiber spinning technology (e.g., single-layer and

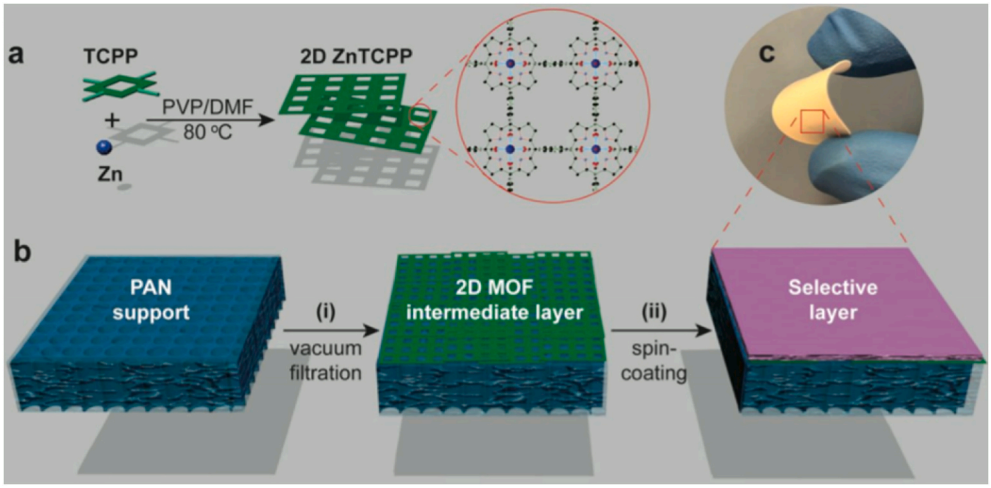

Fig. 29. Schematic illustration of the synthesis process of ZnTCPP membrane. Reproduced with permission from Ref. [172] Copyright 2018 American Chemical Society.

dual-layer spinning) to fabricate hollow fiber MMMs, provided that MOF/polymer dope solution formulation is adequately stable. Several works have demonstrated the formation of MOF-based (i.e., ZIF-8) asymmetric hollow fiber MMMs using single- and dual-layer spinning technology showing improved performances for C_3H_6/C_3H_8 and CO_2/N_2 separations [174,175]. While MOF-based MMMs display inferior separation performances than that of pure MOF membranes, the manufacturability of MMMs is more straightforward with fewer defect generations. However, it should be noted that MOF-based MMMs are not without their own engineering challenges, such as interfacial defects, particle agglomeration and sedimentation, accurate filler positioning, and filler loading limit, among others [173]. For the sake of brevity, these challenges will not be discussed in detail here.

The proposed MOF membrane synthesis protocol would be commercially attractive if it uses a similar manufacturing setup found in the industries and does not require complex state-of-the-art equipment. For current-driven MOF membrane synthesis, we envisioned the mass production of the membrane would use a similar electrolysis bath setup typically found in electroplating plants. Counter-diffusion is among the simplest method to prepare MOF membranes. However, the setup requires membrane sealing and resealing before and after synthesis rendering them unattractive for upscaling [176].

Despite all the excitement surrounding the developments in MOF membranes reported in the past years, the currently reported methods still possess several notable drawbacks preventing commercial scale deployment of the technology. For instance, MOF membrane syntheses still use toxic and environmentally harmful organic solvents that can be troublesome from waste management standpoint. Synthesis of important SOD-type ZIFs such as ZIF-7 and ZIF-90 often require polar aprotic solvents such as dimethylformamide [177–181]. In this case, vapor phase membrane synthesis is attractive as one does not have to deal with hazardous waste management. MOF membrane synthesis also involves the large consumption of expensive precursors. Reported aqueous-based synthesis of ZIF-8 nanocrystal requires Zn^{2+}:2-methylimidazole molar ratio as high as 1:70 [123]. Commercial MOF membrane synthesis protocol should be simple and involve fewer steps as possible. Using a facile synthesis setup, performing the reaction at room temperature, precursor recycling, and switching to more readily available solvents may help make the process more cost attractive.

MOF membrane processing is a complex, low-yield, non-continuous batch process with long synthesis hours, making them unattractive for scale-up. For example, Huang and co-workers [170] obtained continuous ZIF-95 membranes on α-Al_2O_3 supports only after growing the membranes for 7 days. While there have been significant improvements in reducing membrane synthesis time from several days to just a few minutes, they are mostly limited to ZIF-8 membranes and their hybrids [182]. Lastly, some of the proposed synthesis protocols use advanced and specialized tools that require a significant capital investment [181]. Specialized equipment including ALD, CVD, and magnetron sputtering allow for uniform and conformal thin film deposition of metal precursors on supports for the preparation of MOF membranes. However, they are relatively expensive and mostly used for specific applications (e.g., deposition of high-*k* dielectric, gate oxide, and thin metal films for microelectronic applications) [183,184].

In large scale gas separation plants, especially those in the refineries, membrane cost represents only 10–25% of the overall plant cost [185]. The rest is the cost associated with running large gas compressors. Even though membrane cost is smaller relative to compressor operating cost, one should not underestimate the capital investment saving if the cost of inorganic membranes is significantly reduced. Based on the estimated cost and current performances of MOF membranes, the application of the membranes on a commercial scale does not seem cost attractive. Macroporous and mesoporous inorganic membranes (e.g., zirconia, titania, and alumina) have already been commercialized as membrane filtration elements for wastewater treatment, pharmaceutical, food processing, pharmaceutical, and chemical production [186]. These membranes are relatively expensive, marketed at a current market price of \$400 – \$2000 m^{-2} [186]. Growing inorganic zeolite/MOF/CMS membranes on these supports for gas separations would result in a higher membrane price. Lin et al. [186] estimated that such membranes would cost \$1000 – \$5000 m^{-2}, one- or two-order of magnitude higher than polymer membranes. Tsapatsis and co-workers [76] conducted a process-scale evaluation and economic feasibility studies of ZIF-8 membranes for C_3H_6/C_3H_8 separations using the Aspen Plus process simulation package. A conservative estimate of the application ZIF-8 membranes with C_3H_6 permeance of 100 GPU and C_3H_6/C_3H_8 separation factor of 50 at 7 bar in a hybrid C_3H_6/C_3H_8 single-stage membrane-distillation system producing $\sim 2.5 \times 10^5$ tonnes of polymer grade C_3H_6 (99.7 mol%) annually revealed that a membrane with a cost of \$130 m^{-2} is required to just breakeven with distillation system. Meanwhile, an acceptable price ceiling for the membrane system in petrochemical industries is ~\$200 m^{-2} [187]. Based on the estimated inorganic membrane cost, it is unlikely that the membranes to be used as a membrane-distillation hybrid for commercial C_3H_6/C_3H_8 separations.

ZIF-8 membranes are better off being applied as membrane recovery units as the process permits higher membrane cost while maintaining healthy process economics. Recovering unreacted C_3H_6 from a chemical reactor (e.g., polypropylene, iso-propyl alcohol, and cumene) purge stream is a practical short- or medium-term goal for ZIF-8 as purity requirement and scale of separation is much lower. C_3H_6 purity as low as 70–90 mol% is acceptable to be recycled back into the chemical reactor [76,188]. An estimation of the required ZIF-8 membrane area for membrane recovery unit installed in a typical size polypropylene plant producing $\sim 50 \times 10^6$ tons of polypropylene is just 250 m^2 [76]. Note that the estimation is based on ZIF-8 performances with C_3H_6 permeance of 100 GPU and selectivity of 5. Simulation result revealed that ZIF-8 membrane with a whole module cost of \$1000 m^{-2} could result in a payback period of less than one year and net present value (NPV profits) of \$1.5 million and \$2.2 million in the second and the third year of deployment, respectively. For this application, the industry might be able to tolerate a higher membrane cost. A significant reduction in membrane cost needs to be achieved for a broader target, such as retrofitting the membrane into a conventional C_2 or C_3 splitter columns.

Initial cost to set up inorganic membranes for gas separations should not be expensive and neither do their replacement cost [189]. Lin et al. [186] performed a simple estimation of membrane area-saving when inorganic membranes (i.e., CMS) is used, compared to polymer membranes. An estimated CMS membrane area to process 15,000 m^3 h^{-1} refinery gas was found to be six times smaller (i.e., 2200 m^2). Despite requiring a smaller membrane area, overall cost of CMS membrane is still higher due to high membrane cost and low module packing density. Experts believe that a true solution to address high cost of inorganic membranes is productivity/throughput increase to a point where the cost to process a unit of gas is as attractive as polymeric membranes or other competing technologies.

Competitive performances of inorganic membranes can be achieved from fabrication of thinner membranes, ideally to sub-100 nm thickness. Tsapatsis [190] even argues that for certain applications inorganic membrane thickness need to be further downscaled to 50 nm. Theoretically, one can achieve a 10-fold increase in gas flux by reducing membrane thickness by a similar ratio, for example, from 1 μm to 0.1 μm thick. Focusing on C_3H_6/C_3H_8 separation, there are many published works on the synthesis of sub-100 nm thick ZIF-8 membranes exhibiting unprecedentedly high C_3H_6 permeance available in literature and a few have already been discussed in the earlier section. Switching to a more permeable nanoporous material is another option to consider but one may face an issue of finding material with a proper aperture to efficiently isolate gas species of interest. Also, crystalline nature of MOF provides high molecular sieving effect but at the same time limit its usability and effectiveness to a specific gas mixture only. In some cases, material with superior permeability and selectivity might be available but difficult to be processed into ultrathin and defect-free layer.

Inorganic membrane throughput can also be increased by upgrading intrinsic permeability of current membrane materials. Nair et al. [191] proposed a unique "all nanoporous hybrid membrane" (ANHM) concept to provide access to higher permeability and selectivity, unattainable when using single phase nanoporous materials. ANHM is a borrowed membrane concept from the conventional polymer-based mixed-matrix membrane (MMM) but using nanoporous crystalline material as a continuous phase as oppose to organic polymer. Different performance improvement routes (e.g., increased permeability, increased selectivity, or both) can be achieved from different combinatorial scheme between the dispersed phase and continuous phase as illustrated in Fig. 30a. MFI is a medium pore zeolites (5.5 Å) possessing high C_3H_6 permeability of 8085 Barrer but not selective towards C_3H_6. Incorporation of MFI zeolites into pure phase ZIF-8 (C_3H_6 permeability of 390 Barrer) enable performance limit of ZIF-8 for C_3H_6/C_3H_8 separation to be surpassed.

This new membrane concept does not require an entirely new membrane processing. ZIF-8/MFI MMM with thickness of 9 μm was successfully prepared on the lumen side of macroporous poly(amide-imide) hollow fiber using the IMMP method reported in their earlier work [72]. C_3H_6 permeability of ZIF-8/MFI MMM containing 12.9 vol% of MFI backcalculated using the Maxwell equation was 548 Barrer; 45% higher than that of single phase ZIF-8 as shown in Fig. 30b – c. An even simpler method to prepare ZIF-8/MFI nanoporous hybrid membranes on alumina discs based upon simple dip coating and subsequent evaporative membrane crystallization was also reported [192]. Separation performances of ANHM consisting of 2D MFI nanosheets, MFI nanoparticles, and ZIF-8 were superior compared to ZIF-8 membrane prepared using a similar method. The hybrid membranes displayed C_3H_6 permeance and selectivity of 66 GPU and 72, respectively. These works provide insights into the fabrication of next generation nanoporous crystalline membranes with improved permeability and selectivity, resulting in membranes with higher throughput.

A more straightforward approach to decrease inorganic membrane cost is to just switch to inexpensive and more readily available polymer supports. Porous polymeric supports can be fabricated either as flat sheet or hollow fibers at low cost; \$10–100 m^{-2} and \$2–5 m^{-2} for hollow fiber and spiral wound, respectively [185]. That said, membrane researchers are recommended to develop an innovative solution to prepare highly productive membranes and continue developing polymer-supported MOF membrane technology.

3.2. Transitioning from basic plate-and-frame to spiral wound or hollow fiber module

One important area that deserves further attention is transitioning from planar to hollow fiber geometry. Future works should be dedicated to demonstrate MOF membrane fabrication on porous hollow fiber, capillary, or tubular supports. It is worth mentioning that 4 out of 5 (80%) of the total installed gas separation membrane modules are based on hollow fiber geometry. The remainder is shared between spiral-wound and plate-and-frame modules, in which the former is a more popular option [185]. Polycrystalline MOF membranes are inherently brittle and inflexible; unlikely to be packaged into spiral-wound modules. This leaves hollow fiber modules as the most practical choice. In terms of engineering design, hollow fibers provide a high accessible surface area [186,193]. Hollow fiber-supported MOF membranes with an outer diameter of 2 mm can achieve a high packing density as high as 2000 m^2 m^{-3}, resulting in membrane units with smaller footprints. However, growing MOF membranes on hollow fibers is not straightforward as compared to growing the membrane on planar supports.

To date, a large body of works reported ZIF-8 membranes on various planar supports (e.g., α-Al_2O_3, AAO, and metal nets), where the standard 22 mm diameter α-Al_2O_3 discs being the most popular choice. There are only a few works on ZIF-8 membrane fabrication on polymer (e.g., Torlon®, Matrimid®, polysulfone, and PVDF) and inorganic hollow fibers (e.g., α-Al_2O_3, ZnO, ZnO-Al_2O_3, yttria-stabilized zirconia, and carbon) [72,110,133,194–200]. To increase membrane packing density, one might consider using ceramic multichannel monolith, but then one has to face the challenges associated with membrane synthesis on the bore space of the monolith. Moreover, the geometries of the multichannel monolith may result in additional mass transfer resistance of gases through the supports.

It is critical not to underestimate the difficulties in preparing MOF membranes on hollow fiber modules, especially on the lumen side. Similar membrane synthesis protocol performed on planar supports may not work as well on hollow fiber due to mass transfer limitation and curvature effects. Tran et al. [201] found that ZIF-8 did not form a coherent layer when grown on the bore side as opposed to the shell side

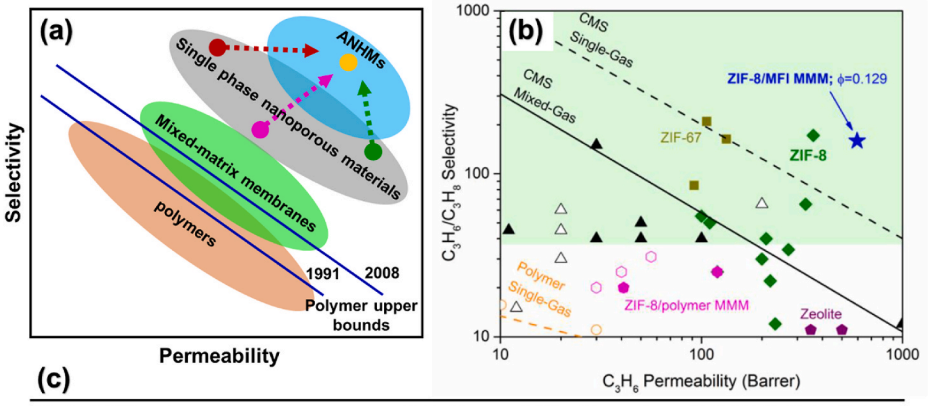

(c)

Material/Membrane	C_3H_6 Permeability (Barrer)	C_3H_6/C_3H_8 Selectivity
MFI[a]	8,085	2.24
ZIF-8[a]	390	135
ZIF-8 membrane: experimental[b]	371 ± 22	156 ± 26
ZIF-8/MFI MMM: experimental[b]	548 ± 67	146 ± 14
ZIF-8/MFI MMM: Maxwell model[c]	538	129

Fig. 30. (a) Schematic illustration of ANHM concept to transcend limitation of single phase nanoporous materials. (b–c) Permeability and selectivity of pure phase ZIF-8, MFI, and ZIF-8/MFI MMM (MFI volume fraction = 0.129) obtained from absorption and diffusion measurements,[a] binary C_3H_6/C_3H_8 measurements,[b] and the Maxwell equation.[c] Image reproduced from Ref. [192] Copyright 2020 American Chemical Society and ref. [191] Copyright 2019 Wiley VCH.

of α-alumina tubes with an outer diameter of 12 mm. This produced ZIF-8 membranes that were not C_3H_6-selective. The authors posit that confined spaces and negative surface curvature of the bore of the α-alumina tubes limit the mass transfer of ZIF-8 particles onto the solid surfaces. As one transition to supports with smaller diameters (i.e., tubes → capillary → hollow fibers), membrane growth is limited by local inhomogeneity and reactant availability [72]. These effects are expected to be even more pronounced when developing full-size industrial modules rather than laboratory-scale modules [202]. Brown et al. [72] found that ZIF-8 membrane growth on the bore of Torlon® hollow fibers under static conditions produced non-continuous ZIF layers, suggesting inadequate reactant concentration to sustain film growth. Continuous replenishment of growth nutrient using a pump helped to maintain a similar reactant concentration throughout for consistent film growth. Also, the effect of fluid dynamics and precursor flow protocol inside the hollow fibers on ZIF membrane microstructures is worthy of investigation as one might see some interesting phenomena along the way.

We should mention here that our reservation with packaging polycrystalline MOF membrane into spiral wound modules stem from requirement of having to grow a continuous membrane layer on support surface and inherent brittleness of the layer. Spiral wound modules is basically a variation of plate-and-frame module. Packaging MOF membranes into spiral wound modules requires robust and mechanically flexible membranes because the membranes, along with feed and permeate spacers need to be wrapped around a permeate collector tube. As mentioned before, growing MOF membrane on flat substrate is more straightforward compared to hollow fiber but designing a robust and mechanically flexible membrane require an innovative solution. Hess et al. [203] proposed an elegant way to prepare a highly flexible ZIF-8 membrane composite by growing the crystals within the pore of polymer support. The method involves plugging of poly(ether sulfone) pores by ZnO seeds followed by solvothermal treatment in 2-methylimidazolate ligand solution to form ZIF-8 islands inside the pores. Exposing the composite membrane in dimethylacetamide vapor allow the polymer molecules to rearrange and fused around ZIF-8 crystals forming a mechanically flexible self-supporting ZIF-8 membrane. In addition, ZIF-8 crystals within the pores are somewhat protected from any mechanical accidents resulting in a more robust membrane.

It is worth to mention that this patent-pending technology has already been commercialized by UniSieve®. UniSieve® is a clean-tech start up company founded in 2018 and is headquartered at the Swiss Federal Institute of Technology (ETH Zurich) [204,205]. UniSieve® molecular sieve membranes are in a form of spiral wound. Among the applications offered by UniSieve® are chemical purifications, biogas upgrading, gas sensing, and liquid-liquid separations. This clearly indicates that in addition to hollow fibers, spiral wound configuration can also be a reasonable choice for membrane scale up. Since growing a continuous and compact membrane layer on the surface of hollow fibers is technically more challenging, membrane researchers are recommended to look into the possibility of adopting a similar method to prepare MOF molecular sieve membranes on hollow fibers. One simple approach that we can suggest is a simple dip coating of metal gel followed by heat treatment to transform the metal gel into metal oxide prior to solvothermal treatment in ligand solution. A selection of substrates with proper pore sizes is critical to prevent infiltration of metal gel throughout the entire substrate cross section.

3.3. Large area membrane synthesis and membrane modulation

Among the different MOFs and ZIFs explored, ZIF-8 has the greatest potential to be commercialized as a C_3H_6 membrane recovery unit in a petrochemical reactor purge stream. Freeman and co-workers [11] argue that membranes with selectivity as low as 5 can recover 90% of the C_3H_6 reactant at reactor purge stream that would otherwise be lost if not recovered and recycled back into the reactor. Moreover, the required membrane area for this application is 100-fold smaller than the area required for a membrane-distillation hybrid system for C_3H_6/C_3H_8 separations. The industry may keen to invest in this particular application as it incurs a lower capital cost, but membrane scientists must first demonstrate large area membrane synthesis and identify several technical challenges associated with making one.

For practical separations, we envisioned tens of thousands of MOF polycrystalline membranes in hollow fiber geometry packaged inside a rigid cylindrical shell to provide high membrane surface area. For plate-and-frame module, the membrane sets are stacked together in a sandwich-like manner for flat substrates with membrane sides facing each other and sealed inside a frame [206]. The majority of research activities in this area still focus on single hollow fiber or single disc synthesis with laboratory scale dimensions. Large area membrane synthesis and packaging them into a module received very little attention as evidenced by the limited scientific works available in the literature [72,75,207]. Fabrication approaches for large area MOF membrane demand further development. Moving away from laboratory scale means higher chances of generating microdefects and cracks, compromising membrane transport properties. The key to make MOF membrane scale-up possible, at least at this stage, would be a feasible fabrication approach on large supports accompanied by a reproducible separation performance at industrial conditions.

Li and co-workers [75] demonstrated the largest area hollow fiber ZIF-8 membrane for gas separation to date. As depicted in Figs. 31a and 30 polysulfone hollow fibers 19 cm in length were coated with a ZIF-8 ultrathin layer yielding a module with membrane area of 340 cm^2. In another work, Ma et al. [182] synthesized ZIF-8 membranes on commercial ceramic flat substrates (8 cm × 8 cm) and assembled several membrane sets into a homemade membrane module. As shown in Fig. 31b, several ZIF-8 membrane sets were stacked together inside a prototypical plate-and-frame module with an effective membrane area of 300 cm^2. An average C_3H_6/C_3H_8 separation factor of the module was 38, much lower than those individually grown on smaller substrates. As a comparison, the reported C_3H_6/C_3H_8 separation factor of similar ZIF-8 membranes but grown on a smaller α-Al_2O_3 disc 1.8 cm in diameter was 165. The finding suggests that synthesizing a high-quality ZIF-8 membrane over large area is not straightforward as it incurs more defects. Nonetheless, the works mentioned above present a significant step forward towards the commercialization of ZIF-8 membranes.

Modulation of MOF membranes can be cumbersome considering the fragile nature of polycrystalline membranes. Certain substrates, particularly ceramic hollow fibers, are prone to fracture, therefore requiring delicate handling and can fail easily under practical conditions [209]. Inorganic membrane sealing or potting during membrane modulation is one of the aspects that are rarely discussed in membrane communities. Fig. 31c shows examples of different sealing technology for inorganic tubular membranes. During membrane modulation, it is critical to assemble sealing materials without damaging membrane surfaces [208]. In this case, growing MOF membranes on the bore of the tubes/hollow fibers is beneficial as there is no direct contact between the membrane layer and sealing materials. This minimizes the possibility of generating defects during module assembly process.

The ability to form large area MOF membranes inside preformed membrane modules is beneficial as it eliminates major issues associated with membrane modulation. In this case, the membrane module itself will serve two purposes: a) a container/reaction vessel for MOF crystallization b) a gas separation module. Nair et al. [72] fabricated a prototype reactor module to house several Torlon® hollow fibers and hold inorganic solvent during ZIF-8 membrane synthesis. Upon the completion of membrane synthesis, the solvent can be removed from the module, and the module is ready for gas testing. If polymer hollow fibers were to be used as substrates, swelling of the polymers in solvents could be a concern. Park et al. [210] observed the folding of polysulfone hollow fibers inside a preformed membrane module during membrane synthesis, resulting in damage to the selective skin layer. Selecting appropriate solvent, switching to inert inorganic substrates, or

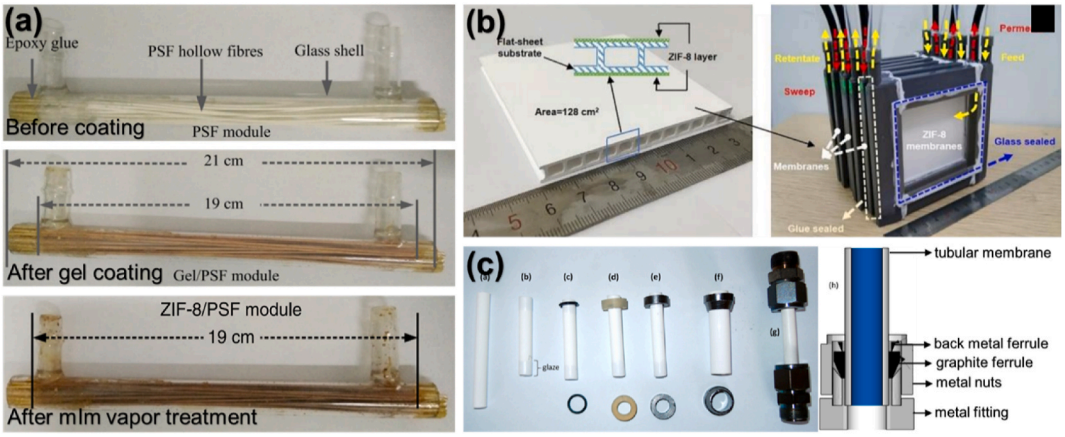

Fig. 31. Successful demonstration of large-area membrane synthesis for (a) hollow fiber module and (b) plate-and-frame module. (c) A variety of membrane sealing materials to seal inorganic ceramic tubes (e.g., (a) support, (b) membrane with glazed ends, (c) Viton O-ring, (d) silicon ferrule, (e) cylindrical graphite ferrule, (f) conical graphite ferrule, (g) assembled membrane, and (h) cut-away of the assembled membrane. Adapted from Ref. [75] Copyright 2017 Springer Nature, ref. [182] Copyright 2020 Wiley VCH and ref. [208] Copyright 2014 American Chemical Society. (For interpretation of the references to color in this figure legend, the reader is referred to the Web version of this article.)

implementing solvent-free synthesis may help to minimize the issue.

3.4. Improving membrane reproducibility and suppressing defect formation

Like zeolites, MOF membranes are polycrystalline in nature. In other words, MOF membrane layer will always possess grain boundaries with channel sizes several times larger than the pore aperture of the MOF itself. Using molecular dynamics simulation, Zhu and co-workers [211] recreated an interface between two ZIF-8 crystal grains and found that the grain boundary channels (8.2 Å and 3.8 Å) along two crystal planes are much larger than the six-membered ring aperture of ZIF-8 (~3.4 Å). Membrane grain boundaries are considered microscopic defects because the channels provide a non-selective transport pathway for gas penetrants through the membranes [212]. This would mean that separation performances of membranes with grain boundary will be lower compared to those without grain boundary (e.g., MOF glass membranes or single-crystal MOF membranes). Moreover, MOF membranes also suffer from mechanical instability due to the structure's intrinsic brittleness, which could induce grain boundary defects and cracks in the membrane. The defects are non-identifiable by the naked eyes. Though fluorescence confocal optical microscopy could be a technique to identify these defects, it does not solve this fundamental problem [213]. Tightening or blocking membrane grain boundary defects through post-synthetic modification or delicate membrane processing can improve MOF membrane selectivity close to the material intrinsic selectivity.

Another consequence of membrane grain boundary is membrane properties are highly dependent on how the membrane is processed. Different MOF membrane processing will result in different membrane thickness, crystal orientation, grain size, defect density, etc., all affecting membrane transport properties. Reproducibility issues are among the concern in MOF membrane processing as the defect density of polycrystalline membranes is hardly controllable. Even after careful manipulation of synthesis conditions, one may end up with membranes with drastically different performances.

A simple caulking method can be adopted to improve membrane reproducibility and minimize grain boundary defects. Henis and Tripodi first developed the caulking technology in the late 1970s, and the technique has been widely practiced in the industry to repair pinholes and other defects of polymer membranes [214]. Covering MOF membrane layers with caulking materials such as silicone rubber (e.g., PDMS) can improve separation performances of the membranes. Pure PDMS has high C_3H_6 permeability of around 7169 Barrer but low C_3H_6/C_3H_8 selectivity of 1.1 [142,215]. For C_3H_6/C_3H_8 separation, coating a thin layer of PDMS on top of the ZIF-8 membrane layer will not severely retard gas flux of the membranes. Li et al. [142] improved reproducibility and C_3H_6/C_3H_8 separation factor of 12 different ZIF-8 membrane samples synthesized from different batches by coating the membranes with PDMS. Selectivity of defective ZIF-8 membranes (initial selectivity of 2) increased to at least 40 after PDMS coating step. PDMS coating penetrated into the underneath of polycrystalline layer and blocked the inter-crystalline grain boundary defects, resulting in improved separation performances. A recently published work by Hua et al. [216] found that applying vacuum during PDMS coating step promotes infiltration of the PDMS into inter-crystalline region of ZIF-8 and increase interfacial contact between PDMS and ZIF-8. This resulted in higher and more consistent selectivity improvements.

In addition to defect minimization, hydrophobic nature of PDMS provides high water repellency, which improves membrane hydrolytic stability. Separation performances of the PDMS-coated ZIF-8 membranes remained unaltered for at least 7 days of operation under humid state feed gas at 35 °C and 6 bar transmembrane pressure compared to those without coating [217]. Other than PDMS, different polymers have also been used to plug polycrystalline membrane defects. Caro and co-workers [218] coated a thin Matrimid® layer on UiO-66 membranes and observed H_2/CH_4 selectivity improved from 12 to 80. The author attributes the selectivity improvement to pore narrowing from the infusion of Matrimid® into UiO-66 frameworks and plugging of membrane microdefects. However, H_2 permeances of the UiO-66/Matrimid® composite membranes severely dropped due to the low H_2 permeability of Matrimid®.

The membrane can also form defects during handling resulting in deterioration in membrane performances. Given the fact that MOF membranes eventually form defects, it is desirable for the membrane to be *in-situ* healed or sealed without disassembling them from membrane modules. Hamid et al. [133] improved the C_3H_6/C_3H_8 separation factor of ZIF-8 membranes pre-assembled into membrane module from 2 to 55 by passing a dilute PDMS solution through the bore of the hollow fibers. In this case, ZIF-8 membranes grown on the bore of the hollow fibers are beneficial as it allows for more straightforward defect sealing via a simple flow processing. Defect healing of the ZIF-8 membranes grown on α-Al_2O_3 discs has also been demonstrated but has never been performed on hollow fibers or planar supports that are pre-assembled in modules [219]. Kwon et al. [219] performed ZIF-8 membrane defect healing by subjecting defective ZIF-8 membranes to Zn and 2-methylimidazole

precursor solutions in a counter-diffusion manner inside a custom made diffusion cell. After defect healing, inter-crystalline gaps of the membranes were filled with ZIF-8 crystals. Unfortunately, the performances of healed ZIF-8 membranes were not fully restored to their original values due to insufficient healing.

Other than caulking method, membrane community is urged to look for innovative strategies to heal and seal MOF membrane defects, especially after module assembly. Another option to consider for future research is the fabrication of MOF glass membranes to completely eliminate membrane grain boundary issues. MOF glass membranes have steadily captured interest from the scientific community. MOF glass membranes are fabricated by solid-liquid transition followed by quenching the liquid MOF. Several ZIFs, including ZIF-62 and ZIF-4, were found to show this behavior [220]. Wang et al. [220] fabricated ZIF-62 glass membranes on alumina support showing high H_2/CH_4 and CO_2/N_2 selectivities owing to the absence of the non-selective grain boundaries. However, one of the concerns in this growing area is the limited number of ZIFs showing similar behavior.

3.5. Membrane performances under the relevant industrial conditions

Membrane performances under elevated pressure need to be carefully evaluated considering that most of the gases to be processed are pressurized. For example, pipeline pressure at purge stream of the chemical reactor (application area: C_3H_6/C_3H_8 membrane recovery unit) or the outlet of hydrocarbon cracker in the refinery (application area: C_3H_6/C_3H_8 membrane-distillation unit) is at high pressure of 20 bar [221,222]. For post-combustion CO_2 capture application using membrane, flue gas pressure needs to be raised to 5–10 bar to provide a sufficient driving force [3,45]. Similarly, H_2 mixtures from a methane reforming unit (H_2/CH_4), an ammonia reactor (H_2/N_2), and a water gas shift reactor (H_2/CO_2) are all under high pressure. For these applications, high-performance MOF membranes must show steady performances under high-pressure conditions throughout the entire membrane service life (3–5 years) [48]. Despite a considerable body of published works on MOF membranes in the past years, investigation of long term performances of MOF membranes under high pressure conditions is inadequate.

In most studies, gas permeation measurements of MOF membranes were mostly limited to room temperature conditions under atmospheric pressure. Based on our review, the highest transmembrane pressure tested for ZIF-8 membranes for H_2 purification and C_3H_6/C_3H_8 separations is at 9 bar [223,224]. Eum et al. [223] observed a steady decline in C_3H_6 permeance from 55 GPU to 27 GPU and in C_3H_6/C_3H_8 separation factor from 180 to 90 when transmembrane pressure was raised to 9 bar. Nonetheless, the membrane performances were still attractive for commercial applications. In another study, Li et al. [75] found that C_3H_6 permeance and C_3H_6/C_3H_8 separation factor of ZIF-8 membranes grown on PVDF hollow fibers decreased by 25% and 70%, respectively, as the feed gas pressure was increased to 9 bar shown in Fig. 32a. Hou et al. [144] reported a significant decrease in C_3H_6/C_3H_8 separation factor by 89% when testing bimetallic Co_{18}-Zn_{82}-ZIF-8 membranes under feed pressure of only 2.5 bar. Based on the above studies, deterioration in ZIF-8 membrane performances at elevated pressure is an issue that needs to be dealt with.

Reduction in C_3H_6 permeance and C_3H_6/C_3H_8 selectivity under high-pressure conditions was due to 'swing effects' of 2-methyimdazole (2-mIm) linkers and structural changes of the frameworks [119]. The 'swing effects' induce methyl groups of 2-mIm linkers to rotate from inside towards outside the aperture window, allowing larger molecules (i.e., C_3H_8) to diffuse into the cages under high pressure [119]. Also, there will be fewer absorbed C_3H_6 and C_3H_8 on the ZIF-8 surface due to

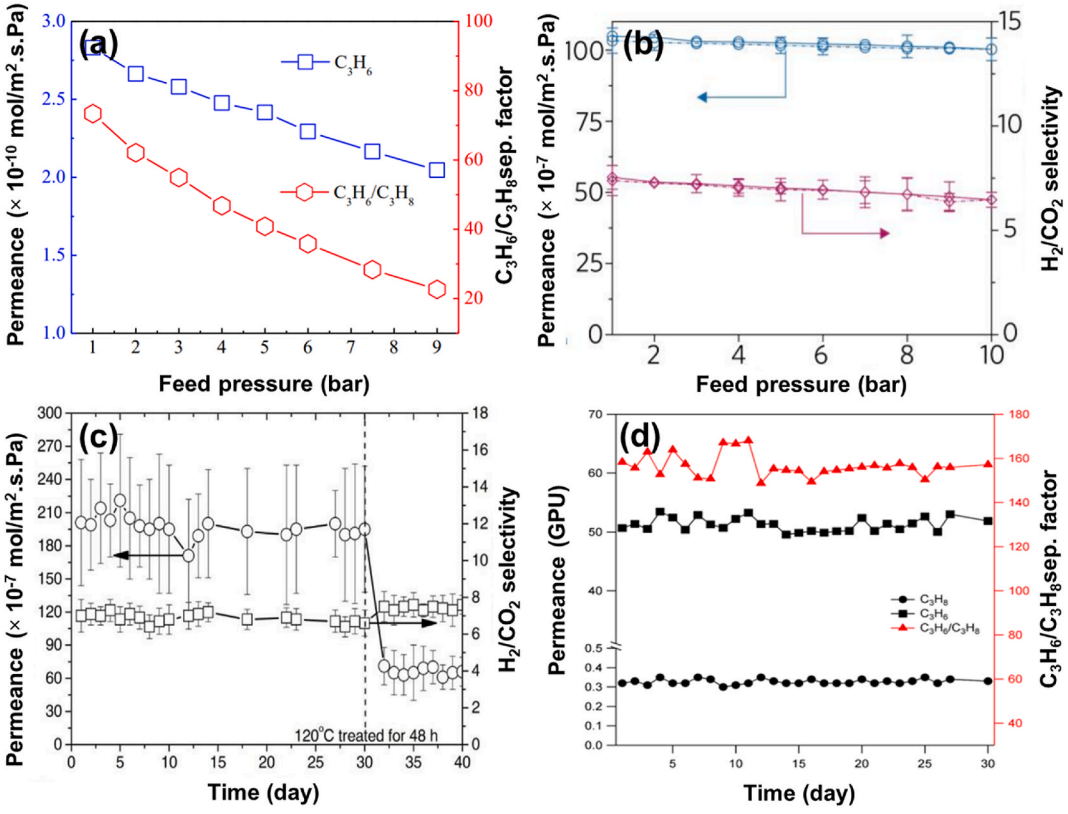

Fig. 32. (a) Binary C_3H_6/C_3H_8 permeances and selectivities of ZIF-8 membranes on PVDF hollow fibers as a function of pressure. (b) H_2 and CO_2 single gas permeances and selectivities of ZIF-8 membranes on PVDF hollow fibers as a function of pressure. Long-term stability of ZIF-8 membranes on (c) PVDF hollow fibers and (d) Torlon® hollow fibers. Reprinted with permission from Ref. [75] Copyright 2017 Springer Nature, ref. [224] Copyright 2019 American Chemical Society, ref. [225] Copyright 2016 Wiley VCH and ref. [223] Copyright 2016 American Chemical Society.

the non-linear adsorption of the gas penetrants in ZIF-8 frameworks [119,226]. A performance decline presents a huge concern, especially when transitioning to a pressure condition much closer to the industrial requirements. For non-condensable gases such as H_2, gas permeances through ZIF-8 membranes appear to be less sensitive to feed gas pressure. H_2 permeance and H_2/CO_2 selectivity reduction of 3% and 10%, respectively, were observed upon increasing feed gas pressure to 10 bar [224].

Pressure-induced reorientation of 2-mIm ligands of ZIF-8 can be suppressed by coating the membrane with a caulking layer. This helps to mitigate unwanted pressure effects and minimize deterioration in ZIF-8 molecular sieving properties [119]. At feed pressure of 7 bar, Li and co-workers [217] observed C_3H_6/C_3H_8 separation factor increased from 93 to 105 (~11% increase) for the PDMS-coated ZIF-8 membranes as oppose to ~80% decrease in C_3H_6/C_3H_8 separation factor for the uncoated membranes. High C_3H_6/C_3H_8 selectivity of 100 was maintained at 7 bar feed pressure for 60 days suggesting that the effect is long-lasting. The increase in C_3H_6/C_3H_8 separation factor for the PDMS-coated ZIF-8 membranes at higher feed pressure was opposite to the general observation of polycrystalline membranes permeation behavior with respect to pressure. They speculated that ZIF-8 frameworks at the outermost layer that was in direct contact with PDMS behaved as if they were rigid, therefore, not affected by the feed gas pressure. PDMS coating was also applied to ZIF-8 membranes grown α-Al_2O_3 tubes. The coated membranes showed similar permeation behavior to those reported by Li and co-workers [142,217] (Fig. 33). The results were encouraging. Nonetheless, enabling the ZIF-8 membrane to be operated at high pressures (~15–20 bar) still demands more research attention.

Ideally, commercial MOF membranes should exhibit steady performances during service throughout the entire membrane lifetime of three to five years [48]. As depicted in Fig. 32c, separation performances of ZIF-8 membranes for H_2/CO_2 were relatively stable under a continuous operation of up to 30 days [225]. Similarly, C_3H_6/C_3H_8 separation performances of ZIF-8 membranes prepared by Nair's group [223] remained unchanged for 30 days (Fig. 32d). Meanwhile, C_3H_6/C_3H_8 selectivity of PDMS-coated ZIF-8 membrane by Li et al. [217] remain constant at 100 for 2 months at a feed pressure of 7 bar. Recently, Li and co-workers [182] found that ZIF-8 membranes grown on flat α-Al_2O_3 substrates maintained a consistent performance for 6 months (4350 h). The as-prepared ZIF-8 membranes were first subjected to continuous permeation testing at 25 °C and 1 bar for 900 h. The membranes were then stored at room temperature for 2880 h. After that, the membranes were tested again at a temperature of 50 °C and pressure of 7 bar for 64 h and finally at a temperature of 25 °C and pressure of 1 bar for 570 h [182]. The membranes did not show any deterioration in separation performances throughout the entire test. Long term stabilities of the prepared ZIF-8 membranes were promising for scale-up.

For the gas separation test, the Wicke-Kallenbach setup is the most commonly used method to measure performances of the prepared MOF membranes. In a typical binary test, a 50/50 mixture of gases is introduced in the feed side while a sweep gas (e.g., Ar, He, and N_2) feeds in the permeate side. In most cases, the pressure on both sides is maintained at ~1 bar. A purging gas is required to sweep away permeating gas for analysis and prevent excessive gas build-up, ensuring transport property measurements are carried out at the linear adsorption region of MOFs. While the Wicke-Kallenbach setup is indispensable for fundamental studies, membrane researchers should recognize the limitation of the setup in industrial gas separation because gas purging is needed. The idea of having purge gas to improve membrane separation performances in a commercial-scale membrane unit is possible only when the permeated gas is not a product and has no real value, and exists at a low concentration in the feed gas. Li et al. [227] studied the effect of purging gas in the CO_2 removal process. A three-component gas mixture of O_2 (56%), N_2 (40%), and CO_2 (4%) was passed through a silicone flat sheet membrane. N_2 was used as purging gas at the permeate stream. Experimental data and mathematical modeling results showed the introduction of purge gas at the permeate side improved CO_2 depletion from the feed gas significantly when running the system at a pressure ratio of 10.

If the permeated gas holds a commercial value, purging gas cannot be used, and without them, a departure from ideal separation performance will occur. This was observed in a study by Li et al. [142]. Without purging gas, the measured C_3H_6/C_3H_8 selectivity of the membrane was only 26, which is significantly lower than those tested with purging gas (C_3H_6/C_3H_8 separation factor of 76). This phenomenon is regarded as concentration polarization, where a buildup of C_3H_6 at the permeate side reduces the concentration gradient of C_3H_6. It is clear that the use of sweep gas can result in an overestimation of the true performance of ZIF membranes. When it comes to the process design of the membrane system, it would be more meaningful to use a more realistic performance indicator instead of ideal membrane performance.

The majority of works still focus on single and binary gas permeation

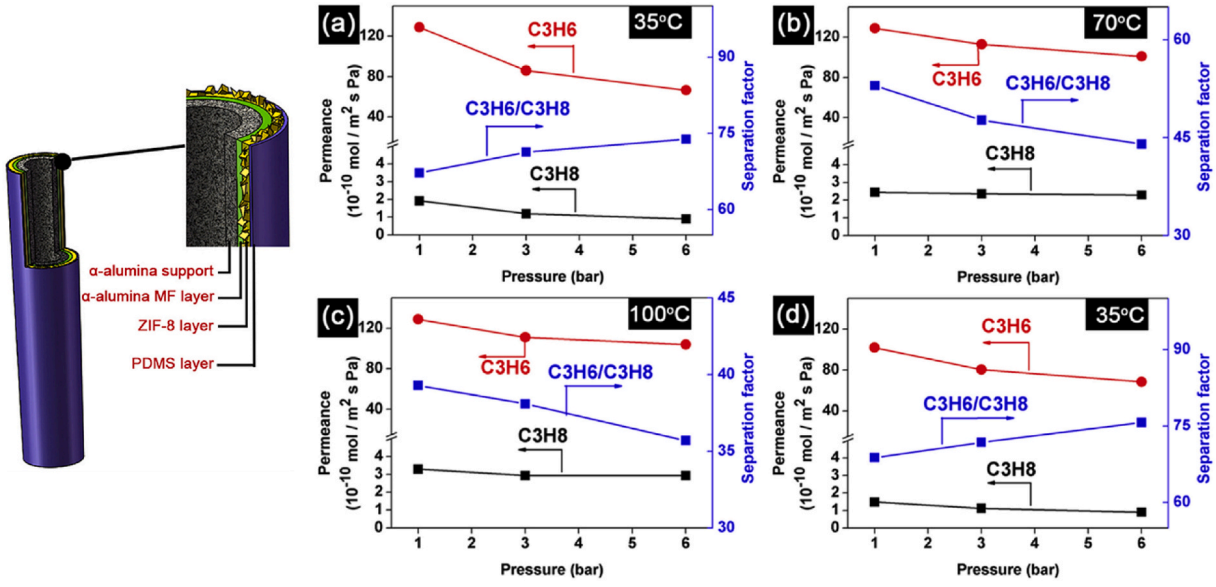

Fig. 33. Schematic illustration of PDMS coating of ZIF-8 membranes on α-alumina tubes. Binary C_3H_6/C_3H_8 separation performances of the PDMS-coated membranes at (a) 35 °C (b) 70 °C (c) 100 °C and (d) return to 35 °C. Reproduced with permission from Ref. [142] Copyright 2019 Elsevier B.V.

measurements to access MOF membrane performances. However, it should be noted that industrial feed gases are much more complex. For example, flue gas from post-combustion normally contains moisture and a trace amount of acidic gases (e.g., SO_2, NO_2, etc.). For C_3H_6/C_3H_8 separation, gases in the downstream of a refinery cracker also contain a mixture of other gases (e.g., H_2, H_2O, C_2H_4, C_2H_6, C_4 mixture, etc.). Thus, multicomponent permeation testing of the membrane under a practical condition demands more research attention. For a starter, membrane communities are suggested to pay attention to ternary/quaternary mixture during separation measurements to observe any deviation in membrane selectivity and permeance. Ma et al. [182] investigated the effect of other components on the performances of ZIF-8 membranes. The membranes remained C_3H_6-selective under coking dry gas feed stream (i.e., C_3H_6 (20.3%), C_3H_8 (49.6%), C_4H_8 (10.1%), n-C_4H_{10} (16.0%) and i-C_4H_{10} (4.0%)) with C_3H_6/C_3H_8 selectivity of 160 which are extremely attractive for commercial applications.

Major efforts should also be directed toward exploring the effects of minor impurities and water vapor in the feed stream and looking for possible mitigation strategies. Unlike zeolites, MOF suffers from poor hydrothermal stability. Most of the reported MOFs to date cannot survive at high humidity, and some cannot even exist under the inert environment [228]. For example, MOF-5 readily transforms to an amorphous phase under ambient humidity. ZIF-8, on the other hand, is relatively stable at high temperatures and atmospheres with moderate humidity [229,230]. Take C_3H_6/C_3H_8 separation as an example, ZIF-8 membrane is quite robust at both on-stream (35 °C, 1 bar) and off-stream storage conditions (relative humidity: 15.6–18.3%, temperature: 23–24 °C) [231]. The membrane, however, suffers from crystallinity loss in aqueous conditions [232–234]. For post-combustion CO_2 capture application, flue gas of coal-fired power plant contains a relatively high amount of water vapor (15%), along with CO_2 (13%), N_2 (69%), O_2 (2.4%), and a trace amount of SO_x and NO_x, all available at a pressure of 1 bar and temperature of 57 °C [235]. In addition to being CO_2-selective, the MOF membranes must also show good long-term stabilities under humid acidic conditions. As previously mentioned, ZIF membranes appear to be relatively stable under dry room temperature conditions. However, as stated in a number of publications, ZIF crystals and membranes are not particularly stable under hydrothermal or humid CO_2 and SO_2 conditions [234,236–238]. The formation of sulfurous-sulfuric acid complexes attacks the Zn-N coordination bonds of ZIFs, which results in a loss in porosity [237,238]. Support surface properties under humid conditions can also affect the stabilities of ZIF membranes.

According to Kim et al. [239], ZIF-7 membranes on α-Al_2O_3 discs experienced structural degradations under mild hydrothermal conditions attributable to the surface acidity of the supports. Acidic metal oxide surfaces under humid conditions catalyzed the breaking of Zn–benzimidazole coordination bonds resulting in structural degradations of ZIF-7. In another work, it is found that the presence of a trace amount of SO_2 could significantly reduce the CO_2/N_2 selectivity of the ZIF-68 membrane [240]. Unless mitigation protocols are proposed, the applications of MOF membranes are likely to be limited to those feed gases with a trace amount of water vapor. Once again, we must remind the membrane communities to take into consideration the above-mentioned aspect of the membranes as we begin to transition to more realistic industry conditions.

3.6. Mechanical property evaluation of MOF-based membranes

Like any other membranes, eventually, the prepared MOF membranes must be assembled into modules. During the module assembly process, mechanical accidents may occur and damage the hollow fiber membranes. On a commercial scale, damaged membranes can result in product loss and/or product with insufficient purity. The membranes need to be handled carefully during the module assembly process. Bending of the membranes should be avoided as both MOF and support layers have different mechanical properties [141]. This may not be a big issue for membranes grown on ceramic tubes because they are rigid and possesses excellent mechanical properties. For instance, Sun et al. [124] used commercial porous ceramic tubes to grow ZIF-8 membrane that possesses radial crushing strength greater than 40 MPa.

However, membranes grown on flexible polymer substrates may need high flexibility to tolerate a high degree of bending without damage. Several groups have evaluated the mechanical properties of MOF membranes grown on polymeric supports. Mechanical testing of MOF membranes is performed by subjecting the supported MOF membranes to a simple bending and/or elongation. This is followed by gas separation measurements and membrane microstructure evaluation [141]. The degree of bending is represented by bending curvature ($K = 1/r$), which can be defined as a reciprocal of bending radius (r). MOF membranes are considered to possess excellent mechanical properties if they do not show any deformation, detachment, crack formation, and maintain similar separation performances after the bending/elongation test.

Chen and co-workers [225] investigated the mechanical properties of ZIF-8 membranes supported on PVDF hollow fibers. The membrane H_2/CO_2 separation performances were not altered after bending the membrane to curvature of 77 m^{-1}. The integrity of the membrane is well-preserved after 3% elongation, which corresponds to the tensile stress of 3.5 MPa. Meanwhile, polysulfone-supported ZIF-8 membranes by Ma et al. [241] and polyethersulfone-supported ZIF-8 membranes Zhang et al. [242] showed good separation performances after bending with a curvature of ~36 m^{-1} and ~46 m^{-1}, respectively. However, these studies focused on the separation of small molecules (e.g., H_2/CO_2 and CO_2/CH_4) where differences between molecule sizes are large. In this case, the existence of microcracks and the worsening of inter-crystalline gaps due to bending may not make a significant difference. It may not be the same for the separation of C_3H_6 from C_3H_8, where the size difference between the molecules is only 0.2 Å. In this case, even tiny defects can result in a sharp decline in separation performances.

Recently, Wang and coworkers [141] reported polypropylene-supported ZIF-8 membranes exhibiting a high degree of flexibility under compressive or tensile stress. Porous polypropylene was selected as substrates for ZIF-8 membranes synthesis for having a relatively similar Young's modulus to that of ZIF-8. This allows for greater flexibility, thus minimizing unwanted defect formation during the synthesis, handling, and module assembly process. No visible cracks were observed after bending the membrane with a curvature of 333–666 m^{-1}. Cracks, however, began to appear when bending curvature was increased to 1000 m^{-1}. The C_3H_6/C_3H_8 separation factor remained unchanged at 105 up to a bending curvature of 92 m^{-1}. Excellent mechanical properties of polypropylene-supported ZIF-8 membranes are highly desirable for industrial applications. The study also provides an important insight into the fabrication of flexible MOF membranes, which opens the possibility of packaging the membrane into spiral-wound modules.

4. Conclusions

In the past decade, numerous research efforts have gravitated towards MOF-based gas separations membranes, particularly ZIF-8. Compared with other MOFs, it seems ZIF-8 is the best candidate for C_3H_6/C_3H_8 separation and a competitive candidate for other gas separations as well. ZIF-8 has largely surpassed polymeric membranes in terms of performances for C_3H_6/C_3H_8 separation. The majority of other MOF-based membranes cannot provide comparable performances not only for C_3H_6/C_3H_8 separation but also other types of separations. A constant research effort has pushed the performances of ZIF-8 membranes for C_3H_6/C_3H_8 separation in terms of both selectivity and permeance to a point where the technology can be seriously considered as an attractive candidate to replace C_3 distillation. However, engineering challenges with respect to membrane scale-up demands further

research. Among the major barriers preventing a commercial scale deployment of the technology is the difficulty of implementing a continuous processing to fabricate a large area membrane with good reproducibility. The difficulty is exacerbated when developing a full module with hollow fiber geometry cost-effectively. For future research, a systematic study on the scale-up production of MOF membrane is suggested as the primary research focus rather than continually pushing the laboratory scale separation performances, which requires a collaborative effort between academia, government agencies, and industries.

Declaration of competing interest

The authors declare that they have no known competing financial interests or personal relationships that could have appeared to influence the work reported in this paper.

Acknowledgements

The authors acknowledge the financial supports of the Universiti Putra Malaysia under Geran Inisiatif Putra Muda (project code – GP-IPM/2020/9689700, vot no. – 9689700). H.-K.J. acknowledges the financial support from the National Science Foundation (CBET-1929596). This publication was made possible in part by NPRP grant # 12S-0209-190064 from the Qatar National Research Fund (a member of Qatar Foundation). Z. Lai acknowledges the financial support from King Abdullah University of Science and Technology URF/1/3769-01.

Appendix A. Supplementary data

Supplementary data related to this article can be found at https://doi.org/10.1016/j.memsci.2021.119802.

References

[1] T. Yang, T.S. Chung, High performance ZIF-8/PBI nano-composite membranes for high temperature hydrogen separation consisting of carbon monoxide and water vapor, Int. J. Hydrogen Energy 38 (2013) 229–239, https://doi.org/10.1016/j.ijhydene.2012.10.045.

[2] F. Jeremias, V. Lozan, S.K. Henninger, C. Janiak, Programming MOFs for water sorption: amino-functionalized MIL-125 and UiO-66 for heat transformation and heat storage applications, Dalton Trans. 42 (2013) 15967–15973, https://doi.org/10.1039/C3DT51471D.

[3] T.C. Merkel, H. Lin, X. Wei, R. Baker, Power plant post-combustion carbon dioxide capture: an opportunity for membranes, J. Membr. Sci. 359 (2010) 126–139, https://doi.org/10.1016/j.memsci.2009.10.041.

[4] R.W. Baker, K. Lokhandwala, Natural gas processing with membranes: an overview, Ind. Eng. Chem. Res. 47 (2008) 2109–2121, https://doi.org/10.1021/ie071083w.

[5] J.-R. Li, R.J. Kuppler, H.-C. Zhou, Selective gas adsorption and separation in metal-organic frameworks, Chem. Soc. Rev. 38 (2009) 1477–1504, https://doi.org/10.1039/B802426J.

[6] S. Kitagawa, Porous materials and the age of gas, Angew. Chem. Int. Ed. 54 (2015) 10686–10687, https://doi.org/10.1002/anie.201503835.

[7] Y. He, R. Krishna, B. Chen, Metal–organic frameworks with potential for energy-efficient adsorptive separation of light hydrocarbons, Energy Environ. Sci. 5 (2012) 9107–9120, https://doi.org/10.1039/C2EE22858K.

[8] X. Li, Y. Liu, J. Wang, J. Gascon, J. Li, B. Van der Bruggen, Metal-organic frameworks based membranes for liquid separation, Chem. Soc. Rev. 46 (2017) 7124–7144, https://doi.org/10.1039/C7CS00575J.

[9] D. Speybrouck, E. Lipka, Preparative supercritical fluid chromatography: a powerful tool for chiral separations, J. Chromatogr. A 1467 (2016) 33–55, https://doi.org/10.1016/j.chroma.2016.07.050.

[10] Q. Qian, P.A. Asinger, M.J. Lee, G. Han, K. Mizrahi Rodriguez, S. Lin, F. M. Benedetti, A.X. Wu, W.S. Chi, Z.P. Smith, MOF-based membranes for gas separations, Chem. Rev. 120 (2020) 8161–8266, https://doi.org/10.1021/acs.chemrev.0c00119.

[11] M. Galizia, W.S. Chi, Z.P. Smith, T.C. Merkel, R.W. Baker, B.D. Freeman, 50th anniversary perspective: polymers and mixed matrix membranes for gas and vapor separation: a review and prospective opportunities, Macromolecules 50 (2017) 7809–7843, https://doi.org/10.1021/acs.macromol.7b01718.

[12] E.M. Hampe, D.M. Rudkevich, Exploring reversible reactions between CO_2 and amines, Tetrahedron 59 (2003) 9619–9625, https://doi.org/10.1016/j.tet.2003.09.096.

[13] C.H. Yu, C.H. Huang, C.S. Tan, A review of CO_2 capture by absorption and adsorption, Aerosol Air Qual. Res. 12 (2012) 745, https://doi.org/10.4209/aaqr.2012.05.0132.

[14] D.F. Sanders, Z.P. Smith, R. Guo, L.M. Robeson, J.E. McGrath, D.R. Paul, B. D. Freeman, Energy-Efficient polymeric gas separation membranes for a sustainable future: a review, Polymer 54 (2013) 4729–4761, https://doi.org/10.1016/j.polymer.2013.05.075.

[15] Z. Lai, Development of ZIF-8 membranes: opportunities and challenges for commercial applications, Curr. Opin. Chem. Eng. 20 (2018) 78–85, https://doi.org/10.1016/j.coche.2018.03.002.

[16] P. Angelini, T. Armstrong, R. Counce, W. Griffith, T. Klasson, G. Muralidharan, C. Narula, V. Sikka, G. Closset, G. Keller, Materials for Separation Technologies: Energy and Emission Reduction Opportunities, vol. 103, DOE, EERE Office, Washington, DC, 2005.

[17] J.L. Humphrey, G.E. Keller, Separation Process Technology, McGraw-Hill, New York, 1997.

[18] J.A. Chavez Velasco, M. Tawarmalani, R. Agrawal, Systematic analysis reveals thermal separations are not necessarily most energy intensive, Joule 5 (2021) 330–343, https://doi.org/10.1016/j.joule.2020.12.002.

[19] D.S. Sholl, R.P. Lively, Seven chemical separations to change the world, Nature 532 (2016) 435–437, https://doi.org/10.1038/532435a.

[20] E. National Academies of Sciences, Medicine, A Research Agenda for Transforming Separation Science, 2019.

[21] A.K. Jana, Advances in heat pump assisted distillation column: a review, Energy Convers. Manag. 77 (2014) 287–297, https://doi.org/10.1016/j.enconman.2013.09.055.

[22] J. Lee, Y. Son, K.S. Lee, W. Won, Economic analysis and environmental impact assessment of heat pump-assisted distillation in a gas fractionation unit, Energies 12 (2019), https://doi.org/10.3390/en12050852.

[23] A.A. Kiss, R. Smith, Rethinking energy use in distillation processes for a more sustainable chemical industry, Energy 203 (2020), 117788, https://doi.org/10.1016/j.energy.2020.117788.

[24] L. Joseph, L.K. Boateng, J.R.V. Flora, Y.-G. Park, A. Son, M. Badawy, Y. Yoon, Removal of bisphenol A and 17α-ethinyl estradiol by combined coagulation and adsorption using carbon nanomaterials and powdered activated carbon, Separ. Purif. Technol. 107 (2013) 37–47, https://doi.org/10.1016/j.seppur.2013.01.012.

[25] P. Westerhoff, Y. Yoon, S. Snyder, E. Wert, Fate of endocrine-disruptor, pharmaceutical, and personal care product chemicals during simulated drinking water treatment processes, Environ. Sci. Technol. 39 (2005) 6649–6663, https://doi.org/10.1021/es0484799.

[26] L. Joseph, J. Heo, Y.-G. Park, J.R.V. Flora, Y. Yoon, Adsorption of bisphenol A and 17α-ethinyl estradiol on single walled carbon nanotubes from seawater and brackish water, Desalination 281 (2011) 68–74, https://doi.org/10.1016/j.desal.2011.07.044.

[27] C. Jung, X. Chen, J. Cai, H. Lei, I. Yun, J. Kim, Boundary-preserving stereo matching with certain region detection and adaptive disparity adjustment, J. Vis. Commun. Image Represent. 33 (2015) 1–9, https://doi.org/10.1016/j.jvcir.2015.08.010.

[28] Y.A.J. Al-Hamadani, K.H. Chu, J.R.V. Flora, D.-H. Kim, M. Jang, J. Sohn, W. Joo, Y. Yoon, Sonocatalytical degradation enhancement for ibuprofen and sulfamethoxazole in the presence of glass beads and single-walled carbon nanotubes, Ultrason. Sonochem. 32 (2016) 440–448, https://doi.org/10.1016/j.ultsonch.2016.03.030.

[29] J.-K. Im, J. Yoon, N. Her, J. Han, K.-D. Zoh, Y. Yoon, Sonocatalytic-TiO_2 nanotube, Fenton, and CCl_4 reactions for enhanced oxidation, and their applications to acetaminophen and naproxen degradation, Separ. Purif. Technol. 141 (2015) 1–9, https://doi.org/10.1016/j.seppur.2014.11.021.

[30] J. Heo, L. Joseph, Y. Yoon, Y.-G. Park, N. Her, J. Sohn, S.-H. Yoon, Removal of micropollutants and NOM in carbon nanotube-UF membrane system from seawater, Water Sci. Technol. 63 (2011) 2737–2744, https://doi.org/10.2166/wst.2011.602.

[31] S. Kim, K.H. Chu, Y.A.J. Al-Hamadani, C.M. Park, M. Jang, D.-H. Kim, M. Yu, J. Heo, Y. Yoon, Removal of contaminants of emerging concern by membranes in water and wastewater: a review, Chem. Eng. J. 335 (2018) 896–914, https://doi.org/10.1016/j.cej.2017.11.044.

[32] Y. Liu, Z. Yang, C. Yu, X. Gu, N. Xu, Effect of seeding methods on growth of NaA zeolite membranes, Microporous Mesoporous Mater. 143 (2011) 348–356, https://doi.org/10.1016/j.micromeso.2011.03.016.

[33] X. Wang, Y. Chen, C. Zhang, X. Gu, N. Xu, Preparation and characterization of high-flux T-type zeolite membranes supported on YSZ hollow fibers, J. Membr. Sci. 455 (2014) 294–304, https://doi.org/10.1016/j.memsci.2014.01.006.

[34] X. Wang, Z. Yang, C. Yu, L. Yin, C. Zhang, X. Gu, Preparation of T-type zeolite membranes using a dip-coating seeding suspension containing colloidal SiO_2, Microporous Mesoporous Mater. 197 (2014) 17–25, https://doi.org/10.1016/j.micromeso.2014.05.046.

[35] Y.S. Lin, M.C. Duke, Recent progress in polycrystalline zeolite membrane research, Curr. Opin. Chem. Eng. 2 (2013) 209–216, https://doi.org/10.1016/j.coche.2013.03.002.

[36] N. Rangnekar, N. Mittal, B. Elyassi, J. Caro, M. Tsapatsis, Zeolite membranes – a review and comparison with MOFs, Chem. Soc. Rev. 44 (2015) 7128–7154, https://doi.org/10.1039/C5CS00292C.

[37] L.M. Robeson, Correlation of separation factor versus permeability for polymeric membranes, J. Membr. Sci. 62 (1991) 165, https://doi.org/10.1016/0376-7388(91)80060-J.

[38] R. Swaidan, B. Ghanem, I. Pinnau, Fine-tuned intrinsically ultramicroporous polymers redefine the permeability/selectivity upper bounds of membrane-based air and hydrogen separations, ACS Macro Lett. 4 (2015) 947–951, https://doi.org/10.1021/acsmacrolett.5b00512.

[39] D.T. Coker, B.D. Freeman, G.K. Fleming, Modeling multicomponent gas separation using hollow-fiber membrane contactors, AIChE J. 44 (1998) 1289–1302, https://doi.org/10.1002/aic.690440607.

[40] L.M. Robeson, The upper bound revisited, J. Membr. Sci. 320 (2008) 390, https://doi.org/10.1016/j.memsci.2008.04.030.

[41] B. Comesaña-Gándara, J. Chen, C.G. Bezzu, M. Carta, I. Rose, M.C. Ferrari, E. Esposito, A. Fuoco, J.C. Jansen, N.B. McKeown, Redefining the Robeson upper bounds for CO_2/CH_4 and CO_2/N_2 separations using a series of ultrapermeable benzotriptycene-based polymers of intrinsic microporosity, Energy Environ. Sci. 12 (2019) 2733–2740, https://doi.org/10.1039/C9EE01384A.

[42] L.M. Robeson, M.E. Dose, B.D. Freeman, D.R. Paul, Analysis of the transport properties of thermally rearranged (TR) polymers and polymers of intrinsic microporosity (PIM) relative to upper bound performance, J. Membr. Sci. 525 (2017) 18–24, https://doi.org/10.1016/j.memsci.2016.11.085.

[43] H. Lin, M. Yavari, Upper bound of polymeric membranes for mixed-gas CO_2/CH_4 separations, J. Membr. Sci. 475 (2015) 101–109, https://doi.org/10.1016/j.memsci.2014.10.007.

[44] S. Park, M.R. Abdul Hamid, H.-K. Jeong, Highly propylene-selective mixed-matrix membranes by in situ metal-organic framework formation using a polymer-modification strategy, ACS Appl. Mater. Interfaces 11 (2019) 25949–25957, https://doi.org/10.1021/acsami.9b07106.

[45] Y. Ding, Perspective on gas separation membrane materials from process economics point of view, Ind. Eng. Chem. Res. 59 (2019) 556–568, https://doi.org/10.1021/acs.iecr.9b05975.

[46] P.E. Jones, U.S. Patent. US 20060151669, 2006.

[47] E. Esposito, L. Dellamuzia, U. Moretti, A. Fuoco, L. Giorno, J.C. Jansen, Simultaneous production of biomethane and food grade CO_2 from biogas: an industrial case study, Energy Environ. Sci. 12 (2019) 281–289, https://doi.org/10.1039/C8EE02897D.

[48] R.W. Baker, B.T. Low, Gas separation membrane materials: a perspective, Macromolecules 47 (2014) 6999–7013, https://doi.org/10.1021/ma501488s.

[49] M.R. Abdul Hamid, T.C. Shean Yaw, M.Z. Mohd Tohir, W.A. Wan Abdul Karim Ghani, P.D. Sutrisna, H.-K. Jeong, Zeolitic imidazolate framework membranes for gas separations: current state-of-the-art, challenges, and opportunities, J. Ind. Eng. Chem. 98 (2021) 17–41, https://doi.org/10.1016/j.jiec.2021.03.047.

[50] D.-Y. Koh, B.A. McCool, H.W. Deckman, R.P. Lively, Reverse osmosis molecular differentiation of organic liquids using carbon molecular sieve membranes, Science 353 (2016) 804–807, https://doi.org/10.1126/science.aaf1343.

[51] N. Rangnekar, N. Mittal, B. Elyassi, J. Caro, M. Tsapatsis, Zeolite membranes - a review and comparison with MOFs, Chem. Soc. Rev. 44 (2015) 7128–7154, https://doi.org/10.1039/C5CS00292C.

[52] M.S. Denny Jr., J.C. Moreton, L. Benz, S.M. Cohen, Metal-organic frameworks for membrane-based separations, Nat. Rev. Mater. 1 (2016), https://doi.org/10.1038/natrevmats.2016.78.

[53] O.M. Yaghi, M.J. Kalmutzki, C. Diercks, Introduction to reticular chemistry, Mol. Front. J. 4 (2019). Wiley-VCH, Weinheim.

[54] O.M. Yaghi, G. Li, H. Li, Selective binding and removal of guests in a microporous metal-organic framework, Nature 378 (1995) 703–706, https://doi.org/10.1038/378703a0.

[55] H. Li, M. Eddaoudi, M. O'Keeffe, O.M. Yaghi, Design and synthesis of an exceptionally stable and highly porous metal-organic framework, Nature 402 (1999) 276–279, https://doi.org/10.1038/46248.

[56] J. Yao, H. Wang, Zeolitic imidazolate framework composite membranes and thin films: synthesis and applications, Chem. Soc. Rev. 43 (2014) 4470–4493, https://doi.org/10.1039/C3CS60480B.

[57] S. Qiu, M. Xue, G. Zhu, Metal-organic framework membranes: from synthesis to separation application, Chem. Soc. Rev. 43 (2014) 6116–6140, https://doi.org/10.1039/C4CS00159A.

[58] S.R. Venna, M.A. Carreon, Metal organic framework membranes for carbon dioxide separation, Chem. Eng. Sci. 124 (2015) 3–19, https://doi.org/10.1016/j.ces.2014.10.007.

[59] Z. Kang, L. Fan, D. Sun, Recent advances and challenges of metal-organic framework membranes for gas separation, J. Mater. Chem. 5 (2017) 10073–10091, https://doi.org/10.1039/C7TA01142C.

[60] B. Seoane, J. Coronas, I. Gascon, M.E. Benavides, O. Karvan, J. Caro, F. Kapteijn, J. Gascon, Metal-organic framework based mixed matrix membranes: a solution for highly efficient CO_2 capture? Chem. Soc. Rev. 44 (2015) 2421–2454, https://doi.org/10.1039/C4CS00437J.

[61] M.A. Carreon, S.R. Venna, Metal-Organic Framework Membranes for Molecular Gas Separations, World Scientific Publishing Europe Ltd, London, 2020.

[62] S.S.Y. Chui, S.M.F. Lo, J.P.H. Charmant, A.G. Orpen, I.D. Williams, A chemically functionalizable nanoporous material $[Cu_3(TMA)_2(H_2O)_3]$(n), Science 283 (1999) 1148–1150, https://doi.org/10.1126/science.283.5405.1148.

[63] M. Eddaoudi, J. Kim, N. Rosi, D. Vodak, J. Wachter, M. O'Keeffe, O.M. Yaghi, Systematic design of pore size and functionality in isoreticular MOFs and their application in methane storage, Science 295 (2002) 469–472, https://doi.org/10.1126/science.1067208.

[64] K.S. Park, Z. Ni, A.P. Côté, J.Y. Choi, R. Huang, F.J. Uribe-Romo, H.K. Chae, M. O'Keeffe, O.M. Yaghi, Exceptional chemical and thermal stability of zeolitic imidazolate frameworks, Proc. Natl. Acad. Sci. U.S.A. 103 (2006) 10186–10191, https://doi.org/10.1073/pnas.0602439103.

[65] R. Banerjee, A. Phan, B. Wang, C. Knobler, H. Furukawa, M. O'Keeffe, O. M. Yaghi, High-throughput synthesis of zeolitic imidazolate frameworks and application to CO_2 capture, Science 319 (2008) 939–943, https://doi.org/10.1126/science.1152516.

[66] J.H. Cavka, S. Jakobsen, U. Olsbye, N. Guillou, C. Lamberti, S. Bordiga, K. P. Lillerud, A new zirconium inorganic building brick forming metal organic frameworks with exceptional stability, J. Am. Chem. Soc. 130 (2008) 13850–13851, https://doi.org/10.1021/ja8057953.

[67] P. Horcajada, T. Chalati, C. Serre, B. Gillet, C. Sebrie, T. Baati, J.F. Eubank, D. Heurtaux, P. Clayette, C. Kreuz, J.-S. Chang, Y.K. Hwang, V. Marsaud, P.-N. Bories, L. Cynober, S. Gil, G. Férey, P. Couvreur, R. Gref, Porous metal-organic-framework nanoscale carriers as a potential platform for drug delivery and imaging, Nat. Mater. 9 (2010) 172–178, https://doi.org/10.1038/nmat2608.

[68] Y. Liu, Z. Ng, E.A. Khan, H.-K. Jeong, C.-b. Ching, Z. Lai, Synthesis of continuous MOF-5 membranes on porous α-alumina substrates, Microporous Mesoporous Mater. 118 (2009) 296–301, https://doi.org/10.1016/j.micromeso.2008.08.054.

[69] H. Guo, G. Zhu, I.J. Hewitt, S. Qiu, "Twin copper source" growth of metal-organic framework membrane: $Cu_3(BTC)_2$ with high permeability and selectivity for recycling H2, J. Am. Chem. Soc. 131 (2009) 1646–1647, https://doi.org/10.1021/ja8074874.

[70] R. Ranjan, M. Tsapatsis, Microporous metal organic framework membrane on porous support using the seeded growth method, Chem. Mater. 21 (2009) 4920–4924, https://doi.org/10.1021/cm902032y.

[71] J. Yao, D. Dong, D. Li, L. He, G. Xu, H. Wang, Contra-diffusion synthesis of ZIF-8 films on a polymer substrate, Chem. Commun. 47 (2011) 2559–2561, https://doi.org/10.1039/C0CC04734A.

[72] A.J. Brown, N.A. Brunelli, K. Eum, F. Rashidi, J.R. Johnson, W.J. Koros, C. W. Jones, S. Nair, Interfacial microfluidic processing of metal-organic framework hollow fiber membranes, Science 345 (2014) 72–75, https://doi.org/10.1126/science.1251181.

[73] O. Shekhah, R. Swaidan, Y. Belmabkhout, M. Du Plessis, T. Jacobs, L.J. Barbour, I. Pinnau, M. Eddaoudi, The liquid phase epitaxy approach for the successful construction of ultra-thin and defect-free ZIF-8 membranes: pure and mixed gas transport study, Chem. Commun. 50 (2014) 2089–2092, https://doi.org/10.1039/C3CC47495J.

[74] H.T. Kwon, H.-K. Jeong, A.S. Lee, H.S. An, T. Lee, E. Jang, J.S. Lee, J. Choi, Defect-induced ripening of zeolitic-imidazolate framework ZIF-8 and its implication to vapor-phase membrane synthesis, Chem. Commun. 52 (2016) 11669–11672, https://doi.org/10.1039/C6CC05433A.

[75] W. Li, P. Su, Z. Li, Z. Xu, F. Wang, H. Ou, J. Zhang, G. Zhang, E. Zeng, Ultrathin metal-organic framework membrane production by gel-vapour deposition, Nat. Commun. 8 (2017) 1–8, https://doi.org/10.1038/s41467-017-00544-1.

[76] X. Ma, P. Kumar, N. Mittal, A. Khlyustova, P. Daoutidis, K.A. Mkhoyan, M. Tsapatsis, Zeolitic imidazolate framework membranes made by ligand-induced permselectivation, Science 361 (2018) 1008–1011, https://doi.org/10.1126/science.aat4123.

[77] G. He, M. Dakhchoune, J. Zhao, S. Huang, K.V. Agrawal, Electrophoretic nuclei assembly for crystallization of high-performance membranes on unmodified supports, Adv. Funct. Mater. 28 (2018), 1707427, https://doi.org/10.1002/adfm.201707427.

[78] S. Zhou, Y. Wei, L. Li, Y. Duan, Q. Hou, L. Zhang, L.-X. Ding, J. Xue, H. Wang, J. Caro, Paralyzed membrane: current-driven synthesis of a metal-organic framework with sharpened propene/propane separation, Sci. Adv. 4 (2018) 1393, https://doi.org/10.1126/sciadv.aau1393.

[79] R. Wei, H.Y. Chi, X. Li, D. Lu, Y. Wan, C.W. Yang, Z. Lai, Aqueously cathodic deposition of ZIF-8 membranes for superior propylene/propane separation, Adv. Funct. Mater. 30 (2020), 1907089, https://doi.org/10.1002/adfm.201907089.

[80] Y. Yoo, H.-K. Jeong, Rapid fabrication of metal organic framework thin films using microwave-induced thermal deposition, Chem. Commun. (2008) 2441–2443, https://doi.org/10.1039/B800061A.

[81] O. Kozachuk, K. Yusenko, H. Noei, Y. Wang, S. Walleck, T. Glaser, R.A. Fischer, Solvothermal growth of a ruthenium metal-organic framework featuring HKUST-1 structure type as thin films on oxide surfaces, Chem. Commun. 47 (2011) 8509–8511, https://doi.org/10.1039/C1CC11107H.

[82] M. Wu, Y. Ai, B. Zeng, F. Zhao, In situ solvothermal growth of metal-organic framework-ionic liquid functionalized graphene nanocomposite for highly efficient enrichment of chloramphenicol and thiamphenicol, J. Chromatogr. A 1427 (2016) 1–7, https://doi.org/10.1016/j.chroma.2015.11.080.

[83] Y. Yoo, Z. Lai, H.-K. Jeong, Fabrication of MOF-5 membranes using microwave-induced rapid seeding and solvothermal secondary growth, Microporous Mesoporous Mater. 123 (2009) 100–106, https://doi.org/10.1016/j.micromeso.2009.03.036.

[84] G.H. Albuquerque, G.S. Herman, Chemically modulated microwave-assisted synthesis of MOF-74(Ni) and preparation of metal-organic framework-matrix based membranes for removal of metal ions from aqueous media, Cryst. Growth Des. 17 (2017) 156–162, https://doi.org/10.1021/acs.cgd.6b01398.

[85] A. Centrone, Y. Yang, S. Speakman, L. Bromberg, G.C. Rutledge, T.A. Hatton, Growth of metal-organic frameworks on polymer surfaces, J. Am. Chem. Soc. 132 (2010) 15687–15691, https://doi.org/10.1021/ja106381x.

[86] J. Caro, Supported zeolite and mof molecular sieve membranes: preparation, characterization, application, in: Zeolites and Zeolite-like Materials, Elsevier, Amsterdam, 2016.

[87] H. Bux, F. Liang, Y. Li, J. Cravillon, M. Wiebcke, J.r. Caro, Zeolitic imidazolate framework membrane with molecular sieving properties by microwave-assisted solvothermal synthesis, J. Am. Chem. Soc. 131 (2009) 16000–16001, https://doi.org/10.1021/ja907359t.

[88] Y. Liu, G. Zeng, Y. Pan, Z. Lai, Synthesis of highly c-oriented ZIF-69 membranes by secondary growth and their gas permeation properties, J. Membr. Sci. 379 (2011) 46–51, https://doi.org/10.1016/j.memsci.2011.05.041.

[89] S.R. Venna, M.A. Carreon, Highly permeable zeolite imidazolate framework-8 membranes for CO_2/CH_4 separation, J. Am. Chem. Soc. 132 (2010) 76–78, https://doi.org/10.1021/ja909263x.

[90] D. Nagaraju, D.G. Bhagat, R. Banerjee, U.K. Kharul, In situ growth of metal-organic frameworks on a porous ultrafiltration membrane for gas separation, J. Mater. Chem. 1 (2013) 8828–8835, https://doi.org/10.1039/C3TA10438A.

[91] A. Huang, H. Bux, F. Steinbach, J. Caro, Molecular-sieve membrane with hydrogen permselectivity: ZIF-22 in LTA topology prepared with 3-aminopropyltriethoxysilane as covalent linker, Angew. Chem. 122 (2010) 5078–5081, https://doi.org/10.1002/ange.201001919.

[92] S. Hermes, F. Schröder, R. Chelmowski, C. Wöll, R.A. Fischer, Selective nucleation and growth of metal-organic open framework thin films on patterned COOH/CF_3− terminated self-assembled monolayers on Au(111), J. Am. Chem. Soc. 127 (2005) 13744–13745, https://doi.org/10.1021/ja053523l.

[93] S. Hermes, D. Zacher, A. Baunemann, C. Wöll, R.A. Fischer, Selective growth and MOCVD loading of small single crystals of MOF-5 at alumina and silica surfaces modified with organic self-assembled monolayers, Chem. Mater. 19 (2007) 2168–2173, https://doi.org/10.1021/cm062854+.

[94] D. Zacher, A. Baunemann, S. Hermes, R.A. Fischer, Deposition of microcrystalline [Cu_3(btc)$_2$] and [Zn_2(bdc)$_2$(dabco)] at alumina and silica surfaces modified with patterned self assembled organic monolayers: evidence of surface selective and oriented growth, J. Mater. Chem. 17 (2007) 2785–2792, https://doi.org/10.1039/B703098C.

[95] Q. Liu, N. Wang, J.r. Caro, A. Huang, Bio-inspired polydopamine: a versatile and powerful platform for covalent synthesis of molecular sieve membranes, J. Am. Chem. Soc. 135 (2013) 17679–17682, https://doi.org/10.1021/ja4080562.

[96] N. Wang, Y. Liu, Z. Qiao, L. Diestel, J. Zhou, A. Huang, J. Caro, Polydopamine-based synthesis of a zeolite imidazolate framework ZIF-100 membrane with high H_2/CO_2 selectivity, J. Mater. Chem. 3 (2015) 4722–4728, https://doi.org/10.1039/C4TA06763K.

[97] Y. Zhu, K.M. Gupta, Q. Liu, J. Jiang, J. Caro, A. Huang, Synthesis and seawater desalination of molecular sieving zeolitic imidazolate framework membranes, Desalination 385 (2016) 75–82, https://doi.org/10.1016/j.desal.2016.02.005.

[98] M.C. McCarthy, V. Varela-Guerrero, G.V. Barnett, H.-K. Jeong, Synthesis of zeolitic imidazolate framework films and membranes with controlled microstructures, Langmuir 26 (2010) 14636–14641, https://doi.org/10.1021/la102409e.

[99] T. Ben, C. Lu, C. Pei, S. Xu, S. Qiu, Polymer-supported and free-standing metal-organic framework membrane, Chem. Eur J. 18 (2012) 10250–10253, https://doi.org/10.1002/chem.201201574.

[100] Z. Kang, M. Xue, L. Fan, J. Ding, L. Guo, L. Gao, S. Qiu, "Single nickel source" in situ fabrication of a stable homochiral MOF membrane with chiral resolution properties, Chem. Commun. 49 (2013) 10569–10571, https://doi.org/10.1039/C3CC42376J.

[101] P. Neelakanda, E. Barankova, K.-V. Peinemann, Polymer supported ZIF-8 membranes by conversion of sputtered zinc oxide layers, Microporous Mesoporous Mater. 220 (2016) 215–219, https://doi.org/10.1016/j.micromeso.2015.08.038.

[102] J. Li, J. Gu, W. Yin, Z. Li, Preparation of ZIF-8 membranes on ZnO modified stainless steel nets, CIESC J. 69 (8) (2018) 3724–3731.

[103] F. Zhang, X. Zou, X. Gao, S. Fan, F. Sun, H. Ren, G. Zhu, Hydrogen selective NH_2-MIL-53(Al) MOF membranes with high permeability, Adv. Funct. Mater. 22 (2012) 3583–3590, https://doi.org/10.1002/adfm.201200084.

[104] Y.-S. Li, H. Bux, A. Feldhoff, G.-L. Li, W.-S. Yang, J. Caro, Controllable synthesis of metal-organic frameworks: from MOF nanorods to oriented MOF membranes, Adv. Mater. 22 (2010) 3322–3326, https://doi.org/10.1002/adma.201000857.

[105] J. Gascon, S. Aguado, F. Kapteijn, Manufacture of dense coatings of Cu_3(BTC)$_2$ (HKUST-1) on α-alumina, Microporous Mesoporous Mater. 113 (2008) 132–138, https://doi.org/10.1016/j.micromeso.2007.11.014.

[106] L. Fan, M. Xue, Z. Kang, H. Li, S. Qiu, Electrospinning technology applied in zeolitic imidazolate framework membrane synthesis, J. Mater. Chem. 22 (2012) 25272–25276, https://doi.org/10.1039/C2JM35401B.

[107] V.V. Guerrero, Y. Yoo, M.C. McCarthy, H.-K. Jeong, HKUST-1 membranes on porous supports using secondary growth, J. Mater. Chem. 20 (2010) 3938–3943, https://doi.org/10.1039/B924536G.

[108] K. Eum, A. Rownaghi, D. Choi, R.R. Bhave, C.W. Jones, S. Nair, Fluidic processing of high-performance ZIF-8 membranes on polymeric hollow fibers: mechanistic insights and microstructure control, Adv. Funct. Mater. 26 (2016) 5011–5018, https://doi.org/10.1002/adfm.201601550.

[109] L. Kong, X. Zhang, Y. Liu, S. Li, H. Liu, J. Qiu, K.L. Yeung, In situ fabrication of high-permeance ZIF-8 tubular membranes in a continuous flow system, Mater. Chem. Phys. 148 (2014) 10–16, https://doi.org/10.1016/j.matchemphys.2014.07.036.

[110] K. Huang, Z. Dong, Q. Li, W. Jin, Growth of a ZIF-8 membrane on the inner-surface of a ceramic hollow fiber via cycling precursors, Chem. Commun. 49 (2013) 10326–10328, https://doi.org/10.1039/C3CC46244G.

[111] A.M. Marti, W. Wickramanayake, G. Dahe, A. Sekizkardes, T.L. Bank, D. P. Hopkinson, S.R. Venna, Continuous flow processing of ZIF-8 membranes on polymeric porous hollow fiber supports for CO2 capture, ACS Appl. Mater. Interfaces 9 (2017) 5678–5682, https://doi.org/10.1021/acsami.6b16297.

[112] J.P. Patterson, P. Abellan, M.S. Denny, C. Park, N.D. Browning, S.M. Cohen, J. E. Evans, N.C. Gianneschi, Observing the growth of metal-organic frameworks by in situ liquid cell transmission electron microscopy, J. Am. Chem. Soc. 137 (2015) 7322–7328, https://doi.org/10.1021/jacs.5b00817.

[113] O. Shekhah, H. Wang, S. Kowarik, F. Schreiber, M. Paulus, M. Tolan, C. Sternemann, F. Evers, D. Zacher, R.A. Fischer, C. Wöll, Step-by-Step route for the synthesis of metal-organic frameworks, J. Am. Chem. Soc. 129 (2007) 15118–15119, https://doi.org/10.1021/ja076210u.

[114] I. Stassen, M. Styles, G. Grenci, Hans V. Gorp, W. Vanderlinden, Steven D. Feyter, P. Falcaro, D.D. Vos, P. Vereecken, R. Ameloot, Chemical vapour deposition of zeolitic imidazolate framework thin films, Nat. Mater. 15 (2016) 304–310, https://doi.org/10.1038/nmat4509.

[115] S.D. Worrall, H. Mann, A. Rogers, M.A. Bissett, M.P. Attfield, R.A.W. Dryfe, Electrochemical deposition of zeolitic imidazolate framework electrode coatings for supercapacitor electrodes, Electrochim. Acta 197 (2016) 228–240, https://doi.org/10.1016/j.electacta.2016.02.145.

[116] X. Zhang, K. Wan, P. Subramanian, M. Xu, J. Luo, J. Fransaer, Electrochemical deposition of metal–organic framework films and their applications, J. Mater. Chem. 8 (2020) 7569–7587, https://doi.org/10.1039/D0TA00406E.

[117] X.C. Huang, Y.Y. Lin, J.P. Zhang, X.M. Chen, Ligand-directed strategy for zeolite-type metal-organic frameworks: zinc (II) imidazolates with unusual zeolitic topologies, Angew. Chem. Int. Ed. 45 (2006) 1557–1559, https://doi.org/10.1002/anie.200503778.

[118] P. Krokidas, M. Castier, S. Moncho, E. Brothers, I.G. Economou, Molecular simulation studies of the diffusion of methane, ethane, propane, and propylene in ZIF-8, J. Phys. Chem. C 119 (2015) 27028–27037, https://doi.org/10.1021/acs.jpcc.5b08554.

[119] D. Fairen-Jimenez, S.A. Moggach, M.T. Wharmby, P.A. Wright, S. Parsons, T. Duren, Opening the gate: framework flexibility in ZIF-8 explored by experiments and simulations, J. Am. Chem. Soc. 133 (2011) 8900–8902, https://doi.org/10.1021/ja202154j.

[120] K. Li, D.H. Olson, J. Seidel, T.J. Emge, H. Gong, H. Zeng, J. Li, Zeolitic imidazolate frameworks for kinetic separation of propane and propene, J. Am. Chem. Soc. 131 (2009) 10368–10369, https://doi.org/10.1021/ja9039983.

[121] C. Zhang, R.P. Lively, K. Zhang, J.R. Johnson, O. Karvan, W.J. Koros, Unexpected molecular sieving properties of zeolitic imidazolate framework-8, J. Phys. Chem. Lett. 3 (2012) 2130–2134, https://doi.org/10.1021/jz300855a.

[122] Y. Pan, T. Li, G. Lestari, Z. Lai, Effective separation of propylene/propane binary mixtures by ZIF-8 membranes, J. Membr. Sci. 390 (2012) 93–98, https://doi.org/10.1016/j.memsci.2011.11.024.

[123] Y. Pan, Y. Liu, G. Zeng, L. Zhao, Z. Lai, Rapid synthesis of zeolitic imidazolate framework-8 (ZIF-8) nanocrystals in an aqueous system, Chem. Commun. 47 (2011) 2071–2073, https://doi.org/10.1039/C0CC05002D.

[124] Y. Pan, B. Wang, Z. Lai, Synthesis of ceramic hollow fiber supported zeolitic imidazolate framework-8 (ZIF-8) membranes with high hydrogen permeability, J. Membr. Sci. 421 (2012) 292–298, https://doi.org/10.1016/j.memsci.2012.07.028.

[125] M. Shah, H.T. Kwon, V. Tran, S. Sachdeva, H.-K. Jeong, One step in situ synthesis of supported zeolitic imidazolate framework ZIF-8 membranes: role of sodium formate, Microporous Mesoporous Mater. 165 (2013) 63–69, https://doi.org/10.1016/j.micromeso.2012.07.046.

[126] J.-W. Wang, N.-X. Li, Z.-R. Li, J.-R. Wang, X. Xu, C.-S. Chen, Preparation and gas separation properties of Zeolitic imidazolate frameworks-8 (ZIF-8) membranes supported on silicon nitride ceramic hollow fibers, Ceram. Int. 42 (2016) 8949–8954, https://doi.org/10.1016/j.ceramint.2016.02.153.

[127] A. Huang, H. Bux, F. Steinbach, J. Caro, Molecular-sieve membrane with hydrogen permselectivity: ZIF-22 in LTA topology prepared with 3-aminopropyltriethoxysilane as covalent linker, Angew. Chem. Int. Ed. 49 (2010) 4958–4961, https://doi.org/10.1002/anie.201001919.

[128] A. Huang, W. Dou, J.r. Caro, Steam-stable zeolitic imidazolate framework ZIF-90 membrane with hydrogen selectivity through covalent functionalization, J. Am. Chem. Soc. 132 (2010) 15562–15564, https://doi.org/10.1021/ja108774v.

[129] S. Tanaka, K. Okubo, K. Kida, M. Sugita, T. Takewaki, Grain size control of ZIF-8 membranes by seeding-free aqueous synthesis and their performances in propylene/propane separation, J. Membr. Sci. 544 (2017) 306–311, https://doi.org/10.1016/j.memsci.2017.09.037.

[130] H. Bux, A. Feldhoff, J. Cravillon, M. Wiebcke, Y.-S. Li, J. Caro, Oriented zeolitic imidazolate framework-8 membrane with sharp H_2/C_3H_8 molecular sieve separation, Chem. Mater. 23 (2011) 2262–2269, https://doi.org/10.1021/cm200555s.

[131] L. Kong, X. Zhang, H. Liu, J. Qiu, Synthesis of a highly stable ZIF-8 membrane on a macroporous ceramic tube by manual-rubbing ZnO deposition as a multifunctional layer, J. Membr. Sci. 490 (2015) 354–363, https://doi.org/10.1016/j.memsci.2015.05.006.

[132] K. Tao, C. Kong, L. Chen, High performance ZIF-8 molecular sieve membrane on hollow ceramic fiber via crystallizing-rubbing seed deposition, Chem. Eng. J. 220 (2013) 1–5, https://doi.org/10.1016/j.cej.2013.01.051.

[133] M.R. Abdul Hamid, S. Park, J.S. Kim, Y.M. Lee, H.-K. Jeong, Synthesis of ultrathin zeolitic imidazolate framework ZIF-8 membranes on polymer hollow fibers using a polymer modification strategy for propylene/propane separation, Ind. Eng. Chem. Res. 58 (2019) 14947–14953, https://doi.org/10.1021/acs.iecr.9b02969.

[134] J. Sun, C. Yu, H.-K. Jeong, Propylene-selective thin zeolitic imidazolate framework membranes on ceramic tubes by microwave seeding and solvothermal secondary growth, Crystals 8 (2018) 373, https://doi.org/10.3390/cryst8100373.

[135] H.T. Kwon, H.-K. Jeong, Improving propylene/propane separation performance of zeolitic-imidazolate framework ZIF-8 membranes, Chem. Eng. Sci. 124 (2015) 20–26, https://doi.org/10.1016/j.ces.2014.06.021.

[136] E. Jang, E. Kim, H. Kim, T. Lee, H.-J. Yeom, Y.-W. Kim, J. Choi, Formation of ZIF-8 membranes inside porous supports for improving both their H_2/CO_2 separation performance and thermal/mechanical stability, J. Membr. Sci. 540 (2017) 430–439, https://doi.org/10.1016/j.memsci.2017.06.072.

[137] N. Hara, M. Yoshimune, H. Negishi, K. Haraya, S. Hara, T. Yamaguchi, ZIF-8 membranes prepared at miscible and immiscible liquid–liquid interfaces, Microporous Mesoporous Mater. 206 (2015) 75–80, https://doi.org/10.1016/j.micromeso.2014.12.018.

[138] N. Hara, M. Yoshimune, H. Negishi, K. Haraya, S. Hara, T. Yamaguchi, Thickness reduction of the zeolitic imidazolate framework-8 membrane by controlling the reaction rate during the membrane preparation, J. Chem. Eng. Jpn. 47 (2014) 770–776, https://doi.org/10.1252/jcej.14we340.

[139] N. Hara, M. Yoshimune, H. Negishi, K. Haraya, S. Hara, T. Yamaguchi, Effect of temperature on synthesis of ZIF-8 membranes for propylene/propane separation by counter diffusion method, J. Jpn. Pet. Inst. 58 (2015) 237–244, https://doi.org/10.1627/jpi.58.237.

[140] A. Knebel, B. Geppert, K. Volgmann, D.I. Kolokolov, A.G. Stepanov, J. Twiefel, P. Heitjans, D. Volkmer, J. Caro, Defibrillation of soft porous metal-organic frameworks with electric fields, Science 358 (2017) 347–351, https://doi.org/10.1126/science.aal2456.

[141] Y. Zhao, Y. Wei, L. Lyu, Q. Hou, J. Caro, H. Wang, Flexible polypropylene-supported ZIF-8 membranes for highly efficient propene/propane separation, J. Am. Chem. Soc. 142 (2020) 20915–20919, https://doi.org/10.1021/jacs.0c07481.

[142] J. Li, H. Lian, K. Wei, E. Song, Y. Pan, W. Xing, Synthesis of tubular ZIF-8 membranes for propylene/propane separation under high-pressure, J. Membr. Sci. 595 (2020), 117503, https://doi.org/10.1016/j.memsci.2019.117503.

[143] H.T. Kwon, H.-K. Jeong, A.S. Lee, H.S. An, J.S. Lee, Heteroepitaxially grown zeolitic imidazolate framework membranes with unprecedented propylene/propane separation performances, J. Am. Chem. Soc. 137 (2015) 12304–12311, https://doi.org/10.1021/jacs.5b06730.

[144] Q. Hou, S. Zhou, Y. Wei, J. Caro, H. Wang, Balancing the grain boundary structure and the framework flexibility through bimetallic MOF membranes for gas separation, J. Am. Chem. Soc. 142 (2020) 9582–9586, https://doi.org/10.1021/jacs.0c02181.

[145] X. Dong, K. Huang, S. Liu, R. Ren, W. Jin, Y.S. Lin, Synthesis of zeolitic imidazolate framework-78 molecular-sieve membrane: defect formation and elimination, J. Mater. Chem. 22 (2012) 19222–19227, https://doi.org/10.1039/C2JM34102F.

[146] Y. Pan, W. Liu, Y. Zhao, C. Wang, Z. Lai, Improved ZIF-8 membrane: effect of activation procedure and determination of diffusivities of light hydrocarbons, J. Membr. Sci. 493 (2015) 88–96, https://doi.org/10.1016/j.memsci.2015.06.019.

[147] M.J. Lee, M.R. Abdul Hamid, J. Lee, J.S. Kim, Y.M. Lee, H.-K. Jeong, Ultrathin zeolitic-imidazolate framework ZIF-8 membranes on polymeric hollow fibers for propylene/propane separation, J. Membr. Sci. 559 (2018) 28–34, https://doi.org/10.1016/j.memsci.2018.04.041.

[148] Z. Qiao, Y. Liang, Z. Zhang, D. Mei, Z. Wang, M.D. Guiver, C. Zhong, Ultrathin low-crystallinity MOF membranes fabricated by interface layer polarization induction, Adv. Mater. 32 (2020), 2002165, https://doi.org/10.1002/adma.202002165.

[149] M.J. Lee, H.T. Kwon, H.K. Jeong, High-flux zeolitic imidazolate framework membranes for propylene/propane separation by postsynthetic linker exchange, Angew. Chem. Int. Ed. 57 (2018) 156–161, https://doi.org/10.1002/anie.201708924.

[150] T. Wu, J. Lucero, M.A. Sinnwell, P.K. Thallapally, M.A. Carreon, Recovery of xenon from air over ZIF-8 membranes, Chem. Commun. 54 (2018) 8976–8979, https://doi.org/10.1039/C8CC04154G.

[151] Q. Wei, J.M. Lucero, J.M. Crawford, J.D. Way, C.A. Wolden, M.A. Carreon, Ammonia separation from N_2 and H_2 over LTA zeolitic imidazolate framework membranes, J. Membr. Sci. 623 (2021), 119078, https://doi.org/10.1016/j.memsci.2021.119078.

[152] X. Wang, C. Chi, J. Tao, Y. Peng, S. Ying, Y. Qian, J. Dong, Z. Hu, Y. Gu, D. Zhao, Improving the hydrogen selectivity of graphene oxide membranes by reducing non-selective pores with intergrown ZIF-8 crystals, Chem. Commun. 52 (2016) 8087–8090, https://doi.org/10.1039/C6CC02013E.

[153] E. Shamsaei, X. Lin, L. Wan, Y. Tong, H. Wang, A one-dimensional material as a nano-scaffold and a pseudo-seed for facilitated growth of ultrathin, mechanically reinforced molecular sieving membranes, Chem. Commun. 52 (2016) 13764–13767, https://doi.org/10.1039/C6CC07709A.

[154] Z. Xie, J. Yang, J. Wang, J. Bai, H. Yin, B. Yuan, J. Lu, Y. Zhang, L. Zhou, C. Duan, Deposition of chemically modified α-Al_2O_3 particles for high performance ZIF-8 membrane on a macroporous tube, Chem. Commun. 48 (2012) 5977–5979, https://doi.org/10.1039/C2CC17607F.

[155] Y. Huang, D. Liu, Z. Liu, C. Zhong, Synthesis of zeolitic imidazolate framework membrane using temperature-switching synthesis strategy for gas separation, Ind. Eng. Chem. Res. 55 (2016) 7164–7170, https://doi.org/10.1021/acs.iecr.6b01290.

[156] Y. Huang, Y. Xiao, H. Huang, Z. Liu, D. Liu, Q. Yang, C. Zhong, Ionic liquid functionalized multi-walled carbon nanotubes/zeolitic imidazolate framework hybrid membranes for efficient H_2/CO_2 separation, Chem. Commun. 51 (2015) 17281–17284, https://doi.org/10.1039/C5CC05061H.

[157] A. Huang, Y. Chen, N. Wang, Z. Hu, J. Jiang, J. Caro, A highly permeable and selective zeolitic imidazolate framework ZIF-95 membrane for H_2/CO_2 separation, Chem. Commun. 48 (2012) 10981–10983, https://doi.org/10.1039/C2CC35691K.

[158] N. Wang, A. Mundstock, Y. Liu, A. Huang, J. Caro, Amine-modified Mg-MOF-74/CPO-27-Mg membrane with enhanced H_2/CO_2 separation, Chem. Eng. Sci. 124 (2015) 27–36, https://doi.org/10.1016/j.ces.2014.10.037.

[159] Y. Peng, Y. Li, Y. Ban, W. Yang, Two-Dimensional metal–organic framework nanosheets for membrane-based gas separation, Angew. Chem. Int. Ed. 56 (2017) 9757–9761, https://doi.org/10.1002/anie.201703959.

[160] X. Wang, C. Chi, K. Zhang, Y. Qian, K.M. Gupta, Z. Kang, J. Jiang, D. Zhao, Reversed thermo-switchable molecular sieving membranes composed of two-dimensional metal-organic nanosheets for gas separation, Nat. Commun. 8 (2017) 14460, https://doi.org/10.1038/ncomms14460.

[161] A. Jomekian, R.M. Behbahani, T. Mohammadi, A. Kargari, Innovative layer by layer and continuous growth methods for synthesis of ZIF-8 membrane on porous polymeric support using poly(ether-block-amide) as structure directing agent for gas separation, Microporous Mesoporous Mater. 234 (2016) 43–54, https://doi.org/10.1016/j.micromeso.2016.07.008.

[162] D.J. Babu, G. He, J. Hao, M.T. Vahdat, P.A. Schouwink, M. Mensi, K.V. Agrawal, Restricting lattice flexibility in polycrystalline metal-organic framework membranes for carbon capture, Adv. Mater. 31 (2019), 1900855, https://doi.org/10.1002/adma.201900855.

[163] Q. Hou, Y. Wu, S. Zhou, Y. Wei, J. Caro, H. Wang, Ultra-tuning of the aperture size in stiffened ZIF-8_Cm frameworks with mixed-linker strategy for enhanced CO_2/CH_4 separation, Angew. Chem. Int. Ed. 58 (2019) 327–331, https://doi.org/10.1002/anie.201811638.

[164] Z.Y. Yeo, P.W. Zhu, A.R. Mohamed, S.-P. Chai, An enhanced hybrid membrane of ZIF-8 and zeolite T for CO_2/CH_4 separation, CrystEngComm 16 (2014) 3072–3075, https://doi.org/10.1039/C3CE42468E.

[165] F. Cacho-Bailo, M. Etxeberría-Benavides, O. Karvan, C. Téllez, J. Coronas, Sequential amine functionalization inducing structural transition in an aldehyde-containing zeolitic imidazolate framework: application to gas separation membranes, CrystEngComm 19 (2017) 1545–1554, https://doi.org/10.1039/C7CE00086C.

[166] N. Hara, M. Yoshimune, H. Negishi, K. Haraya, S. Hara, T. Yamaguchi, Metal–organic framework membranes with layered structure prepared within the porous support, RSC Adv. 3 (2013) 14233–14236, https://doi.org/10.1039/C3RA22733B.

[167] C. Kong, H. Du, L. Chen, B. Chen, Nanoscale MOF/organosilica membranes on tubular ceramic substrates for highly selective gas separation, Energy Environ. Sci. 10 (2017) 1812–1819, https://doi.org/10.1039/C7EE00830A.

[168] H. Yin, J. Wang, Z. Xie, J. Yang, J. Bai, J. Lu, Y. Zhang, D. Yin, J.Y.S. Lin, A highly permeable and selective amino-functionalized MOF CAU-1 membrane for CO_2-N_2 separation, Chem. Commun. 50 (2014) 3699–3701, https://doi.org/10.1039/C4CC00068D.

[169] W. Wu, Z. Li, Y. Chen, W. Li, Polydopamine-modified metal-organic framework membrane with enhanced selectivity for carbon capture, Environ. Sci. Technol. 53 (2019) 3764–3772, https://doi.org/10.1021/acs.est.9b00408.

[170] Z. Rui, J.B. James, A. Kasik, Y.S. Lin, Metal-organic framework membrane process for high purity CO_2 production, AIChE J. 62 (2016) 3836–3841, https://doi.org/10.1002/aic.15367.

[171] Y. Zhang, H. Wang, J. Liu, J. Hou, Y. Zhang, Enzyme-embedded metal-organic framework membranes on polymeric substrates for efficient CO_2 capture, J. Mater. Chem. 5 (2017) 19954–19962, https://doi.org/10.1039/C7TA03719H.

[172] M. Liu, K. Xie, M.D. Nothling, P.A. Gurr, S.S.L. Tan, Q. Fu, P.A. Webley, G.G. Qiao, Ultrathin metal-organic framework nanosheets as a gutter layer for flexible composite gas separation membranes, ACS Nano 12 (2018) 11591–11599, https://doi.org/10.1021/acsnano.8b06811.

[173] M.R. Abdul Hamid, H.-K. Jeong, Recent advances on mixed-matrix membranes for gas separation: opportunities and engineering challenges, Kor. J. Chem. Eng. 35 (2018) 1577–1600, https://doi.org/10.1007/s11814-018-0081-1.

[174] C. Zhang, K. Zhang, L. Xu, Y. Labreche, B. Kraftschik, W.J. Koros, Highly scalable ZIF-based mixed-matrix hollow fiber membranes for advanced hydrocarbon separations, AIChE J. 60 (2014) 2625–2635, https://doi.org/10.1002/aic.14496.

[175] Y. Dai, J.R. Johnson, O. Karvan, D.S. Sholl, W.J. Koros, Ultem®/ZIF-8 mixed matrix hollow fiber membranes for CO_2/N_2 separations, J. Membr. Sci. 401–402 (2012) 76–82, https://doi.org/10.1016/j.memsci.2012.01.044.

[176] Y.S. Lin, Metal organic framework membranes for separation applications, Curr. Opin. Chem. Eng. 8 (2015) 21–28, https://doi.org/10.1016/j.coche.2015.01.006.

[177] T. Xiao, D. Liu, Progress in the synthesis, properties and applications of ZIF-7 and its derivatives, Mater. Today Energy 14 (2019), 100357, https://doi.org/10.1016/j.mtener.2019.100357.

[178] A. Huang, J. Caro, Covalent post-functionalization of zeolitic imidazolate framework ZIF-90 membrane for enhanced hydrogen selectivity, Angew. Chem. Int. Ed. 50 (2011) 4979–4982, https://doi.org/10.1002/anie.201007861.

[179] A. Huang, Q. Liu, N. Wang, J. Caro, Organosilica functionalized zeolitic imidazolate framework ZIF-90 membrane for CO_2/CH_4 separation, Microporous Mesoporous Mater. 192 (2014) 18–22, https://doi.org/10.1016/j.micromeso.2013.09.025.

[180] Y. Go, J.H. Lee, I.K. Shamsudin, J. Kim, M.R. Othman, Microporous ZIF-7 membranes prepared by in-situ growth method for hydrogen separation, Int. J. Hydrogen Energy 41 (2016) 10366–10373, https://doi.org/10.1016/j.ijhydene.2015.09.060.

[181] V.M.A. Melgar, H.T. Kwon, J. Kim, Direct spraying approach for synthesis of ZIF-7 membranes by electrospray deposition, J. Membr. Sci. 459 (2014) 190–196, https://doi.org/10.1016/j.memsci.2014.02.020.

[182] Q. Ma, K. Mo, S. Gao, Y. Xie, J. Wang, H. Jin, A. Feldhoff, S. Xu, J.Y.S. Lin, Y. Li, Ultrafast semi-solid processing of highly durable ZIF-8 membranes for propylene/propane separation, Angew. Chem. Int. Ed. 59 (2020), 21909, https://doi.org/10.1002/anie.202008943.

[183] R.W. Johnson, A. Hultqvist, S.F. Bent, A brief review of atomic layer deposition: from fundamentals to applications, Mater, Today Off. 17 (2014) 236–246, https://doi.org/10.1016/j.mattod.2014.04.026.
[184] A. Kafizas, C.J. Carmalt, I.P. Parkin, CVD and precursor chemistry of transition metal nitrides, Coord. Chem. Rev. 257 (2013) 2073–2119, https://doi.org/10.1016/j.ccr.2012.12.004.
[185] R.W. Baker, Future directions of membrane gas separation technology, Ind. Eng. Chem. Res. 41 (2002) 1393–1411, https://doi.org/10.1021/ie0108088.
[186] Y.S. Lin, Inorganic membranes for process intensification: challenges and perspective, Ind. Eng. Chem. Res. 58 (2018) 5787–5796, https://doi.org/10.1021/acs.iecr.8b04539.
[187] J. Caro, Hierarchy in inorganic membranes, Chem. Soc. Rev. 45 (2016) 3468–3478, https://doi.org/10.1039/C5CS00597C.
[188] M.T. Castoldi, J.C. Pinto, P.A. Melo, Modeling of the separation of propene/propane mixtures by permeation through membranes in a polymerization system, Ind. Eng. Chem. Res. 46 (2007) 1259–1269, https://doi.org/10.1021/ie060333q.
[189] J. Caro, M. Noack, P. Kölsch, R. Schäfer, Zeolite membranes - state of their development and perspective, Microporous Mesoporous Mater. 38 (2000) 3–24, https://doi.org/10.1016/S1387-1811(99)00295-4.
[190] M. Tsapatsis, Toward high-throughput zeolite membranes, Science 334 (2011) 767–768, https://doi.org/10.1126/science.1205957.
[191] F. Rashidi, J. Leisen, S.J. Kim, A.A. Rownaghi, C.W. Jones, S. Nair, All-nanoporous hybrid membranes: redefining upper limits on molecular separation properties, Angew. Chem. Int. Ed. 131 (2019) 242–245, https://doi.org/10.1002/ange.201811629.
[192] K. Eum, S. Yang, B. Min, C. Ma, J.H. Drese, Y. Tamhankar, S. Nair, All-nanoporous hybrid membranes: incorporating zeolite nanoparticles and nanosheets with zeolitic imidazolate framework matrices, ACS Appl. Mater. Interfaces 12 (2020) 27368–27377, https://doi.org/10.1021/acsami.0c06227.
[193] D. Li, R. Wang, T.-S. Chung, Fabrication of lab-scale hollow fiber membrane modules with high packing density, Separ. Purif. Technol. 40 (2004) 15–30, https://doi.org/10.1016/j.seppur.2003.12.019.
[194] W. Li, W. Wu, Z. Li, J. Shi, Y. Xia, Sol–gel asynchronous crystallization of ultra-selective metal-organic framework membranes for gas separation, J. Mater. Chem. 6 (2018) 16333–16340, https://doi.org/10.1039/C8TA06083E.
[195] M.R. Abdul Hamid, H.-K. Jeong, Flow synthesis of polycrystalline ZIF-8 membranes on polyvinylidene fluoride hollow fibers for recovery of hydrogen and propylene, J. Ind. Eng. Chem. 88 (2020) 319–327, https://doi.org/10.1016/j.jiec.2020.04.031.
[196] F. Cacho-Bailo, S. Catalan-Aguirre, M. Etxeberria-Benavides, O. Karvan, V. Sebastian, C. Tellez, J. Coronas, Metal-organic framework membranes on the inner-side of a polymeric hollow fiber by microfluidic synthesis, J. Membr. Sci. 476 (2015) 277–285, https://doi.org/10.1016/j.memsci.2014.11.016.
[197] K. Eum, C. Ma, D.Y. Koh, F. Rashidi, Z. Li, C.W. Jones, R.P. Lively, S. Nair, Zeolitic imidazolate framework membranes supported on macroporous carbon hollow fibers by fluidic processing techniques, Adv. Mater. Interfaces 4 (2017), 1700080, https://doi.org/10.1002/admi.201700080.
[198] K. Huang, B. Wang, Y. Chi, K. Li, High propylene selective metal-organic framework membranes prepared in confined spaces via convective circulation synthesis, Adv. Mater. Interfaces 5 (2018), 1800287, https://doi.org/10.1002/admi.201800287.
[199] X. Wang, M. Sun, B. Meng, X. Tan, J. Liu, S. Wang, S. Liu, Formation of continuous and highly permeable ZIF-8 membranes on porous alumina and zinc oxide hollow fibers, Chem. Commun. 52 (2016) 13448–13451, https://doi.org/10.1039/C6CC06589A.
[200] Y. Wang, H. Chen, X. Wang, B. Meng, N. Yang, X. Tan, S. Liu, Preparation of ZIF-8 membranes on porous ZnO hollow fibers by a facile ZnO-induced method, Ind. Eng. Chem. Res. 59 (2020) 15576–15585, https://doi.org/10.1021/acs.iecr.0c02750.
[201] N.T. Tran, T. Yu, J. Kim, M.R. Othman, ZIF-8 tubular membrane for propylene purification: effect of surface curvature and zinc salts on separation performance, Separ. Purif. Technol. 251 (2020), 117354, https://doi.org/10.1016/j.seppur.2020.117354.
[202] M. Pera-Titus, R. Mallada, J. Llorens, F. Cunill, J. Santamaría, Preparation of inner-side tubular zeolite NaA membranes in a semi-continuous synthesis system, J. Membr. Sci. 278 (2006) 401–409, https://doi.org/10.1016/j.memsci.2005.11.026.
[203] S.C. Hess, R.N. Grass, W.J. Stark, MOF channels within porous polymer film: flexible, self-supporting ZIF-8 poly(ether sulfone) composite membrane, Chem. Mater. 28 (2016) 7638–7644, https://doi.org/10.1021/acs.chemmater.6b02499.
[204] W.J. Stark, S.C. Hess, U.S. Patent App., 20200306698, 2020.
[205] Gas Separation Membranes UniSieve®, 2020. https://www.unisieve.com/. (Accessed 7 August 2021).
[206] D. Enrico, G. Lidietta, Encyclopedia of Membranes, Springer, Berlin, 2015.
[207] B.P. Biswal, A. Bhaskar, R. Banerjee, U.K. Kharul, Selective interfacial synthesis of metal-organic frameworks on a polybenzimidazole hollow fiber membrane for gas separation, Nanoscale 7 (2015) 7291–7298, https://doi.org/10.1039/C5NR00299K.
[208] C.A. Scholes, J. Motuzas, S. Smart, S.E. Kentish, Membrane adhesives, Ind. Eng. Chem. Res. 53 (2014) 9523–9533, https://doi.org/10.1021/ie501036p.
[209] G. Xu, K. Wang, Z. Zhong, C.-s. Chen, P.A. Webley, H. Wang, SiC nanofiber reinforced porous ceramic hollow fiber membranes, J. Mater. Chem. 2 (2014) 5841–5846, https://doi.org/10.1039/C3TA15348G.
[210] S. Park, H.-K. Jeong, Transforming polymer hollow fiber membrane modules to mixed-matrix hollow fiber membrane modules for propylene/propane separation, J. Membr. Sci. 612 (2020), 118429, https://doi.org/10.1016/j.memsci.2020.118429.
[211] Y. Zhu, J. Ciston, B. Zheng, X. Miao, C. Czarnik, Y. Pan, R. Sougrat, Z. Lai, C.-E. Hsiung, K. Yao, I. Pinnau, M. Pan, Y. Han, Unravelling surface and interfacial structures of a metal-organic framework by transmission electron microscopy, Nat. Mater. 16 (2017) 532–536, https://doi.org/10.1038/nmat4852.
[212] C. Chen, A. Ozcan, A.O. Yazaydin, B.P. Ladewig, Gas permeation through single-crystal ZIF-8 membranes, J. Membr. Sci. 575 (2019) 209–216, https://doi.org/10.1016/j.memsci.2019.01.027.
[213] J. Choi, H.-K. Jeong, M.A. Snyder, J.A. Stoeger, R.I. Masel, M. Tsapatsis, Grain boundary defect elimination in a zeolite membrane by rapid thermal processing, Science 325 (2009) 590, https://doi.org/10.1126/science.1176095.
[214] J.M.S. Henis, M.K. Tripodi, U.S. Patent, 1980, p. US4230463.
[215] M. Sadrzadeh, M. Amirilargani, K. Shahidi, T. Mohammadi, Gas permeation through a synthesized composite PDMS/PES membrane, J. Membr. Sci. 342 (2009) 236–250, https://doi.org/10.1016/j.memsci.2009.06.047.
[216] J. Hua, C. Li, H. Tao, L. Wang, E. Song, H. Lian, C. Wang, J. Jiang, Y. Pan, W. Xing, Improved C_3H_6/C_3H_8 separation performance on ZIF-8 membranes through enhancing PDMS contact-dependent confinement effect, J. Membr. Sci. 636 (2021), 119613, https://doi.org/10.1016/j.memsci.2021.119613.
[217] L. Sheng, C. Wang, F. Yang, L. Xiang, X. Huang, J. Yu, L. Zhang, Y. Pan, Y. Li, Enhanced C_3H_6/C_3H_8 separation performance on MOF membranes through blocking defects and hindering framework flexibility by silicone rubber coating, Chem. Commun. 53 (2017) 7760–7763, https://doi.org/10.1039/C7CC03887A.
[218] S. Friebe, B. Geppert, F. Steinbach, J.r. Caro, Metal-organic framework UiO-66 layer: a highly oriented membrane with good selectivity and hydrogen permeance, ACS Appl. Mater. Interfaces 9 (2017) 12878–12885, https://doi.org/10.1021/acsami.7b02105.
[219] H.T. Kwon, H.-K. Jeong, In situ synthesis of thin zeolitic-imidazolate framework ZIF-8 membranes exhibiting exceptionally high propylene/propane separation, J. Am. Chem. Soc. 135 (2013) 10763–10768, https://doi.org/10.1021/ja403849c.
[220] Y. Wang, H. Jin, Q. Ma, K. Mo, H. Mao, A. Feldhoff, X. Cao, Y. Li, F. Pan, Z. Jiang, A MOF glass membrane for gas separation, Angew. Chem. Int. Ed. 59 (2020) 4365–4369, https://doi.org/10.1002/anie.201915807.
[221] H.R. Amedi, M. Aghajani, Economic estimation of various membranes and distillation for propylene and propane separation, Ind. Eng. Chem. Res. 57 (2018) 4366–4376, https://doi.org/10.1021/acs.iecr.7b04169.
[222] M.W. Niu, G.P. Rangaiah, Retrofitting an isopropanol process based on reactive distillation and propylene-propane separation, Chem. Eng. Process 108 (2016) 164–173, https://doi.org/10.1016/j.cep.2016.07.013.
[223] K. Eum, C. Ma, A. Rownaghi, C.W. Jones, S. Nair, ZIF-8 membranes via interfacial microfluidic processing in polymeric hollow fibers: efficient propylene separation at elevated pressures, ACS Appl. Mater. Interfaces 8 (2016) 25337–25342, https://doi.org/10.1021/acsami.6b08801.
[224] J. Hou, P.D. Sutrisna, T. Wang, S. Gao, Q. Li, C. Zhou, S. Sun, H.-C. Yang, F. Wei, M.T. Ruggiero, Unraveling the interfacial structure–performance correlation of flexible metal-organic framework membranes on polymeric substrates, ACS Appl. Mater. Interfaces 11 (2019) 5570–5577, https://doi.org/10.1021/acsami.8b20570.
[225] J. Hou, P.D. Sutrisna, Y. Zhang, V. Chen, Formation of ultrathin, continuous metal-organic framework membranes on flexible polymer substrates, Angew. Chem. Int. Ed. 55 (2016) 3947–3951, https://doi.org/10.1002/anie.201511340.
[226] C. Zhang, Y. Dai, J.R. Johnson, O. Karvan, W.J. Koros, High performance ZIF-8/6FDA-DAM mixed matrix membrane for propylene/propane separations, J. Membr. Sci. 389 (2012) 34–42, https://doi.org/10.1016/j.memsci.2011.10.003.
[227] K. Li, D.R. Acharya, R. Hughes, Membrane gas separation with permeate purging, Gas Separ. Purif. 4 (1990) 81–86, https://doi.org/10.1016/0950-4214(90)80032-G.
[228] X. Zhao, Y. Zhang, J. Han, H. Jing, Z. Gao, H. Huang, Y. Wang, C. Zhong, Design of "turn-on" fluorescence sensor for L-Cysteine based on the instability of metal-organic frameworks, Microporous Mesoporous Mater. 268 (2018) 88–92, https://doi.org/10.1016/j.micromeso.2018.04.019.
[229] J.B. James, Y.S. Lin, Kinetics of ZIF-8 thermal decomposition in inert, oxidizing, and reducing environments, J. Phys. Chem. C 120 (2016) 14015–14026, https://doi.org/10.1021/acs.jpcc.6b01208.
[230] L. Sheng, F. Yang, C. Wang, J. Yu, L. Zhang, Y. Pan, Comparison of the hydrothermal stability of ZIF-8 nanocrystals and polycrystalline membranes derived from zinc salt variations, Mater. Lett. 197 (2017) 184–187, https://doi.org/10.1016/j.matlet.2017.03.077.
[231] D. Liu, X. Ma, H. Xi, Y.S. Lin, Gas transport properties and propylene/propane separation characteristics of ZIF-8 membranes, J. Membr. Sci. 451 (2014) 85–93, https://doi.org/10.1016/j.memsci.2013.09.029.
[232] X. Liu, Y. Li, Y. Ban, Y. Peng, H. Jin, H. Bux, L. Xu, J. Caro, W. Yang, Improvement of hydrothermal stability of zeolitic imidazolate frameworks, Chem. Commun. 49 (2013) 9140–9142, https://doi.org/10.1039/C3CC45308A.
[233] S. Tanaka, Y. Tanaka, A simple step toward enhancing hydrothermal stability of ZIF-8, ACS Omega 4 (2019) 19905–19912, https://doi.org/10.1021/acsomega.9b02812.
[234] H. Zhang, D. Liu, Y. Yao, B. Zhang, Y.S. Lin, Stability of ZIF-8 membranes and crystalline powders in water at room temperature, J. Membr. Sci. 485 (2015) 103–111, https://doi.org/10.1016/j.memsci.2015.03.023.
[235] L.-X. Ren, F.-L. Chang, D.-Y. Kang, C.-L. Chen, Hybrid membrane process for post-combustion CO_2 capture from coal-fired power plant, J. Membr. Sci. 603 (2020), 118001, https://doi.org/10.1016/j.memsci.2020.118001.

[236] S. Bhattacharyya, R. Han, W.-G. Kim, Y. Chiang, K.C. Jayachandrababu, J. T. Hungerford, M.R. Dutzer, C. Ma, K.S. Walton, D.S. Sholl, Acid gas stability of zeolitic imidazolate frameworks: generalized kinetic and thermodynamic characteristics, Chem. Mater. 30 (2018) 4089–4101, https://doi.org/10.1021/acs.chemmater.8b01394.

[237] S. Bhattacharyya, S.H. Pang, M.R. Dutzer, R.P. Lively, K.S. Walton, D.S. Sholl, S. Nair, Interactions of SO2-containing acid gases with ZIF-8: structural changes and mechanistic investigations, J. Phys. Chem. C 120 (2016) 27221–27229, https://doi.org/10.1021/acs.jpcc.6b09197.

[238] S. Bhattacharyya, K.C. Jayachandrababu, Y. Chiang, D.S. Sholl, S. Nair, Butanol separation from humid CO_2-containing multicomponent vapor mixtures by zeolitic imidazolate frameworks, ACS Sustain. Chem. Eng. 5 (2017) 9467–9476, https://doi.org/10.1021/acssuschemeng.7b02604.

[239] J. Kim, D. Lee, Marked inducing effects of metal oxide supports on the hydrothermal stability of zeolitic imidazolate framework (ZIF) membranes, J. Mater. Chem. 4 (2016) 5205–5215, https://doi.org/10.1039/C5TA10190E.

[240] Y. Liu, J. Liu, Y.S. Lin, M. Chang, Effects of water vapor and trace gas impurities in flue gas on CO_2/N_2 separation using ZIF-68, J. Phys. Chem. C 118 (2014) 6744–6751, https://doi.org/10.1021/jp4113969.

[241] Y. Ma, Y. Sun, J. Yin, H. Sun, H. Wu, H. Wang, Y. Zhang, X. Feng, J. Meng, A MOF membrane with ultrathin ZIF-8 layer bonded on ZIF-8 in-situ embedded PSf substrate, J. Taiwan Inst. Chem. Eng. 104 (2019) 273–283, https://doi.org/10.1016/j.jtice.2019.08.012.

[242] H. Zhang, X. Wang, L. Wei, B. Meng, X. Tan, W. Jin, S. Liu, A simple seed-embedded method to prepare ZIF-8 membranes supported on flexible PESf hollow fibers, J. Ind. Eng. Chem. 72 (2019) 222–231, https://doi.org/10.1016/j.jiec.2018.12.022.